STRUCTURAL AND BIOLOGICAL INVESTIGATIONS OF METAL COMPLEXES OF SOME SUBSTITUTED THIOSEMICARBAZONES

Thesis submitted to
Cochin University of Science and Technology
In partial fulfillment of the requirements
for the degree of

DOCTOR OF PHILOSOPHY
in
CHEMISTRY

by

ROHITH P. JOHN

Department of Applied Chemistry
Cochin University of Science and Technology
Kochi- 682 022

JANUARY 2002

To My Beloved Parents and Dear Brother.

DECLARATION

I hereby declare that the work presented in this thesis entitled "**STRUCTURAL AND BIOLOGICAL INVESTIGATIONS OF METAL COMPLEXES OF SOME SUBSTITUTED THIOSEMICARBAZONES**" is entirely original and was carried out independently under the supervision of **Professor. M. R. Prathapachandra Kurup**, Department of Applied Chemistry, Cochin University of Science and Technology, and has not been included in any other thesis submitted previously for the award of any degree.

Rohit P. John

Kochi-22
21st January 2002.

Phone Res. 0484-542904
Telex: 885-5019 CUIN
Fax: 0484-532495
Email: mrp@cusat.ac.in

COCHIN UNIVERSITY OF SCIENCE AND TECHNOLOGY

DEPARTMENT OF APPLIED CHEMISTRY

KOCHI - 682 022, INDIA

Dr. M.R. PRATHAPACHANDRA KURUP
Professor

January 21, 2002

CERTIFICATE

This is to certify that the thesis entitled '**Structural and biological investigations of metal complexes of some substituted thiosemicarbazones**", submitted by **Mr. Rohith P. John**, in partial fulfillment of the requirements of the degree of Doctor of Philosophy, to the Cochin University of Science and Technology (CUSAT), Kochi is an authentic and bonafied record of the original research work carried out by him under my guidance and supervision. Further, the results embodied in this thesis, in full or in part, have not been submitted for the award of any other degree.

M. R. Prathapachandra Kurup

(Supervisor)

For I am grateful to...

It's a pleasure and a great privilege to be thankful to those who have come across our lives and have made an impact on us by being what they are and without having our own knowledge. But as an important and significant period in my life I have to be felt indebted to all of those who had been of much help during my research stint over here at Cochin University.

The person to whom I am extremely grateful and committed to is my research supervisor Prof. (Dr.) M. R. Prathapachandra Kurup who gave me the freedom and flexibility in accordance with educational principles. As a humble and simple teacher he had been behind all my motivation and used to be with me in hours of distress as well. Not to mention of his valuable contribution to my academic and research work for when I try to make it out I fall short of words. I wish to express my deep gratitude to (Dr.) S. Sugunan, Head, Dept. of Applied Chemistry for his helps through out my period of work.

The fatherly support and encouragement of former Head of the department Prof. (Dr.) P. Madhavan Pillai in the initial stages of research, was of immense help and I am extremely thankful to him for the same.

The help and useful advise offered by all the faculty members of this department during crucial stages of my work and at times when I confronted with chaos and confusion had been of much value and I am grateful to all of them for their kind-heartedness. The fruitful discussion hours with Prof. (Dr.) A. G. Ramachandran Nair, Visiting Professor, is to be specially remembered for and I am thankful to him for the valuable inputs. The help offered by Prof (Dr.) K. K. Mohammed Yusuff cannot be left-out.

My friends were the chief contributors to what all had I been able do as part of research and I am heavily indebted to some of them. Dr. Binoy Jose who had been with me for more than three years, had been of much solace and encouragement during hours of anvil. He had been of much help in untying much of the puzzled situations and solve-out the imbroglios that often seemed to block the road ahead. Dr. Sreekumar Kurungot and Dr. Jyothi T.M., were also of much help during their stint over here and after wards as well, in my research work. I am heavily indebted to Mr. Jacob Samuel, for his valuable help in crucial junctures.

I appreciate my lab-mates P. B. Sreeja, Chandini R. Nayar, A. Sreekanth and V. Suni for their whole-hearted support during the period. The role of my colleagues Jean John Vadakkan, Preetha G. Prasad, Dr. S. Mayadevi, K. Anas, and Bejoy Thomas was not only limited to as good friends but had always been at my privilege on matters of academics as well. I am thankful to Mr. Sukesh T.V, who had offered much assistance in simulation work. It is a privilege for me to be thankful to Dr. P. Bindu who worked as senior in our lab and who offered valuable advises and assistance during the initial stages of my research career and often lead me to formulate strategies and goals for further work. Her determination to overcome trouble and hardships had been a source of strength and constant motivation for me. The role of Sulatha M. S., Shiju, Sreejith, NCL, Pune has to be remembered for its value. Mr. T. N. Jayaprakash, chemist, Directorate of Mining and Geology had been very helpful at various junctures of my research.

I am grateful to the Mr. T.A. Ajith, Research Scholar, Amala Cancer Research Centre, Trichur, for his immense help during my stint there to carryout the biological screening. I am also thankful Dr. Janardanan, and Dr. Ramadas Kuttan for providing the opportunity to work under them for about two months. I was much benefited by the help of Dr. Suresh Kumar and Ms. Pyroja S. in the early stages of biological study. I am thankful to Prof.(Dr.) D. Velmurugan, Mr. V. Rajakannan, and Dr. L. Govindasamy, Department of Crystallography and Biophysics, Madras University for their collaboration in crystallographic studies. I thankfully remember Sri. K.V. Chary, scientist, corrosion division and Ms. Jayaprabha for their consent and help in carrying out the electrochemical studies at CECRI, Karaikudy. I am immensely grateful to Prof. M.V. Rajasekharan, School of Chemistry, Central University of Hyderabad, for the ESR simulation package and the help offered thereafter at various junctures that added flavour to my work. I am happy to acknowledge the services of RSICs of CDRI Lucknow, IIT Bombay, and SIF, IISc., SICART, Gujarat for the help in sample analyses.

I owe greatly to CSIR for the award of Junior and Senior Research Fellowship without which research here would have been a misery rather than a mystery.

Above all my praises are due to The Almighty, JESUS CHRIST without the grace of whom the whole episode would have had reduced to nothing.

Rohit

PREFACE

From the very child hood the 'chemistry of color' had always fascinated me as I was playing with those 'fascinating small pieces of varied colors'. But as I grew up and science had made its humble introduction into my little mind my views began to change, but it only strengthened my quest for delving into this mystery of nature and of course with a plethora of the rest. The ubiquitous color of green found in nature and the mystery behind it, the brilliant pink of the disinfecting agent potassium permanganate, the fascinating brilliant blue of copper sulfate used in the preparation of Bordeaux Mixture- a common fungicide, all had been a source of intuitive hunger for me. But the chemistry of transition metal complexes caught me for ransom then that of dyes and pigments, may be because a plethora of its other importance than that of simple color. The importance of transition metal complexes has been wide and varied as catalysts in industry, reagents in spectroscopic determination of trace metals, and as important drugs against potential deceases. Metal complexes serve as effective homogeneous catalysts in the industrial preparation of acetic acid, manufacture of formaldehyde etc. Their importance as catalysts lies with their ability to vary their oxidation state and valance with respect to coordination during the process. In addition metal complexes also offer as effective catalysts for stereo selective reactions such as olefin epoxidation and Diels-Alder reactions. Transition metal complexes have potential use in biology and medicine. It has also been found that metal complexes are used as useful drugs against several deceases. One such example is that of *cis*-Platin used as a drug against common cancer. It is also known that metal complexes of drugs sometimes show enhanced biological activities by virtue of coordination to metal. The thesis is only an introduction to our attempts to assess the activity of a few compounds of our interest. The compounds are basically metal complexes of copper, oxovanadium, zinc, manganese, cobalt and dioxouranium. In majority of the cases the primary ligand was ONS donor and a bidentate heterocyclic base. We have also made attempts to elucidate the structure of the compounds prepared by using various spectral techniques and also to study the red-ox behavior. The following is a brief summary of the contents:

CHAPTER 1: Carry a brief introduction into the field of study and an extensive survey of the related literature.

CHAPTER 2: Deals with synthesis and Characterization of thiosemicarbazones and their copper(II) complexes.

CHAPTER 3: Deals with synthesis and spectral characterization of oxovanadium(IV) complexes.

CHAPTER 4: Deals with synthesis, spectral characterization and biological studies of zinc(II) complexes.

CHAPTER 5: Deals with synthesis and spectral characterization of cobalt(III) complexes.

CHAPTER 6: Deals with synthesis and spectral characterization of dioxouranium(VI) complexes.

CHAPTER 7: Deals with synthesis and spectral characterization of manganese(IV) complexes.

CONTENTS

Chapter 1	**Thiosemicarbazones And Their Metal Complexes- A Brief Introduction**	1
1.1	Introduction	1
1.2	Structure, Bonding And Stereochemistry	2
1.3	Structural Characterization Techniques	4
1.3.1	Magnetic Measurements	4
1.3.2	Electronic Spectroscopy	5
1.3.3	Infrared Spectroscopy	6
1.3.4	EPR Spectroscopy	6
1.3.5	X-Ray Crystallography	6
1.3.6	Cyclic Voltammetry	6
1.4	Biological Significance	7
1.5	Present Trends	9
1.6	Objective And Scope of The Work	10
1.7	References	12
Chapter 2a.	**Synthesis And Characterization of Thiosemicarbazones**	16
2a.1	Introduction	16
2a.2	Experimental	16
2a.2.1	Synthesis	16
2a.3.1.	Synthesis of Thiosemicarbazones	17
2a.3.2	Spectral Characterizations	21
2a.3.2.1.	Infrared And NMR Spectroscopy	21
2a.3.2.2	Electronic Spectroscopy	22
	References	25
Chapter 2b	**Structural, Spectroscopic, Biological And Electrochemical Studies of Copper(II) Complexes**	26
2b.1	Introduction	26
2b.2	Experimental	27
2b.2.1.	Materials And Methods	27
2b.2.2.	Physical Measurements	27
2b.2.3	Preparation of The Complexes	27
2b.2.4	Crystal Structure Determination of Complex	28
2b.3	Results And Discussion	28
2b.3.1	Preparation of Complexes	28
2b.3.2	X-Ray Diffraction Studies	29
2b.3.3.	Electronic And IR Spectra	34
2b.3.4	EPR Spectra	34
2b.3.5	Cyclic Voltammetry	37
2b.3.6	Biological Activity	37
	References	46

Chapter 3	**Synthesis, Spectral Characterisation And Electrochemical Studies of Oxovanadyl (IV) Complexes**	48
3.1	Introduction	48
3.2	Experimental	48
3.2.1.	Materials And Methods	48
3.2.2.	Physical Measurements	49
3.2.3	Preparation of The Complexes	49
3.3.	Results And Discussion	50
3.3.1.	Preparation of Compounds	50
3.3.2.	IR And Electronic Spectra	50
3.3.3.	EPR Spectra	53
3.3.4	Cyclic Voltammetry	55
	References	61
Chapter 4	**Spectral And Biological Studies of Zinc(II) Complexes**	62
4.1	Introduction	62
4.2	Experimental	62
4.2.1	Materials	62
4.2.2	Preparation of The Complexes	63
4.2.3	Physical Measurements	64
4.3	Results And Discussion	64
4.3.1	Preparation of The Complexes	64
4.3.2	FAB Spectra	65
4.3.3	IR Spectra	65
4.3.4	NMR Spectra	65
4.3.5	Biological Studies	67
	References	70
Chapter 5	**Synthesis And Spectral Studies of Cobalt(III) Complexes**	71
5.1	Introduction	71
5.2	Experimental	71
5.2.1.	Materials	71
5.2.2.	Preparation of Complexes	71
5.2.3.	Physical Measurements	73
5.3.	Results And Discussion	73
5.3.1.	Preparation of Complexes	73
5.3.2.	Electronic And IR Spectra	74
5.3.3	^{1}H-NMR Spectra	75
	References	79
Chapter 6	**Synthesis And Spectral Studies of Some Dioxouranium(VI) Complexes**	80
6.1	Introduction	80
6.2.	Experimental	80
6.2.1.	Materials	80
6.2.2.	Preparation of The Complexes	80
6.2.3.	Physical Measurements	81
6.3.	Results And Discussion	81
6.3.1	Preparation of The Complexes	81
6.3.2.	IR Spectra	82
6.3.3.	Electronic Spectra	82
6.3.4.	^{1}H-NMR Spectra	83
	References	87

Chapter 7	**Spectral, Magnetic And Cyclic Voltammetric Studies of Manganese(IV) Complexes**	88
7.1.	Introduction	88
7.2.	Experimental	88
7.2.1.	Materials And Methods	88
7.2.2.	Physical Measurements	88
7.2.3.	Preparation of The Complexes	88
7.3.	Results And Discussion	89
7.3.1.	Preparation of The Compounds	89
7.3.2.	Electronic Spectra	89
7.3.3.	IR Spectra	90
7.3.4.	EPR Spectra	90
7.3.5.	Cyclic Voltammetry	91
7.4.	References	94
	Summary And Conclusion	95

CHAPTER 1

THIOSEMICARBAZONES AND THEIR METAL COMPLEXES A BRIEF INTRODUCTION

1.1. INTRODUCTION

Thiosemicarbazones (TSCs) have attracted attention as potential drugs in the early years of twentieth century. They were found to be effective against a variety of diseases. There are scores of reports regarding the biological activity of this class of compounds as potential antitumour [1], antiviral [2], antimalarial [3], antibacterial [4], and antifungal [5] agents.

The TSCs are having a general formula **1.** When TSCs have substituents at the thioamide nitrogen (^{4}N of TSC moiety) they can be represented by the formula **2.**

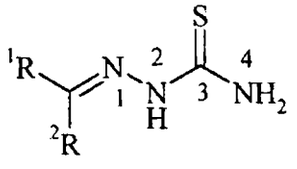

1

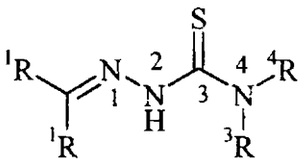

2

The ^{1}R is generally an alkyl or aryl group and ^{2}R is hydrogen, methyl, higher aliphatic or aromatic groups. In the formula **2,** the ^{4}R and ^{3}R can be the same aliphatic or aromatic group or both can be a part of a cyclic system. Intensive research initiated in the first half of the twentieth century has zeroed down some selected type of TSC systems that are found to have better biological activity. Most often the ^{1}R group can be an aromatic ring, having some active functional group bearing on it or by themselves being some heterocyclic aromatic systems.

The general method of preparation of this class of compounds involves condensation of a ketone or an aldehyde with the TSC moiety or with that of a ^{4}N substituted one. Depending upon the nature of the ketone or aldehyde the nature of resulting thiosemicarbazone may vary.

The efforts to evaluate the biological activity of TSCs involve the following strategy:

a) Replacement of sulfur atom of the thiocarbonyl group by oxygen, selenium, imine or oxime.
b) Modification of sulfur center by alkylation
c) Changing the TSC moiety's point of attachment to the heterocyclic ring.
d) Substitution on the terminal ^{4}N position.
e) Variation in the nature of condensing aldehyde or ketone

Extensive research has been carried out on TSC of heterocyclic ketones and aldehydes especially the 2-acetylpyridine and 2-formylpyridine TSCs [6] that are reported to have considerable biological activity. The ^{4}N position can also be a part of a ring system. The ^{4}N position can also be substituted by heterocyclic aromatic groups or groups that can offer an additional binding site. The importance of such heterocyclic

compounds in the TSC moiety is that they can act as a point of attachment which is an essential factor in deciding the biological and other properties of these compounds.

The mechanism of action of these compounds had also been a subject of intensive research, which is still progressing. Their action is proposed to be by inhibiting the ribonucleotide reductase (RDR), a key enzyme in the synthesis of DNA precursors [7]. Their non-heme iron subunit was inactivated by TSC, which is attributed to their chelating ability [8]. It has also been found that the iron complexes are more active in cell destructions than uncomplexed TSC [9]. These observations triggered an era of intensive scientific research in the field of TSCs. Many attempts were made by altering the structure of the TSC by changing the oxygen and sulfur as donor atoms moiety, by changing the condensing ketone or aldehyde, modifying sulfur center by alkylation, substitution at the ^{4}N position etc. Attempts were also made to solve the problem of solubility of thiosemicarbazones in water, which is important in the medical administration. This is achieved by incorporating ionic or polar groups into the TSC moiety [10].

Metal complexes of TSCs have attracted attention as improved drugs because of the following advantages:

1. The long-term side effects of therapeutic agents can be avoided since metal complexes could break down and the metal ion may interact with the organism.
2. Metal complexes may act as a vehicle for the activation of ligand, which is the principal cytotoxic agent.
3. The complexation with metal ion may lead to reduction of drug resistance by several orders of magnitude
4. A large number of such complexes involve biologically essential elements such as copper, iron and zinc.

1.2. STRUCTURE, BONDING AND STEREOCHEMISTRY

The TSCs generally exist in the thione form in the solid state but in solution it would tend to exist as an equilibrium mixture of thiol and thione forms as shown below.

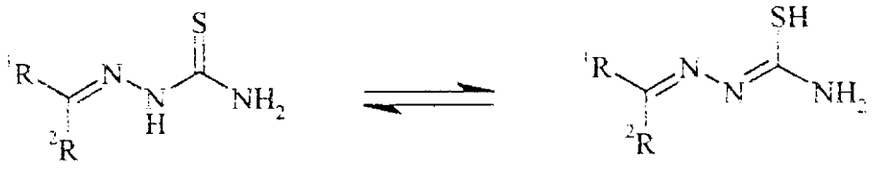

Thione Thiol

The previously mentioned strategies to vary the structural features of the TSCs could in fact bring about changes in the bonding and stereochemistry of the compound, which in turn may decide the mechanism of action of the compound in biological systems. It is expected that the TSC may generally exist in the *E* form (*trans*) but in such situation the compound may act as a unidentate ligand, by bonding through sulfur only [11]. In case the sulfur center is substituted, the bonding may occur through the hydrazine nitrogen and the amide nitrogen [12].

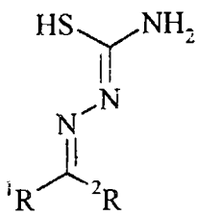

Z (cis)

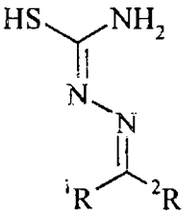

E (trans)

But the studies have shown that the stereochemistry of the ligand is much decided by steric effects of the various substituents in the TSC moiety [13]. It is found that in most cases the compound is in the Z-form while coordinating to the metal ions. This phenomenon is assumed to be due to the "chelate effect" - increased stability due to better electron delocalisation in a chelated ring system- resulting from the coordination with the metal center.

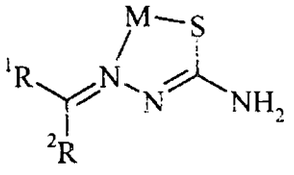

Chelate effect

Generally, the coordination occurs through the thiol/thione sulfur and the hydrazine nitrogen. When additional binding sites are available adjacent to the SN donor system the ligand was found to act as tridentate species. In most of the reported cases the third coordinating species will be in the aldehydic or ketonic moiety [14]. The availability of the third coordinating site brings so many other options when it comes to complexation. Some of them could lead to the formation of polymeric complexes [15] or it could change the oxidation state of the metal or could bring changes in the coordination environment of the metal ion. These changes could in turn affect the biological properties of the compound. The alkylation of the thiocarbonyl sulfur induces a complexation through terminal amido group and hence accounts for the mono acidic character of the ligand [16]. Sometimes such ligands condense with a second aldehyde or ketone to yield quadridentate ligands.

The stereochemistry adopted by the TSC ligands with the transition metal ion depends essentially on the presence of additional coordination sites in the ligand moiety and the charge on the ligand, which in turn is influenced by the thiol-thione equilibrium in the reaction medium. The thiol-thione equilibrium and the nature of complexation depend on the pH of the medium/solvent(s) used for reaction. Generally, the TSCs act as a neutral bidentate ligands, leading to octahedral and square planar geometries as found common among their metal complexes. But some 5-coordinate complexes are also formed by 2-acetylpyridine TSC derivatives that show increased biological activity as antitumour, antimalarial agents [17].

The oxidation state of the metal ion determines the degree of softness and hardness and hence plays an important role in predicting the stability of the complexes that are formed with the TSC ligands. Some d^8 and d^{10} ions exhibit higher stability with sulfur donor ligands due to the formation of strong bonds and $d_\pi - d_\pi$ bonds by donation of a pair of electron to the ligands [18].

It has been established that the arrangement of the hydrogen in the TSC molecule is nearly planar [19] and the sulfur atom and the hydrazinic NH_2 group are trans with respect to the C-N bond. But when an additional coordination site is available the sulfur atom tends to form a weak bond with the adjacent or with the same metal ion [20] leading to multi nuclear species.

The *E* and *Z* forms of the 2-formylpyridine TSC were isolated and were identified [21], based on the difference in the in the δ values of the respective forms using NMR spectroscopy. The *E* isomer of 2-acetylpyridine ^{4}N-methyl TSC was found to be stable [22]. However for a bulky group at the ^{4}N position of the TSC such as azabicyclononyl group a third isomer can also be observed- a bifurcated E-hydrogen-bonded ring isomer.

There are some reports on MLX type complexes. In addition, reports on the mixed ligand complexes of cobalt(II) and nickel(II), 5-coordinate complexes and bimetallic compounds have also appeared. The iron complexes of 2-acetylpyridine and 2-formylpyridine ^{4}N substituted TSCs [23] are found to have a distorted octahedral geometry with iron(III) metal ions coordinated by two deprotonated thiosemicarbazones so that each ligand is essentially planar and azomethine nitrogens are *trans* to each other. The iron(III) complexes of ^{4}N-phenyl substituted derivatives of 2-acetylpyridine thiosemicarbazone was found to form complexes of the formula $[Fe(HL)A_2]$ where A= Cl, NCS, NO_3 etc [17]. Most of the species have rhombic spectra indicating distorted square pyramid geometry [24]. Pyruvaldehyde, pyruvic acid, pyridoxal TSCs of copper and nickel are of interest in investigating their structural aspects by various spectral techniques [25].

1.3 STRUCTURAL CHARACTERIZATION TECHNIQUES

Various techniques are used to elucidate the bonding structure and stereochemistry of the ligands and the complexes prepared. While the ligands are characterized by usual methods such as elemental analysis, IR, UV-visible and NMR spectral techniques, it differs for complexes depending on the nature of the ligands and the metal ions involved. Ligands on complexation with some metal ions having paired or unpaired electrons give diamagnetic or paramagnetic complexes respectively. Some of the common physicochemical methods adopted by inorganic chemists are discussed below.

1.3.1 Magnetic measurements

In a magnetic field, the paramagnetic compounds will be attracted while the diamagnetic compounds repelled. In paramagnetic complexes, often the magnetic moment gives the spin only value corresponding to the number of unpaired electron. The variation from the spin only value is attributed to the orbital contribution and it

varies with the nature of coordination and consequent delocalisation. In some cases two magnetic centers may be coupled together and may result in extraordinary increase or decrease in the magnetic moment of the complex. For example, a mononuclear complex of copper of the formula [CuLX] where Cu is in the +2 oxidation state, the complex is expected to have magnetic moment of 1.73 BM -corresponding to d^9 configuration, but in case of $[Cu(OAc)_2]_2$ the value is lower than 1.73 BM. This is explained on the basis of the assumption that the individual magnetic moments are aligned in opposite directions so that they cancel each other to some extent or can be ascribed as due to antiferromagnetic coupling. Thus the value of magnetic moment of a complex would give valuable insights into its constitution and structure. In some cases the variation in the magnetic moment can be explained on the assumption that the compound may be an equilibrium mixture of tetrahedral and square planar geometries- the number of unpaired electrons differ in either geometries and hence the magnetic moment. The magnetic susceptibility measurements thus help to predict the oxidation state of the metal ion to a limited extent and to establish the possible geometry of the compound.

The most widely adopted method for determining the magnetic moment of a complex is by Gouy method in which the weight difference experienced by a given amount of a substance in the presence and absence is measured. This is compared with that of a standard substance and magnetic moment is determined with the help of suitable equations. Faraday Balance and Vibration Susceptibility Magnetometer are the other instruments used for the magnetic susceptibility measurements [26].

1.3.2 Electronic spectroscopy

Electronic spectroscopy is an important and valuable tool for most chemists to draw important information about the structural aspects of the complexes. The ligands, which are mainly organic compounds, have absorption in the ultraviolet region -hence do have bands in the region of the 200 to 350 nm of the electromagnetic spectrum- and in some cases these bands extends over to higher wavelength region due to conjugation. But upon complexation with transition metal ions, due to interaction with the metal ion there will be an interesting change in the electronic properties of the system. New features or bands in the visible region due to d-d absorption and charge transfer spectra from metal to ligand (M→L) or ligand to metal (L→M) can be observed and this data can be processed to obtain information regarding the structure and geometry of the compounds [27]. This technique along with other spectral techniques viz., EPR serves to find out the structural features and to calculate the bonding parameters such (α^2, β^2, γ^2, $K_{\parallel}$, $K_{\perp}$ etc.) [28, 29a,b] and Racah Parameters (B and C) [29c].

The electronic spectroscopy is also widely used to explore the change in the structural features with change in the pH of the medium. The electronic and structural features of the complexes are widely utilized to investigate the kinetics and mechanisms of the reactions involving transition metal complexes [30a,b]. The kinetics of 4-nitrophenylacetate cleavages, by oxime in the presence of Zn^{2+} ions was investigated [31].

1.3.3 Infrared Spectroscopy

The IR spectroscopy is the widely used as a characterization technique for metal complexes. The basic theory involved is that the stretching modes of the ligands changes upon complexation due to weakening/strengthening of the bonds involved in the bond formation resulting in subsequent change in the position of the bands appearing in the IR spectrum. The changes in the structural features of the ligands are observed as changes in bands observed, mainly in the fingerprint region i.e., in the 1500 - 750 cm^{-1}. Nakamoto discusses at length the characterization of metal complexes with the help of IR spectroscopy [32]. The bands due to the metal ligand bonds are mainly observed in the far IR region i.e., 50 - 500 cm^{-1}.

1.3.4 EPR spectroscopy

For complexes those are paramagnetic, in addition to the elemental analysis, IR, and electronic spectroscopic techniques, Electron Paramagnetic Resonance (EPR) spectroscopy acts as an effective and valuable tool to explore the structural features and bonding characteristics of metal complexes. The advances in the ESR spectroscopy have benefited the inorganic chemists with the help of high field and high-resolution spectrometers that helps to resolve the $g_{\parallel}$ and $g_{\perp}$ features of the paramagnetic species. The information obtainable from a low temperature spectrum of diamagneticaly diluted paramagnetic species provides important clues to structural traits and bonding properties of the complexs [33]. The single crystal EPR spectrum measurements are also widely employed to derive more information about the geometry of the paramagnetic species formed [34]. Hathaway had extensively surveyed the studies on complexes by using EPR spectroscopy [29b]. Various simulation packages are extensively used to simulate the experimental spectrum and hence help to establish the absolute geometry and accurate bonding and structural characteristics of the complexes [35]. However, for diamagnetic complexes, NMR spectroscopy still remains as a valuable tool for establishing the structural characterizations.

1.3.5 X-ray crystallography

The diffraction/scattering of X-ray radiations by array of atoms in a single crystal of a compound is exploited to establish the structure and geometry of the complexes. At present this versatile techniques is valued as the final word by many chemists for establishing the accurate structure of the complex compounds.

1.3.6 Cyclic Voltammetry

Cyclic voltammetry is widely used to study the red-ox behavior of the coordinated complexes. It gives an insight into the stability of the compound under investigation against electrolytic oxidation and reduction in the solution. In this technique, the potential of a small stationary working electrode is changed linearly with the time starting from a potential where no electrode reaction occurs and moving to potentials where reduction or oxidation of a solute (material being studied) occurs. After traversing the potential region in which one or more electrode reaction takes place, the direction of the linear sweep is reversed and the electrode reactions of the intermediates and products formed during the forward scan, often can be detected. The technique can be carried out using a suitable reference, working and counter electrodes, the selection of

which can be made depending on the nature of the compound and the solvent used, in the presence of a supporting electrolyte [36a]. The supporting electrolyte is usually added to repress the migration of charged reactants and products.

Having knowledge of the species involved and an idea about the redox properties, one can select the range of voltages, and the variation in voltammogram can be recorded at different sweep rates. The peaks in the forward and reverse sweeps can be interpreted to assess the stability of the species. Depending on the nature of the voltammogram obtained they may be termed as reversible ($i_{pa}=i_{pc}$), quasi-reversible ($i_{pa}>i_{pc}$) and irreversible process. If some chemical reaction occurs the return peak of the cyclic voltammogram will be reduced in magnitude, and it will be completely absent if the reaction half-life is much less than the scan duration [36b]. The cyclic voltammetric techniques can also be utilized, coupled with electronic spectroscopy, to obtain information about the presence of a new species formed during the oxidation-reduction process and the related stereo chemical and structural changes [37].

1.4 BIOLOGICAL SIGNIFICANCE

Biological activity or therapeutic ability of any compound depends on the minimum amount by which the chemical or the substance is required to inhibit the growth or to kill the microorganism that causes the disease, along with a minimum cytotoxicity –the potential to act as a toxin that may generate undesirable symptoms that are harmful to health of a living organism- and hence decides the drug value of the same. They do so mainly by acting upon the reproductive chain of the causative microorganism. But the mode of drug action differs from one to the other and also on the nature of the microorganism. For example, the heterocyclic TSCs exercise their therapeutic property by inhibiting the ribonucleotide reductase a key enzyme in the synthesis of DNA precursors [38]. The non-heme iron subunit of the enzyme has been shown to be inhibited /inactivated by the TSC [8]. Their ability to provide such inhibitory action is thought to be due to the coordination of the iron in their NNS tridentate ligating system either by a pre-formed iron complex or by the free ligand complexing with the iron charged enzyme [39]. The studies in iron and copper complexes indicate that they are active in cell destruction and in the inhibition of DNA synthesis than the uncomplexed TSCs [9].

The compound, 5-hydroxy-2-formyl TSC has been shown to cause lesions in DNA [40], which speculate the possibility of second site of action in addition to inhibition of ribonucleotide reductase. Certain substituted benzaldehyde and heterocyclic TSC possess antitubercular [41a,b,c] and antileprotic property [42a,b], the most potent being p-acetamido benzaldehyde TSC and are used in combination with other drugs so as to minimize the side effects such as a hemolytic anaemia, cerebral endema, hepatic dysfunction etc. [43a,b]. Derivatives of 2-acetylpyridine TSCs are found to act as antileprotic agents [44] because of their better chelating ability and are found to reduce toxicity on introduction of substituents on C-6 position of the heterocyclic ring or on substitution of thiocarbonyl sulfur by selenium [45a,b]. The presence of N-H group is also proposed to be essential, as it is assumed to be involved in the crucial radical formation step of the overall mechanism of ribonucleotide diphosphate reductase [46].

The heterocyclic TSCs are found to be active against *Asperigilus Niger* and *Chaotomium Globsum* in concentration of 10 μg/ml [47]. On replacing the aldehyde or the

ketonic moiety on the TSC by various heterocycles such as pyridine, isatin, benzene, thiophene, quinoline etc they are found to be more active against vaccinia-induced encephalitis [48a,b]. But the TSC moiety was found to be more important for viral activity. 2-acetylpyridine ^{4}N-methyl and ^{4}N-ethyl TSC are reported to be effective against smallpox virus [49a,b]. The isatin TSC has shown less activity against herpes simplex virus (HSV), however 2-heterocyclic TSC derivatives were found to be active against both HSV1 and HSV2 (Herpes Simplex Virus) types [50]. Some TSCs inhibit the *in vivo* replication of the virus to a greater extent than they inhibit the cellular DNA or protein synthesis. The substituted 2-acetylpyridine TSC inhibit the viral enzyme HSV reductase significantly and preferentially and without affecting the cellular enzyme [51]. 2-acetylpyridine ^{4}N-dibutyl TSCs inhibited all the four types of polioviruses found by blocking the viral RNA synthesis [52]. Ttriazine indole derivative of isatin was effective against rhinoviruses [53]. Some of the metal complexes inhibit the RNA dependant DNA polymerases and the transforming ability of Rous Sarcoma Virus (RSV) [54]. The most active compound being the 1:1 copper complex of 2-formylpyridine TSC [55].

2-acetylpyridine TSC and their ^{4}N-cyclic and phenyl substituted derivatives of TSCs are found to be more active against *Plasmodium Berghei*, the causative malarial microorganism in mice [56]. Similarly, the 2-formylpyridine TSC inhibited the adenosine uptake in rodents infected with malaria caused by *Plasmodium Berghei* [57]. This indicates that the interaction with adenosine receptor is an additional mode of action beside chelation. The TSCs of 3-formyl and 3-acetyl-B-carboline effectively inhibit the promastigate form of *Leishmania donavani* [58].

Some hydroxy derivative of 2-formyl TSC was found to be good anticancer drugs having activity lying in the range of glyoxal TSCs [59a, b]. It has also been established that the chelating ability of the NNS TSC is an essential criteria for antileaprotic activity [60a, b]. The biological activity of the heterocyclic TSC stems from the fact that they inhibit the biosynthesis of DNA in mammalian cells [61]. This is accomplished by interfering with RDR, an obligatory enzyme for the biosynthesis of DNA [7]. The presence of substituents at the C-6 position of 2-acetylpyridine–3-azabicyclononyl TSCs actually decreases the inhibitory activity of the compound, however it increases on introducing a *m*-amino phenyl group at the pyridine moiety due to increase in lyophobic interaction with the enzyme's inhibitory binding sites [62]. However, following chelation with the metal ion such as copper and iron, TSCs are found to show enhanced inhibitory activity.

The extreme insolubility of most TSCs in water causes difficulty in their oral administration. The efforts to overcome this limitation by introducing hydrophilic groups such as NH_2 or OH in the heterocyclic ring system with the ultimate aim of obtaining a soluble acid or sodium salt were met with little success [10]. Therefore, since the medicinal activity of TSC may in part related to their chelating ability, metal complexes may prove to be useful forms of TSCs as they effectively modify their biological activity. From further studies it is known that structural alterations hindering the TSCs ability to function as a chelating agent with transition metal ions tend to diminish or destroy the biological activity.

Copper(II) and iron(III) complexes of 2-formylpyridine TSC were found to be better inhibitors of DNA synthesis than their TSCs without apparent cytotoxicity [63]. Both of them prevent successful cell transplantation [64]. Methyl substitution in the fifth

position of the heterocyclic ring also makes the metal complexes potent agents along with zinc complexes that are active against the *Asperigillus fumigatus* - a wild variety of fungus of higher drug resistance [65].

The iron complexes of quinoline and derivatives of quinoline TSCs were found to be six times more active inhibitors of partially purified ribonucleotide reductase than the uncomplexed TSC [63]. The nuclease activity of the copper complexes TSCs derived from hetero aromatic compounds, have also been investigated [66]. The mechanism of action was assumed to be that the TSC remove iron from ferritin to form iron(III) complex, these are rapidly reduced by the hemoglobin and are then slowly re oxidized by oxygen in aqueous solution or plasma [67]. The iron complex however is bound to the enzyme leading to the inhibition of ribonucleotide diphosphate reductase. Besides *cis*-platin derivatives, the complexes of heterocyclic TSCs could constitute the second largest group of anticancer drugs.

The copper(II) complexes along with iron(III) complexes are effective inhibitors of DNA synthesis at much lower concentrations than free TSCs without apparent cytotoxicity [68]. The mechanism of action was proposed to involve the accumulation of CuL^+ rapidly in the cells [64] where it blocked the G/S interface of the cell cycle, which is consistent with the ribonucleotide reductase being affected [9]. It is argued that the interaction of CuL^+ with the thiols may promote generation of toxic oxygen species that might be responsible for cellular damage [69].

Ruthenium(II) and ruthenium(III) complexes of 2-formylpyridine TSC were found to be active against *E. Coli.* [70], and that of oxovanadium also shows significant inhibitory activity against some of the bacterial and fungal cultures [71]. The dioxomolybdenum(VI) complexes of heterocyclic thiosemicarbazones are active against some familiar fungal cultures [72]. There are reviews on the TSC complexes of cobalt(II), cobalt(III) and nickel(II) [73].

1.5. PRESENT TRENDS

The TSC chemistry is not merely been confined to the field of biological activity and medicinal importance but there is a spurt in the research involving a lot of complexes of main group metals due to their ability to form complexes of a variety of interesting structures. The complexes of germanium, organo metallic complexes, such as organotin [74] and organomercury [75] complexes involving TSCs are found to offer a rich source of gathering structural information due to their peculiar structural features and variety of spectroscopic techniques that can be employed for their characterization. Attempts are being made by Lobana *et al* to correlate the energy barrier to rotation of the amino group with the bonding parameters of the thioamide group in phenyl mercuric complexes of thiosemicarbazones [76].

Though the most widely investigated complexes are that of copper – due to their biological activity catalytic and insulin mimetic property the studies on oxovanadium, iron, cobalt, nickel and manganese offer to follow. There have been reports on copper complexes effecting catalysis of addition of alcohols to ketenes [77] and assisting the ring closure reaction of 1,2- bisketenes. Spectroscopically also copper and oxovanadium complexes has much to offer for an enthusiastic researcher. Complexes of titanium, tungsten and molybdenum are also been explored in depth. The recent research work on

TSCs are much more centered on platinum and palladium [78a,b], Ruthenium [79] and osmium [80] complexes the first being biologically important and the later ones for being known as good homogeneous catalysts. There are reports of trimeric nickel complexes of TSCs functioning as effective homogeneous catalysts for the alcoholysis of silanes giving silyl ethers [81] and in the reduction of imines into primary or secondary amines [82].

There are reports of supramolecular analogs of cyclohexane –self assembled systems of ferrocene containing TSC complexes of zinc and nickel [83] and of the structural dependence on d_{π}-p_{π} interactions of some nickel TSC complexes [84]. Recently the TSC complexes of elements of lanthanide series have also gained interest and their interaction in solution is a matter of further and on going research [85]. The transition metal complexes of vitaminK_3-TSCs are also been investigated for their structural and anti bacterial activity [86]. Some electrochemically synthesized binuclear zinc complexes of phenyl glyoxal derivative of TSC [87] and that of some transition metal complexes of isatin TSC [88] are also been recently reported. There are reports of redox active copper complexes of TSCs that are useful for imaging hypoxic tissues [89]. A recent report by Padhye *et al* deals with the antitumour activity of copper complex of 10-deacetylbaccatin TSC [90]. Ferrari *et al* have reported the versatile chelating behavior of some TSCs with respect to their coordination to zinc and cobalt metal ions [91]. A recent report by Ebenso *et al* puts forward TSCs as a promising group of compounds having corrosion inhibition properties [92]. Besides there also studies on electrochemical and positron annihilation studies of TSCs [93]. Of late, the copper(I) chemistry of TSC complexes have also appeared [94]. Quite recently reports have appeared on novel kind of photochromic TSC compounds [95]. Kovala-Demertzi *et al* reports of a novel kind of trinuclear palladium(II) complex of substituted 2-hydroxyacetophenone TSCs [96]. Molecular rectangles and squares of copper and nickel complexes of TSCs are also been appeared recently [97]. Researchers have also not left out Gold in their attempt to study their interaction with TSCs [98]. The catalytic property of polystyrene supported transition metal complexes of TSCs are been reported by Sreekumar *et al* [99]. The induction of apoptosis by cycloplatinated complexes of some TSCs in *cis*-DDP resistant cells is also been reported [100]. The contribution to the filed of analytical chemistry also is not meager as revealed by the recent reports [101]. Ranford *et al* have reported TSC copper complexes as anti cancer drug analogues [102]. Structural studies of copper complexes of open chain and macro cyclic TSCs [103] and also of cyclometallated platinum(II) [104] have also been recently appeared. Souza *et al* have reported on the cytotoxic activity and DNA binding of palladium(II) benzyl bis(TSC)[105].

1.6 OBJECTIVE AND SCOPE OF THE WORK

Reports of the structural and biological activities of some substituted salicylaldehyde TSCs and their copper(II) [106] and nickel(II) [107] complexes have recently appeared. Not only these compounds showed significant biological activity but also found to possess interesting structural and stereo chemical properties upon complexation with metal ions.

In the light of the above discussion we have decided to prepare some ternary base adducts of N-protected TSCs of 2-hydroxyacetophenone.

We undertook the present work with the following objectives.

To investigate

i) The effect of ^{4}N substituents in the thiosemicarbazone moiety and their biological activity.

ii) The effect of incorporation of bases into the coordination sphere of various metal ions, such as copper, oxovanadium, cobalt, zinc, manganese and dioxouranium in their structure and biological properties.

iii) The changes in biological activity upon complexation with metal ions.

iv) The red-ox behavior of coordinated metal ions of our interest.

The investigations are done to bring about an overall understanding of the structure-activity relationship and to aid the development of better and effective metal based drugs.

In this attempt we have prepared four N-protected TSC ligands of 2-hydroxyaceto- phenone, about eight ternary base adducts of copper(II), eight base adducts of oxovanadium(IV), eight base adducts of zinc(II), eight complexes of cobalt(III), five complexes of dioxouranium(VI) and three complexes of manganese(IV). The bases used were bipyridine and phenanthroline. All of them were characterized by using various spectral techniques and about sixteen of them were screened for their biological activity.

REFERENCES

1. E. J. Blanz Jr., F. A. French, *Cancer Res.*, 1968.
2. J. C. Logan, M.P.Fox, J. H. Morgan, A. M. Makohon, C. J. Pfau , *J. Gen. Virol.*, 1975, **28**, 271.
3. D. L. Klayman, J. E. Bartosevic, T. S. Griffin, C. J. Mason, J. P. Scovill, *J. Med. Chem.*, 1979, **22**, 855 and references therein
4. A. S. Dobek, D. L. Klayman, E. J. Dickson Jr., J. P. Scovill, E. C. Tramont, *Antimicrob. Agents Chemother.*, 1980, **18**, 27 and references therein
5. S. P. Mittal, S. K. Sharma, R.V. Singh, J. P. Tandon, *Curr. Sci.*, 1981, **50**, 483 and the references therein
6. A. B. DeMilo, R. E. Redfurn, A. B. Borkovec, *J. Agri. Food Chem.*, 1983, **31**, 713.; D. L. Klayman, J. P. Scovill, C. Ambros, G. E. Child, J. D. Notsch, *J. Med. Chem.*, 1984, **27**, 87; R. W. Brockman, R. W. Sidwell, G. Arnett, S. Shaddix, *Proc. Soc. Expt. Biol. Med.*, 1970, **133**, 609
7. E. C. Moore, M. S. Zedek, K. C. Agrawal, A. C. Sartorelli, *Biochemistry*, 1970, **9**, 4492
8. J. G. Cory, A. E. Fleischer, *Cancer Res.*, 1979, **39**, 4600
9. L. A. Saryan, E. Ankel, C. Krishnamurthi, W. Antholine, D. H. Petering, *Biochem. Pharmacol.*, 1981, **30**, 1595
10. K. C. Aggrawal, A. C. Sartorelli, *J. Pharm. Sci.* 1968, **57**, 1948
11. P. Domiano, G. G. Fava, M. Nardelli and P. Sagarabotto, *Acta Crystallogr.*, 1969, 25B, 343; G. D. Andreetti, G. Fava, M. Nardelli and P. Sagarabotto, *Acta Crystallogr.*, 1970, 26B, 1005
12. N. V. Gebeleu, M. D. Revenko and V. M. Leovats, *Russ. J. Inorg. Chem.*, 1977, **22**, 1009
13. L. Cogi, A. M. M. Lanfredi and A. Tiripicchio, *J. Chem. Soc., Perkin Trans.*, 1976, **2**, 1808
14. M. Mathew, G. J. Palenick and G. R. Clark, *Inorg. Chem.*, 1973, **12**, 446
15. (a) J. Jezierska, A. Jezierski, J-T. Boguslawa and A. Ozarowski, *Inorg. Chim. Acta.* 1983, **68**, 7-13. (b) N. R. Sangeetha, S. Pal, *Polyhedron*, 2000, **19**,1593
16. V. M. Leovac, N. V. Gebeleu, D. Canic, *Russ. J. Chem.*, 1982, **27**, 514
17. Y. K. Bhoon, S. Mitra, J. P. Scovill and D. L. Klayman, *Trans. Met. Chem.*, 1982, **7**, 264
18. G. Keresztury, *J. Mol. Structure.*, 1978, **46**, 12
19. H. K. Parwana, G. Singh, *Ind. J. Chem.*, 1987, **26**A, 58
20. M. D. Timken, S. R. Wilson, D. N. Hendrickson, *Inorg. Chem.*, 1985, **24**, 3450
21. I. Antonini, F. Claudia, P. Franchetti, M. Grifantini, S. Martelli, *J. Med. Chem.*, 1977, **20**, 447
22. D. X. West, J. P. Scovill, J. Silverton, A. Bavoso, *Trans. Met. Chem.*, 1986, **11**, 123
23. D. X. West, P. M. Ahrweiler, G. Ertem, J. P. Scovill, D.L. Klayman, J. L. Flippen-Anderson, R. Gilardi, C. George, L.K. Pannel, *Trans. Met. Chem.*, 1985, **10**, 264.
24. S. K. Jain, Y.K. Bhoon, B. S. Garg, *Trans. Met. Chem.*, 1986, **11**, 89
25. M. B. Ferrari, G.G. Fava, C. Pelizzi, G. Pelosi, P. Tarasconi, *Inorg. Chim. Acta.*, 1998, **269**, 297; L. J. Ackerman, P. E. Fanwick, M. A. Green, E. John, W. E. Running, J.K. Swearingen, J. W. Web, D.X. West, *Polyhedron*, 1999, **18**, 2759
26. Stephan J. Lippard, *Progress in Inorganic Chemistry*, John Wiley and Sons, **29**, 1982
27. A. B. P. Lever, *Inorganic Electronic Spectroscopy*, 2nd Edn., Elsevier, NY, 1984

28. A. H. Maki and B. R. McGarvey, *J. Chem. Phy.*, 1958, **29**, 31-38.
29. (a) B. N. Figgis, *Introduction to Ligand Fields*, Interscience, NewYork, 1966, 295; (b) B. J. Hathaway, *Structure and Bonding*, Springer Verlag, 1973, **14**, 60; (c) B.N. Figgis, *Introduction to ligand fields*, Wiley Eastern Ltd., India, 1976, p163.
30. (a) A. K. Yatsimirsky, G-T. Paola, E-T. Sigfrido, R-R. Lena, *Inorg. Chim. Acta.*, 1998, **273**, 167; (b) M. J. Sisley and R. B. Jordan, *J. Chem. Soc., Dalton Trans.*,1997, 3883
31. J. Suh and H. Han, *Bioorg. Chem.*, 1984, **12**, 177; J. Suh, M. Cheong and H. Han, *Bioorg. Chem.*, 1984,**12**, 188.
32. K. Nakamoto, *Infrared and Raman Spectra of Raman and Coordination Compounds*, 3rd edn, John Wiley and Sons, NY, 1978.
33. J. E. Wertz and J. R. Boltzon, *Electron Spin Resonance: Elementary Theory and Practical Applications*, McGraw-Hill, 1979
34. P. S. Subramanian, E. Suresh and D. Srinivas, *Inorg. Chem.*, 2000, **39**, 2053 and the references therein
35. (a) M. Pasenkiewics-Gierula, J. S. Hyde and J. R. Pilbrow, *J. Mag. Resonance*, 1983, **55**, 255. (b) D. L. Liczwek, R. L. Belford, J. S. Hyde and J. R. Pilbrow, *J. Chem. Phy.*, 1983, **87**, 2509. (c) A. Diaz, R. Pogni, R. Cao, R. Basosi, *Inorg. Chim. Acta.* 1998, **552**, 275; R. Pogni, M. C. Baratto, A. Diaz, R. Basosi, *J. Inorg. Biochem.*, 2000, **79**, 333
36. (a) M. Noel and K. I. Vasu, *Cyclic Voltammetry and the frontiers of electrochemistry*. Oxford & IBH Co., New Delhi, 1990; (b) R. S. Nicholson, I. Shain., *Anal. Chem.*, 1964, **36**, 706
37. A. Saha, P. Majumdar, S. Goswami, *J. Chem. Soc., Dalton Trans.*, 2000, 1703
38. F. A. French, E. J. Blanz Jr., Do. J. R. Amaral, D. A. French, *J. Med Chem.*, 1970, **13**, 1117
39. A. C. Sartorelli, K. C. Agrawal, A. S. Tsiftsoglou, E. C. More, *Advances in Enzyme Regulation*, 1977, **15**. 117.
40. M. Karen, W.F. Benedict, *Science*, 1972, **178**, 62
41. (a) E. Hogarth, A. Martin, M. Storey, E. Young, *Br. J. Pharmacol.*, 1949, **4**, 248; (b) R. Donovick, F. Pansy, G. Stryker, J. Bernstein, *J. Bacteriol.*, 1950, **59**, 667; (c) D. Hamre, J. Bernstein, R. Donovick, *J. Bacteriol.*, 1950, **59**, 675
42. (a) M. Hooper, M. G. Purohit, in *Prog. Med. Chem.*, ed G. P. Ellis, G. B. West, Vol 20, Elsevier, North Holland, 1983, p1. (b) R. J. W. Rees, *Int. J. Lepr.*, 1987, **55**, 11
43. (a) A. Berger, "*Medicinal Chemistry*" 3rd edn. Vol. II, Wiley-Interscience, p 429. (b) A. Miller, W. Fox, R. Tall, *Tubercule.*, 1966, **47**, 33
44. F. M. Collins, D. L. Klayman, N. E. Morrison, *J. Gen. Microbiology*, 1982, **128**, 1349
45. (a) J. K. Syndell, *Int. J. Lepr.*, 1951, **49**, 90; (b) D. L. Klayman, J. P. Scovill, C. J. Mason, J. F. Bartosevic, *Eur. J. Med. Chem.*, 1979, **14**, 317
46. K. J. Schaper, J. K. Seydel, M. Rosenfeld, J. Kazda, *Lepr. Rev.*, 1986, **57**, Suppliment **3**, 254
47. D. M. Wiles, T. Supruchunk, *J. Med. Chem.*, 1969, **12**, 526
48. (a) D. Hamre, K. Brownlee, R. Donovick, *J. Immunol.*, 1950, **67**, 305; (b) D. Hamre, J. Bertnstein,R. Donovick, *Proc. Soc. Expt. Biol. Med.*, 1953, **84**, 496
49. (a) D. Bauer, P. Sadler, Lancent, 1960, **1**, 1110; (b) D. Bauer, St. L. Vincent, C. Kempe, A. Downie, Lancent, 1963, **2**, 494
50. C. Chipman Jr., S. H. Smith, J. C. Drach, D. L. Klayman, *Antimicrob. Agents. Chemother.*, 1981, **19**, 682
51. S. R. Turk, C. Shipman Jr., J.C. Drach, *Biochem. Pharmacology*, 1986, **35**, 1539
52. G. Pearson, E. Zimmerman, *Virology*, 1969, **38**, 641

53. J. Gladych, J. Hunt, D. Jack, R. Haff, J. Boyle, R. Stewart, R. Ferlauto, *Nature* London, 1969, **221**, 226
54. W. Levinson, B. Woodson, J. Jackson, *Nat. New. Biol.*, 1971, **232**, 116
55. W. Levinson, A. Faras, B. Woodson, J. Jackson, J. M. Bishop, *Proc. Nat. Acad. Sci. USA.*, 1973, **70**, 164
56. D.L. Klayman, J.P. Scovill, J.F. Bartosevich, C.J. Mason, *J. Med. Chem.*, 1979, **22**, 1367
57. C. E. Emery, F. A. Stancato, R. E. Brown, D. A. Prichard, A. D. Wolfe, *Life Sci.*, **33**, 1285
58. R.H. Dodd, C. Ouannes, M. Robert-Gero, P. Potier, *J. Med. Chem.*, 1989, **32**, 1272
59. (a) F. A. French, E. J. Blanch Jr., *Cancer Res.*, 1966, **26**,1638; (b) F. A. French, E. J. Blanch Jr., J. Med. Chem., 1966, **9**, 585
60. (a) D. H. Petering, W. E. Antholine, L. A. Saryan In R. M. Ottenbrite, G. B. Butter (eds), *Metal Complexes as Antitumour Agents in anticancer and Interferron Agents*, Marcel Decker, NY, p 203; (b) W. K. Subczynski, W. E. Antholine, J. S. Hyde, D. H. Petering, *J. Am. Chem. Soc.*, 1987, **109**, 46
61. A. C. Sartorelli, *Biochem. Biophys. Res. Comm.*, 1967, **27**, 26
62. A. C. Sartorelli, K. C. Agarwal, E. C. Moore, *Biochem. Pharmacol.*, 1971, **20**, 3119
63. L. A. Saryan, E. Ankel, C. Krishnamurthi, D. H. Petering, H. Elford, *J. Med. Chem.*, 1979, **22**, 1218
64 W. E. Antholine, J.M. Knight, D.H. Petering, *J. Med. Chem.* 1976, **19**, 339
65. H. K. Parwana, G. Singh, P. Talwar, *Inorg. Chim. Acta.*, 1985, **108**, 87
66. K. H. Reddy, P. S. Reddy, P. R. Babu, *Trans. Met. Chem.*, 2000, **25**, 505-510
67. R. C. DeConti, B. R. Toftness, K. C. Agrawal, R. Tomchick, J. A. R. Mead, J.R. Bertino, A.C. Sartorelli, W.A. Creasy, *Cancer Res.*, 1972, **32**, 455
68. N.E. Spingarn, A.C. Sartorelli, *J. Med. Chem.*, 1977, **22**, 1314
69. W.E. Antholine, F. Taketa, *J. Inorg. Biochem.*, 1984, **20**, 69
70. S.K. Chatopadhyay, S. Ghosh, *Inorg. Chim. Acta*, 1989, **163**, 245
71. A. Maiti, A. K. Guhu, S. Ghosh, *J. Inorg. Biochem.*, 1988, **33**, 57
72. N. Kanoongo, R. Singh, J.P. Tandon, *Bull. of Chem. Soc. Japan*, 1989, **62**, 1385
73. D. X. West, S.B. Padhye and P.B. Sonaware, *Structure and Bonding*, Springer Verlag, Heidelberg, 1991, **76**, p 31-43
74. A. Saxena, J. P. Tandon, *Polyhedron*, 1984, **3**(6), 681
75. T. S. Lobana, A. Sanchez, J. S. Casas, A. Castineiras, J. Sordo, M. S. Garcia-Tasende, *Polyhedron*, 1998, **17**, 21, 3701-3709.; T. S. Lobana, A. Sanchez, J. S. Casas, J. Sordo, M. S. Garcia-Tasende *Inorg. Chim. Acta*, 1998, **267**, 169-172
76. T. S. Lobana, A. Sanchez, J. S. Casas, A. Castineiras, J. Sordo, M. S. Garcia-Tasende and E. M. Vazquez-Lopez *J. Chem. Soc., Dalton Trans.*, 1997, 4289-4299
77. Pracejus H., Samtleben R. *Z Chem.* 1972, 153; B. L. Hodous, J. C. Rouble, G.C. Fu, *J. Am. Chem. Soc.* 1999, **121**, 2637
78. (a) A. G. Quiroga, J. M. Perez, D. X. West, E. I. Monrtero, C. Alonso, N-R. Carmen *J. Inorg. Bio. Chem.*, 1999, **75**, 293. (b) D. Kovala-Demertzi, M. A. Demertzis, A. Castineiras, D. X. West *Polyhedron* 1998, **17**(21), 3739
79. M. Maji, M. Cattaerjee, S. Ghosh, S. K. Chattopadhyay, Bo-Mu Wu and T. C. W. Mak, *J. Chem. Soc., Dalton Trans.*, 1999, 135-140; M. Hussain, S. K. Chattopadhyay, S. Ghosh, *Polyhedron*, 1997, **16**, 24, 4313-4321
80. K. Manjumdar, S. M. Peng, S. Bhattacharya, *J. Chem.Soc., Dalton Trans.*, 2001, 284; A. Das, , S. M. Peng, S. Bhattacharya, *Polyhedron*, 2000, **19**(10), 1227.
81. D. E. Barber, Z. Lu, T. Richardson, R. H. Crabtree, *Inrog. Chem.*, 1992, **31**, 4709
82. A. H. Vetter, A. Berkessel, *Synthesis*, 1995, 419

83. Fang Chen-jie, Duan Chun-ying, He Cheng, Han Gang and Meng Qing-jin, *New J. Chem.*, 2000, **24**, 697
84. Liu Ze-hua, Duan Chun-ying, Li Ji-hui, Liu Yong-jiang, Mei Yu-hua and Xiao-zeng, *New J. Chem.*, 2000, **24**, 1057
85. A. A. Khan and K. Iftikhar, *Polyhedron*, 1997, **16**, 23, 4153-4161.
86. Q. Li, H. Tang, Y. Li, M. Wang, L-F. Wang, Chun-Gu Xia, *J. Inorg. Biochem.*, 2000, **78**, 167-174
87. M.L. Duran, A. Sousa, J. Romero, A. Castineiras, E. Bermejo, D. X. West, *Inorg. Chim. Acta*, 1999, **294**, 79
88. E. Labisbal, A. Sousa, A. Castineiras, , J. A. Gracia-Vazquez, J. Romero, D. X. West, *Polyhedron*, 2000, **19**(10), 1255.
89. J. L. J. Dearling, J. S. Lewis, D. W. McCarthy, M. J. Welch and P. J. Blower, *Chem. Commun.*, 1998, 2531.
90. A. Murugkar, S. Padhye, S. Guha-Roy, Ullas Wag, *Inorg. Chem. Comm.* 1999, **2**, 545
91. M. B. Ferrari, G. G. Fava, G. Pelosi, P. Tarasconi, *Polyhedron*, 2000, **19** (16-17) 1895
92. E.E. Ebenso, U.J. Ekpe, B.I. Ita, O.E. Offiong, U.J. Ibok, *Mat. Chem. Phy.*, 1999, **60**, 79.
93. J. E. J. C. Graudo, C. A. L. Filgueiras, A. Marques-Netto, A. A. Batista, *J. Braz. Chem. Soc.*, 2000, **11** (3), 237.
94. C. Argay, A. Klayman, L. Parkanyi, V. M. Leovac, I. D. Birceski, P. N. Radivojsa, *J. Coord. Chem.*, 2000, **51**(1), 9
95. X. C. Tang, D. Z. Jia, L. Kai, X. G. Zhang, X. Xi, Z. Y. Zhou, *J. Photochem. Photobiol., A. Chem.*, 2000, **134**(1-2), 23
96. D. Kovala-Demertzi, N. Kourkoumelis, M. A. Demertzis, J. R. Miller, C. S. Frampton, J. K. Swearingen, D. X. West, *Eur. J. Inorg. Chem.*, 2000, (4), 727
97. H. Cheng, C. Y. Duan, C. J. Fang, Y. J. L. Y. Liu and Q. J. Meng, *J. Chem. Soc., Dalton Trans.*, 2000, **7**, 1207
98. U. Abram, K. Ortner, R. Gust and K. Sommer, *J. Chem. Soc., Dalton Trans.*, 2000, (5), 735.
99. K. S. Chettiar, K. Sreekumar, *Polymer International*, 1999, **48**(6), 455
100. J. M. Perez, A. G. Quiroga, E. I. Montero, C. Alonso and C. Navarro-Ranninger, *J. Inorg. Biochem.*, 1999, **73**(4), 235.
101. J. Y. Qu, M. Liu and K. Z. Liu, *Analytical Letters*, 1999, **32**, 10; J. A. S. Coello, G. P. Andreu and O. B. Guerra, *Afinidad*, 1999, **56**, 165.
102. B. Moubaraki, K. S. Murray, J. D. Ranford, J. J. Vittal, X. Wang and Yan Xu, *J. Chem. Soc., Dalton Trans.*, 1999, 3573.
103. E. Franco, E. Lopez-Torres, M. A. Mendiola and M. T. Sevilla, *Polyhedron*, 2000, **19**, 441.
104. D. Vazquez- Garcia, A. Fernandez, J. J. Fernandez, M. Lopez-Torres, A. Suarez, J. M. Ortuguiera, J. M. Vila and Harry Adams, *J. Org. Met. Chem.*, 2000, **595**, 199.
105. A. I. Matesanz, J. M. Perez, P. Navarro, J. M. Moreno, E. Colacio and P. Souza, *J. Inorg. Biochem.*, 1999, **76**, 29.
106. (a) P. Bindu and M. R.P. Kurup, *Trans. Met. Chem.*, 1997, **22**, 578; (b) P. Bindu, M. R. P. Kurup and T. R. Satyakeerthy, *Polyhedron*, 1998, **18**, 321.
107. P. Bindu and M. R. P. Kurup, *Ind. J. Chem.*, 1997, **36A**, 1094.

CHAPTER 2

SYNTHESIS AND CHARACTERIZATION OF THIOSEMICARBAZONES

2a.1. INTRODUCTION

The importance of TSCs as potential bioactive agents have already been covered in the last chapter [1-9]. The use of TSC as an analytical reagent is also well established. Besides, works are still going on about the other useful characteristics of TSCs in various fields [10-12]. A recent study discusses the synthesis of heterocyclic compounds by the cyclisation of carbohydrate TSCs [13]. There are also some reports on synthesis of TSCs employing microwave.

In this chapter we discuss various methods of synthesis and techniques used for the characterization of the ligands.

2a.2. EXPERIMENTAL

2a.2.1. Synthesis

Methods:

There are several methods by which the TSCs can be synthesized.

Method 1. It involves the condensation of thiosemicarbazide with an aldehyde or a ketone.

Method 2. It involves the condensation of an aldehyde or a ketone with methyl hydrazine carbodithioate to form an intermediate. The S-methyl group of the latter compound on displacement with an amine gives the desired thiosemicarbazone. The rate of the displacement reaction depends on the basicity of the amine.

Method 3. The procedure for this method involves the condensation of an isothiocyanate with hydrazones of an aldehyde or ketone

Method 4. It is based on the one reported by Holmberg and Psilanderhielm [11] and later modified by Scovill [3]. The procedure involves the reaction of carbondisulfide and N-methyl aniline in the presence of sodium hydroxide followed by the treatment with sodiumchloroacetate. The product isolated is then treated with hydrazine hydrate leading to the formation of N-methyl-N-phenylthiosemicarbazide. This is used as precursor for the synthesis of the desired ligand. It is a single step process in which the required ketone or aldehyde and the amine that is to be transaminated into the parent TSC are treated in one pot in a suitable solvent.

Materials:

The reagent grade 2-hydroxyacetophenone (Merck), carbon disulfide (Merck), N-methyl aniline (Merck), sodiumchloroacetate (Merck) and hydrazine hydrate 98% (Glaxo –Fine Chemicals) were used as received. Cyclohexylamine (Merck), hexamethyleneimine (Fluka) and morpholine (Glaxo-Fine chemicals) were purified by distillation and kept under nitrogenous atmosphere. The solvents were purified and dried by using standard methods and procedures. Methanol was dried over fused calcium chloride and was in the presence of magnesium isopropoxide; acetonitrile was dried overnight and distilled over from activated alumina.

Synthesis of thiosemicarbazones

The TSC ligands were synthesized from N-methyl-N-phenylthiosemicarbazide.

2a.2.1.1. *Synthesis of N-phenyl-N-methylthiosemicarbazide*:

Synthesis of *N*-phenyl-*N*-methyl thiosemicarbazide involves two steps.

i) Preparation of Carboxymethyl *N*-methyl-*N*-phenyldithiocarbamate

A mixture of 12.0 mL (15.2 g, 0.20 mol) of carbon disulfide and 21.6 mL (21.2 g, 0.20 mol) of *N*-methylaniline was treated with a solution of 8.4 g of (0.21 mol) NaOH in 250 mL, was stirred at room temperature for about two hours, when a pale orange colored homogeneous solution resulted. To this solution was then added in small portions about 23.2 g (0.20 mol) of sodiumchloroacetate with stirring. It was allowed to continue for 6-7 hrs. To the resulting pale golden yellow solution was added 25mL of conc. HCl and the resulting solid was collected and dried. The yield was 39.0 g (82%). mp. 197-198°C.

ii) Preparation of *N*-methyl-*N*-phenylthiosemicarbazide (4-methyl-4-phenyl-3 thiosemicarbazide).

A solution of 17.7 g of (0.0733 mol) Carboxymethyl-*N*-methyl-*N*-phenyldithiocarbamate in 20 mL of 98% hydrazine hydrate and 10 mL of water was heated in a water bath for about 10 minutes when colorless crystals began to appear, the heating was continued for another 5 minutes, filtered washed with water, and dried under lamp. The crude product was recrystallised from a mixture of ethanol and water when colorless triclinic crystals appeared. About 10 g (81%) of the product was obtained. Mp. 125°C.

2a.2.1.2. Synthesis of 2-hydroxyacetophenone ^{4}N-cyclohexylthiosemicarbazone (H_2L^1)

A solution of 1.00 g (5.52 mmol) 4-methyl-4-phenyl-3-thiosemicarbazide in 5 mL of acetonitrile was treated with 0.664 mL (5.52 mmol) of 2-hydroxyacetophenone and 0.620 mL (5.52 mmol) of cyclohexylamine and warmed in a water bath for 20-25 minutes. The solution was kept at room temp for 15 minutes and then chilled in a freezer, when pale yellow plate like crystals of 2-hydroxyacetophenone ^{4}N-cyclohexylthiosemicarbazone separated out. The crystals were filtered and washed with cold acetonitrile followed by water and then dried *in vacuo* over P_4O_{10}. The compound was recrystallised from dry acetonitrile. mp 154°C. Yield 1.16 mg (72%). Analytical data: Elemental; Calcd for $C_{15}H_{21}N_3OS$: C, 61.82; H, 7.26; N, 14.42. Found: C, 61.75; H, 7.24;

N, 14.37. IR (KBr): 3310m(sh), 3109s, 2523m, 1620m, 1599m, 1448m, 1365m, 1219s, 1118m, 988m, 864w, 652w cm^{-1}. ^1H NMR (300 MHz, $CDCl_3$, δ(ppm) vs internal TMS): 10.89 (s, 1H, OH, phenolic); 8.74 (s, 1H, NH, hydrazide); 7.46 (d, 1H, Ar-H); 7.33, 7.28 (AB, dd, 1H, Ar-H); 6.98, 6.92 (AB, dd, 1H, Ar-H); 6.72 (d, 1H, Ar-H); 4.31 (t, 1H, NH, imine); 2.38 (s, 3H, CH_3); 1.22-2.12 (m, 11H, aliphatic).

The ^{13}C NMR spectral assignments for the compound is given in Figure. 2a.1

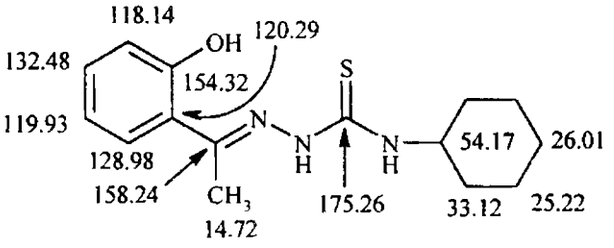

Figure. 2a.1 ^{13}C NMR spectral assignments for 2-hydroxyacetophenone ^4N-cyclohexylthiosemicarbazone (H_2L^1)

2a.2.1.3. Synthesis of 2-hydroxyacetophenone-3-hexamethyleneiminylthiosemicarbazone(H_2L^2)

A solution of 1.00 g (5.52 mmol) 4-methyl-4-phenyl-3-thiosemicarbazide in 5 mL of acetonitrile was treated with 0.664 mL (5.52 mmol) of 2-hydroxyacetophenone and 0.71 mL (5.52 mmol) of hexamethyleneimine and refluxed for about 40 minutes. The solution was allowed to cool when fine colorless needles of the compound separated out. The solution was filtered, washed with cold acetonitrile and dried *in vacuo* over P_4O_{10}. The compound was recrystallised from absolute ethanol. mp 182°C. Yield 1.28 mg (80%). Analytical data: Elemental; Calcd for $C_{15}H_{21}N_3OS$: C, 61.82; H, 7.26; N, 14.42. Found: C, 61.85; H, 7.20; N, 14.48. IR (KBr): 3470s (b), 1603sh, 1452m, 1383s, 1252s, 1163m, 1101m, 997m, 839m, 642w cm^{-1}. ^1H NMR (400 MHz, $CDCl_3$, δ(ppm) vs internal TMS): 12.75 (s, 1H, OH, phenolic); 8.36 (s, NH, hydrazide); 7.32 (d, 1H, Ar-H); 7.25 (t, 1H, Ar-H); 7.00 (d, 1H, Ar-H); 6.81 (t, 1H, Ar-H); 3.76 (s, 4H, aliphatic); 2.24 (s, 3H, CH_3); 1.79 (s, 4H, aliphatic); 1.55 (s, 4H, aliphatic).

The ^{13}C NMR spectral assignments for the compound is given in Figure. 2a.2

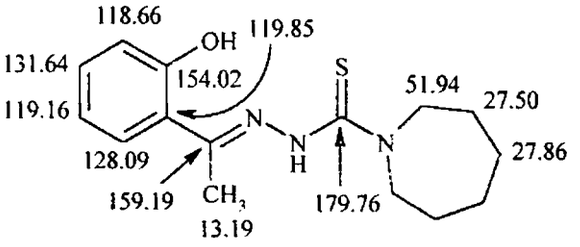

Figure. 2a.2 ^{13}C NMR spectral assignments for 2-hydroxyacetophenone-3-hexamethyleneiminyl thiosemicarbazone (H_2L^2)

2a.2.1.4. Synthesis of 2-hydroxyacetophenone-3-morpholyl thiosemicarbazone (H_2L^3)

A solution of 1.00 g (5.52 mmol) 4-methyl-4-phenyl-3-thiosemicarbazide in 10 mL of methanol was treated with 0.664 mL (5.52 mmol) of 2-hydroxyacetophenone and 0.480 mL (5.52 mmol) of morpholine and refluxed in a water bath for about an hour. The solution was allowed to cool or chilled when fine crystals of a cream colored compound separated out. The solution was filtered, washed with cold methanol and dried *in vacuo* over P_4O_{10}. The compound was recrystallised from absolute ethanol. mp 208°C. Yield 1.35 mg (87%). Analytical data: Elemental; Calcd for $C_{13}H_{17}N_3O_2S$: C, 55.89; H, 6.13; N, 15.04. Found: C, 55.91; H, 6.12; N, 15.01. IR (KBr): 3401s (b), 3385sh, 1605s, 1458m, 1374s, 1246s, 1118s(d), 1043m, 1017m, 835m, 646w cm^{-1}. ^1H NMR (400 MHz, DMSO-d_6, δ(ppm) vs internal TMS): 12.90 (s, 1H, OH, phenolic), 10.38 (s, NH, hydrazide), 7.60 (d, 1H, Ar-H), 7.28 (t, 1H, Ar-H), 6.88 (d, 2H, Ar-H), 3.91 (t, 4H, aliphatic), 3.66 (t, 4H, aliphatic), 3.35 (s, 3H, CH_3).

The ^{13}C NMR spectral assignments for the compound are given in Figure. 2a.3

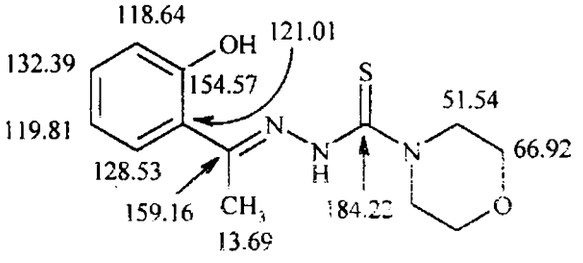

Figure. 2a.3 ^{13}C NMR spectral assignments for 2-hydroxyacetophenone-3-morpholyl thiosemicarbazone (H_2L^3)

2a.2.1.5. Synthesis of 2-hydroxyacetophenone 4-methyl-4-phenylthiosemicarbazone (H_2L^4)

A solution of 1.00 g (5.52 mmol) 4-methyl-4-phenyl-3-thiosemicarbazide in 10 mL of methanol was treated with 0.664 mL (5.52 mmol) of 2-hydroxyacetophenone and a slight excess of a base viz., cyclohexylamine and refluxed in a water bath for about for 10-15 min., when fine cubic crystals of compound started separating in the medium. The solution was allowed to cool. The solution was filtered, washed with cold methanol and dried *in vacuo* over P_4O_{10}. The compound was recrystallised from absolute ethanol. Mp 197°C. Yield 1.30 mg (78%). Analytical data: Elemental; Calcd for $C_{17}H_{17}N_3O_2S$: C, 64.19; H, 5.72; N, 14.03. Found: C, 64.20; H, 5.70; N, 13.99. IR (KBr): 3400s, 3268sh, 1601m, 1575s, 1250s, 1001 m, 791m cm^{-1}. ^1H NMR (400 MHz, $CDCl_3$, δ(ppm) vs internal TMS): 12.64 (s, 1H, OH, phenolic); 8.31 (s, NH, hydrazide); 7.56 (t, 2H, Ar-H); 7.49 (t, 1H, Ar-H); 7.34 (d, 2H, Ar-H); 7.21-7.28(m, 2H, Ar-H); 7.00 (d, 1H, Ar-H); 6.81 (t, 1H, Ar-H); 3.70 (s, 3H, CH_3, N-methyl); 1.79 (s, 3H, CH_3).

2a.2.1.4. Synthesis of 2-hydroxyacetophenone-3-morpholyl thiosemicarbazone (H_2L^3)

A solution of 1.00 g (5.52 mmol) 4-methyl-4-phenyl-3-thiosemicarbazide in 10 mL of methanol was treated with 0.664 mL (5.52 mmol) of 2-hydroxyacetophenone and 0.480 mL (5.52 mmol) of morpholine and refluxed in a water bath for about an hour. The solution was allowed to cool or chilled when fine crystals of a cream colored compound separated out. The solution was filtered, washed with cold methanol and dried *in vacuo* over P_4O_{10}. The compound was recrystallised from absolute ethanol. mp 208°C. Yield 1.35 mg (87%). Analytical data: Elemental; Calcd for $C_{13}H_{17}N_3O_2S$: C, 55.89; H, 6.13; N, 15.04. Found: C, 55.91; H, 6.12; N, 15.01. IR (KBr): 3401s (b), 3385sh, 1605s, 1458m, 1374s, 1246s, 1118s(d), 1043m, 1017m, 835m, 646w cm^{-1}. ^1H NMR (400 MHz, DMSO-d_6, δ(ppm) vs internal TMS): 12.90 (s, 1H, OH, phenolic), 10.38 (s, NH, hydrazide), 7.60 (d, 1H, Ar-H), 7.28 (t, 1H, Ar-H), 6.88 (d, 2H, Ar-H), 3.91 (t, 4H, aliphatic), 3.66 (t, 4H, aliphatic), 3.35 (s, 3H, CH_3).

The ^{13}C NMR spectral assignments for the compound are given in Figure. 2a.3

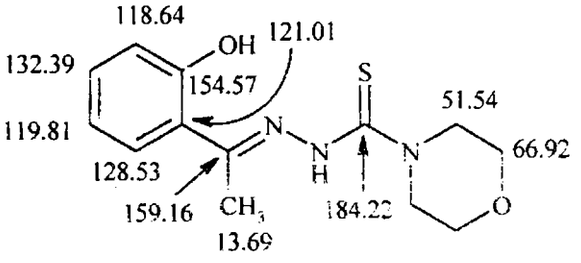

Figure. 2a.3 ^{13}C NMR spectral assignments for 2-hydroxyacetophenone-3-morpholyl thiosemicarbazone (H_2L^3)

2a.2.1.5. Synthesis of 2-hydroxyacetophenone 4-methyl-4-phenylthiosemicarbazone (H_2L^4)

A solution of 1.00 g (5.52 mmol) 4-methyl-4-phenyl-3-thiosemicarbazide in 10 mL of methanol was treated with 0.664 mL (5.52 mmol) of 2-hydroxyacetophenone and a slight excess of a base viz., cyclohexylamine and refluxed in a water bath for about for 10-15 min., when fine cubic crystals of compound started separating in the medium. The solution was allowed to cool. The solution was filtered, washed with cold methanol and dried *in vacuo* over P_4O_{10}. The compound was recrystallised from absolute ethanol. Mp 197°C. Yield 1.30 mg (78%). Analytical data: Elemental; Calcd for $C_{13}H_{17}N_3O_2S$: C, 64.19; H, 5.72; N, 14.03. Found: C, 64.20; H, 5.70; N, 13.99. IR (KBr): 3400s, 3268sh, 1601m, 1375s, 1250s, 1001 m, 791m cm^{-1}. ^1H NMR (400 MHz, $CDCl_3$, δ(ppm) vs internal TMS): 12.64 (s, 1H, OH, phenolic); 8.31 (s, NH, hydrazide); 7.56 (t, 2H, Ar-H); 7.49 (t, 1H, Ar-H); 7.34 (d, 2H, Ar-H); 7.21-7.28(m, 2H, Ar-H); 7.00 (d, 1H, Ar-H); 6.81 (t, 1H, Ar-H); 3.70 (s, 3H, CH_3, N-methyl); 1.79 (s, 3H, CH_3).

The ^{13}C NMR spectral assignments for the compound are given in Figure. 2a.4

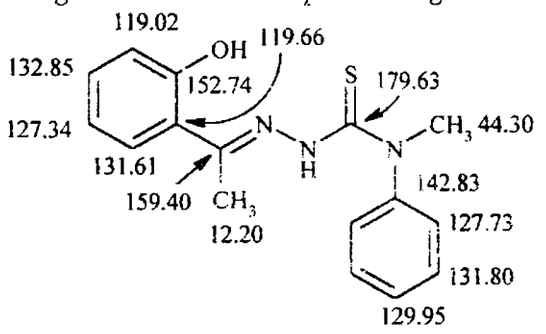

Figure. 2a.4 ^{13}C NMR spectral assignments for 2-hydroxyacetophenone 4-methyl-4-phenylthiosemicarbazone (H_2L^4)

2a.2.2. Analytical methods

Elemental analyses were carried out using a Heraeus elemental analyzer, at CDRI, Lucknow. Infrared spectra were recorded on a Shimadzu DR 8001 series FTIR instrument as KBr pellets and electronic spectra were recorded on Shimadzu 160A UV-visible spectrophotometer from a solution in CH_2Cl_2/DMF. ^1H and ^{13}C NMR spectra were recorded on a Bruker AMX 400 in $CDCl_3$/DMSO-d_6 ($CHCl_3$, δ 7.26, and $^{13}CDCl_3$, δ 77) with TMS as internal standard.

2a.3. RESULTS AND DISCUSSION

2a.3.1. Synthesis of thiosemicarbazones

The preparation of the thiosemicarbazones from 4-methyl-4-phenyl thiosemicarbazide in a single step involves a simultaneous occurrence of two processes a) the condensation of the ketone or aldehyde with the $^1NH_2$ of the thiosemicarbazide moiety b) transamination in which the N-methyl aniline from 4-methyl-4-phenyl thiosemicarbazide is replaced by the amine present in the solution. Here the amines assume the role of a catalyst as well. Since the base viz. amines used are stronger and the N-methyl aniline is a good leaving group and the reaction is facilitated. The rate and extent of the reaction is found to be a function of the strength of the bases used. The solvent is also found to play an important role in the end product and the rate of the reaction. In the synthesis of 2-hydroxyacetophenone 4-methyl-4-phenyl thiosemicarbazone the reaction is better effected in methanol. It is assumed that the condensation reaction is initiated first and overrides the transamination when methanol is used as solvent and mild refluxing condition is adopted. However longer refluxing hours leads to a mixture of the transaminated and non-transaminated products. The transamination slows down for deactivated amines and the major product in such cases is the non-transaminated product.

The status of the end product formed depends on the mode of preparation and the basicity of the medium. The more polar the medium and higher the pH the compound isolated will have a greater percentage of the thiol tautomer than the thione form as revealed by the IR and ^1H-NMR spectra of the compound. However recrystallisation from methanol shifts the percentage to thione tautomer.

Our attempts to effect transamination by using 2-aminopyridine, 2-aminopyrimidine and 2-phenylethylamine ended up with unexpected products. Attempts of transamination using piperidine in acetonitrile and in methanol were unsuccessful. The appearance of the crystals depends on the nature of the solvents used and the methods adopted for crystallization.

2a.3.2. Spectral characterizations

2a.3.2.1. Infrared and NMR spectroscopy

The tentative assignments for the IR spectral bands to establish the structural identity of the compounds are listed in Table 1

The compounds contain thioamide function –NH-C(S)-NHR and consequently they may exhibit thione-thiol tautomerism (fig. 2a.5). The IR spectra of the compound 2-hydroxyacetophenone ^4N-cyclohexylthiosemicarbazone (H_2L^1) shows a broad medium absorption band centered at 2523 cm^{-1} indicating that the compound exists predominantly in the thiol form in the solid state. A low intensity peak at 1620 cm^{-1} characteristic of the thione tautomer and a medium intensity new peak at 1599 cm^{-1}, due to newly formed $^2N=^9C$ in the thiol tautomer, further supports this. The IR spectra of the rest of the compounds do not show any ν(S-H) band at *ca* 2570 cm^{-1} [18], but exhibit a sharp ν(N-H) band at 3385 cm^{-1} for H_2L^3, at 3318 cm^{-1} for H_2L^1. However, for H_2L^2 and H_2L^4 the ν(N-H) cannot be clearly identified as the peak is assumed to be involved in the broad band due to the phenolic ν(O-H) stretching vibration centered at 3500 cm^{-1}. This observation indicates that in the solid state, the compounds, except H_2L^3, remain predominantly as the thioketo tautomer. The proton NMR spectra of the compounds in $CDCl_3$/DMSO-d_6 do not show a resonance peak at 4.00 ppm attributable to the S-H proton- except for H_2L^1 that have a peak at 4.31 δ (ppm) due to S-H -but they do show a peak at 8.3-8.7 ppm ($CDCl_3$) and 10.35 ppm (DMSO-d_6) assignable to the secondary N-H protons. These evidences suggest that in the solution also the thioketo tautomer is the predominant species. The low value of the peak due to NH proton in the 1H NMR spectrum indicates that the compound is predominantly in the *E* form [14b,15]. The high δ values observed for OH and NH proton for 2-hydroxyacetophenone-3-morpholyl thiosemicarbazone (H_2L^3) was assumed to be due to the hydrogen bonding with DMSO. The ^1H NMR assignments- given in Table 2a.2 is in agreement with the values already reported [15- 17].

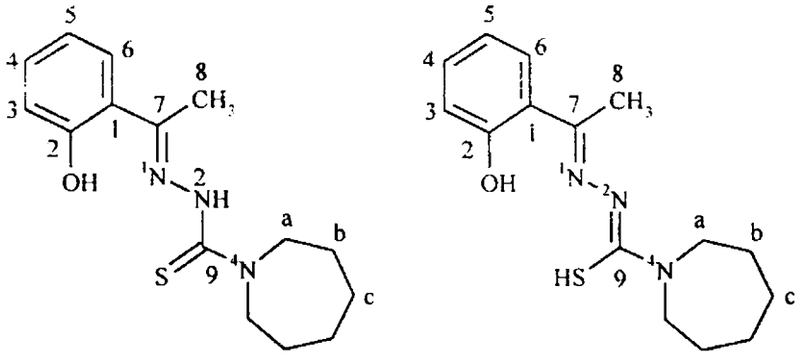

1a (thione form) 1b (thiol form)

Figure. 2a.5 Thiol-thione tautomerism

In all the four ligands the broad band due to phenolic ν(O-H) stretching vibration is found centered on 3300-3500 cm^{-1}. The compounds show azomethine ν(C=^{1}N) stretching vibration in the range 1601-1605 cm^{-1}. The bands in the range 1350 - 1460 cm^{-1} are due to the ν(^{2}N-C), ν(^{4}N-C) stretching vibrations. This region is rather obscured by combination with the aromatic ν(C=C) and ν(C-C-O) stretching vibrations that are found in the form of medium and strong absorption bands in the range of 1400 –1550 cm^{-1} The ν(O-H) bending vibrations are found in the range of 1290 -1330 cm^{-1}. ν(C=S) bending vibrations are found in the range 790 – 840 cm^{-1} while the stretching vibrations are seen in the range 1360 - 1390 cm^{-1}.

The numbering scheme for carbon atoms of 2-hydroxyacetophenone thiosemicarbazone (**I**) is given in the Figure 2a.6.. The ^{13}C spectral assignments, listed in table 3, are consistent with the earlier reports [13,14]. The numbering scheme for thiosemicarbazide –structure **II**- is also given in Figure. 2a.6.

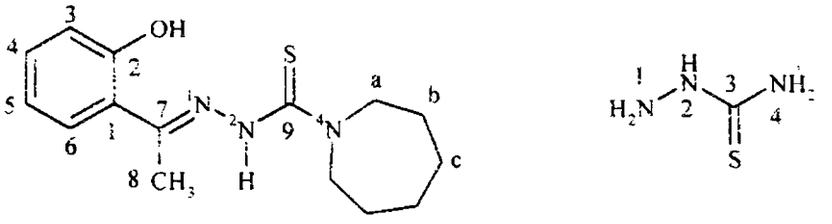

Figure. 2a.6. Numbering scheme for 2-hydroxyacetophenone thiosemicarbazone and thiosemicarbazide moieties.

2a.3.2.2. Electronic spectroscopy

The electronic spectral details are listed in Table 1. The compounds show absorption bands due to n-π* transition at around 30000 cm^{-1} that is characteristic of the thiosemicarbazone compounds. Bands around 35000 cm^{-1} and higher, are attributed to π- π* transitions.

Table 2a.1: IR and Electronic spectral assignments for four ligands. (All absorptions are given in units of cm^{-1}), (log ε is given in parentheses).

Comp.	$\nu_{(^7C=^1N)}$	$\nu_{(^3N-^9C)}$ $\nu_{(^2N-^9C)}$	$\nu_{(^1N-^2N)}$	$\nu_{(C=S)}$	$\delta_{(C-S)}$	$\nu_{(C-O)}$	$\nu_{(C-C-O)}$/ $\nu_{(C-O-C)}$	$\nu_{(^9C-N)}$	$\nu_{(O-H)}$	$\nu_{(2NH)}$	n-π*	π-π*
$H_2L^{1[1]}$	1620m	1599s	988 m	1365m	826 m	1219 s	1118w	1448m	3109s	-----	30300 (4.05) 32342sh (4.32)	35000 (4.26)
H_2L^2	1603 s	1489s	997 m	1383 s	839 m	1252 s	1101m	1452m	3470s, br	-----	30581 (4.19) 32372sh (4.23)	35587 (4.48)
H_2L^3	1605 s	1485s	1017 m	1374m	835 m	1219 s	1118s, d 1043m	1458m	3401s, br	3385sh	30030 (4.43) 32895sh (4.41)	42370 (4.25)
H_2L^4	1601 s	1483s	995 m	1375 s	808 m	1222 s	1129m	1491m	3400s, br	3328sh	30211 (4.19) 35524sh (4.40)	42370 (4.32)

s = strong, m = medium, w = weak, sh = sharp, d = doublet

Table 2a.2 : ^1H NMR spectral assignments for four thiosemicarbazone compounds. [All absorptions are given in units of δ (ppm)]

Sl no	Compound	OH	^2NH	^3CH	^4CH	^5CH	^6CH	^8CH	H^a	H^b	H^c	$^4NH/^4NCH$	SH
1	H_2L^1	10.89	08.74	6.97	7.31	6.93	7.46	2.38	1.69	1.22-2.19[2]	---	6.72	4.30
2	H_2L^2	12.75	08.36	7.00	7.25	6.81	7.32	2.24	3.76	1.79	1.55	---	---
3	H_2L^3	12.90	10.38	6.88	7.28	6.88	7.60	3.35	3.66	3.91	---	---	---
4	H_2L^4	12.64	08.31	7.00	7.23	6.81	7.56	3.70	7.34	7.28	7.49	1.79	---

[1] ν (^4N-H) absorbs at 3318sh cm^{-1}

[2] Multiplet due to aliphatic CH_2 of the cyclohexyl group

Table 2a.3 : ^{13}C NMR spectral assignments for four thiosemicarbazone compounds. (All absorptions are given in units of (ppm)

Sl no	Compound	^{1}C	^{2}C	^{3}C	^{4}C	^{5}C	^{6}C	^{7}C	^{8}C	^{9}C	C^{a}	C^{b}	C^{c}	C^{d}	^{4}NC
1	H_2L^1	120.29	154.32	118.14	132.48	119.93	128.98	158.24	14.72	175.26	54.17	33.12	25.22	26.01	----
2	H_2L^2	119.85	154.02	118.66	131.64	119.16	128.09	159.19	13.19	179.76	51.94	27.50	27.86	----	----
3	H_2L^3	121.01	154.57	118.64	132.39	119.81	128.53	159.16	13.69	184.22	51.54	66.92	----	----	----
4	H_2L^4	119.66	152.74	119.02	132.85	127.34	131.61	159.40	12.20	179.63	142.83	127.73	131.80	129.95	44.30

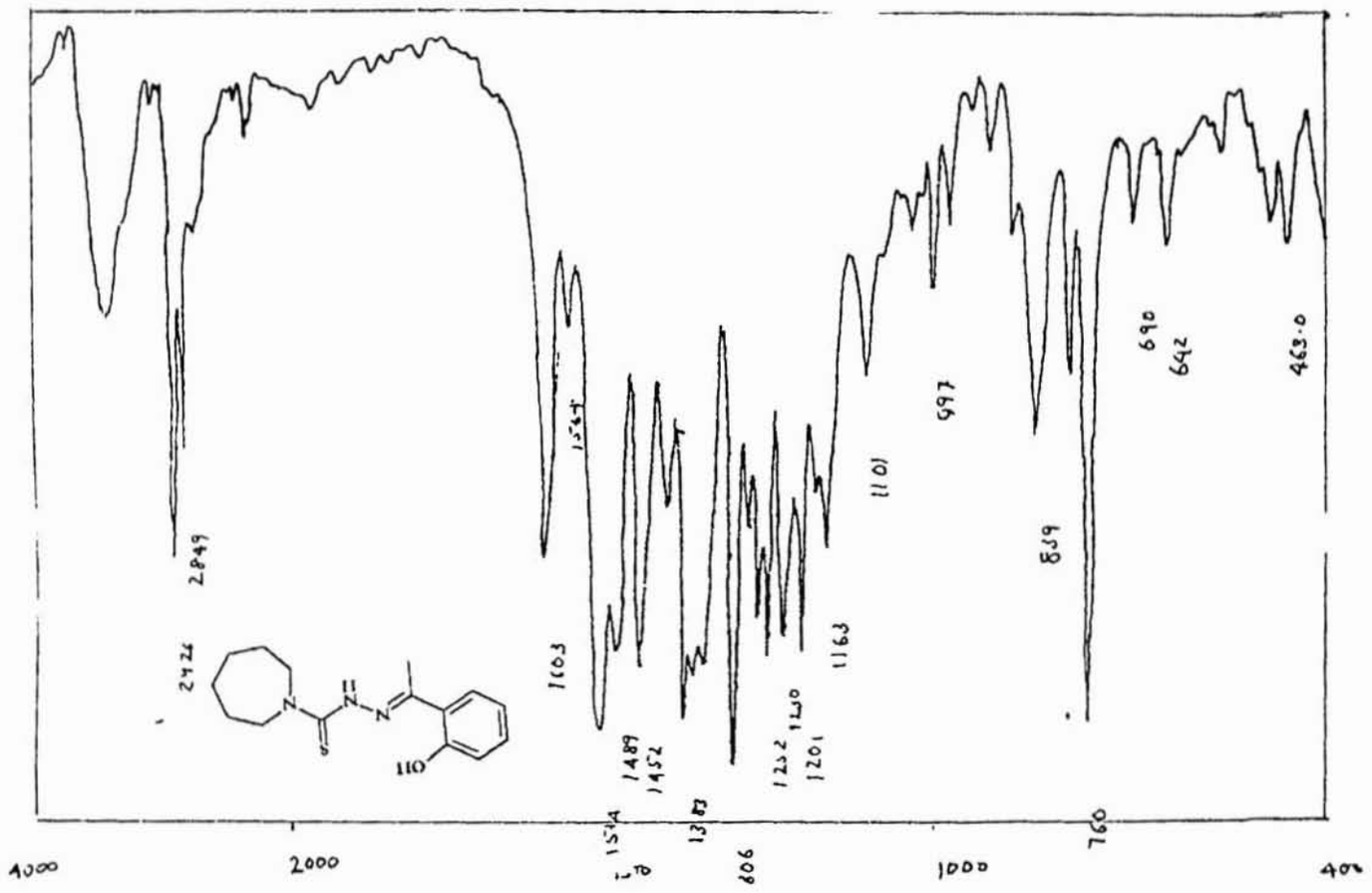

Figure 2a.7 a. IR spectrum of 2-hydroxyacetophenone hexamethylenimine-3-thiosemicarbazone (H_2L^2).

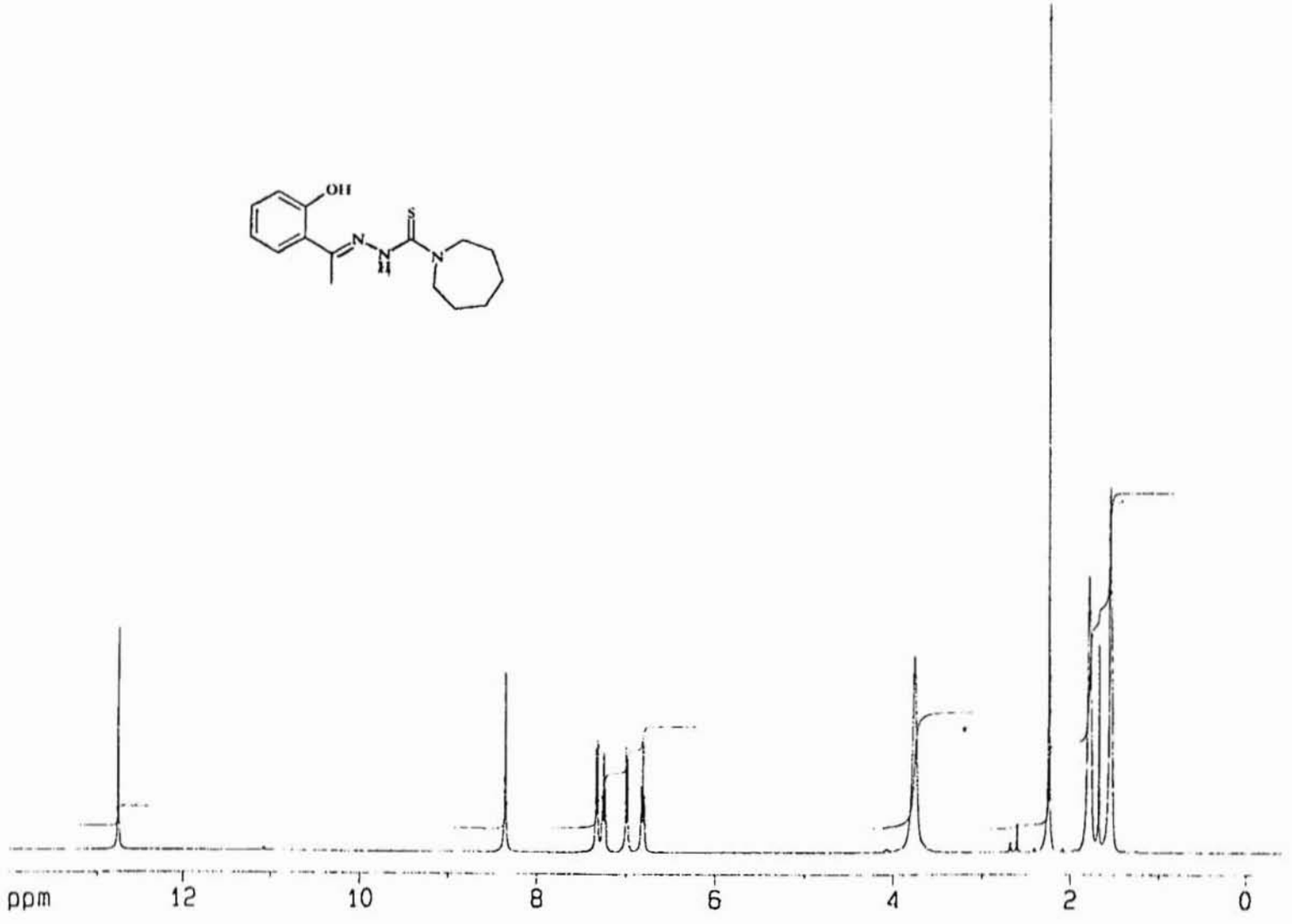

Figure 2a.7b. ^{1}H NMR spectrum of 2-hydroxyacetophenone hexamethyleneimine-3-thiosemicarbazone (H_2L^2).

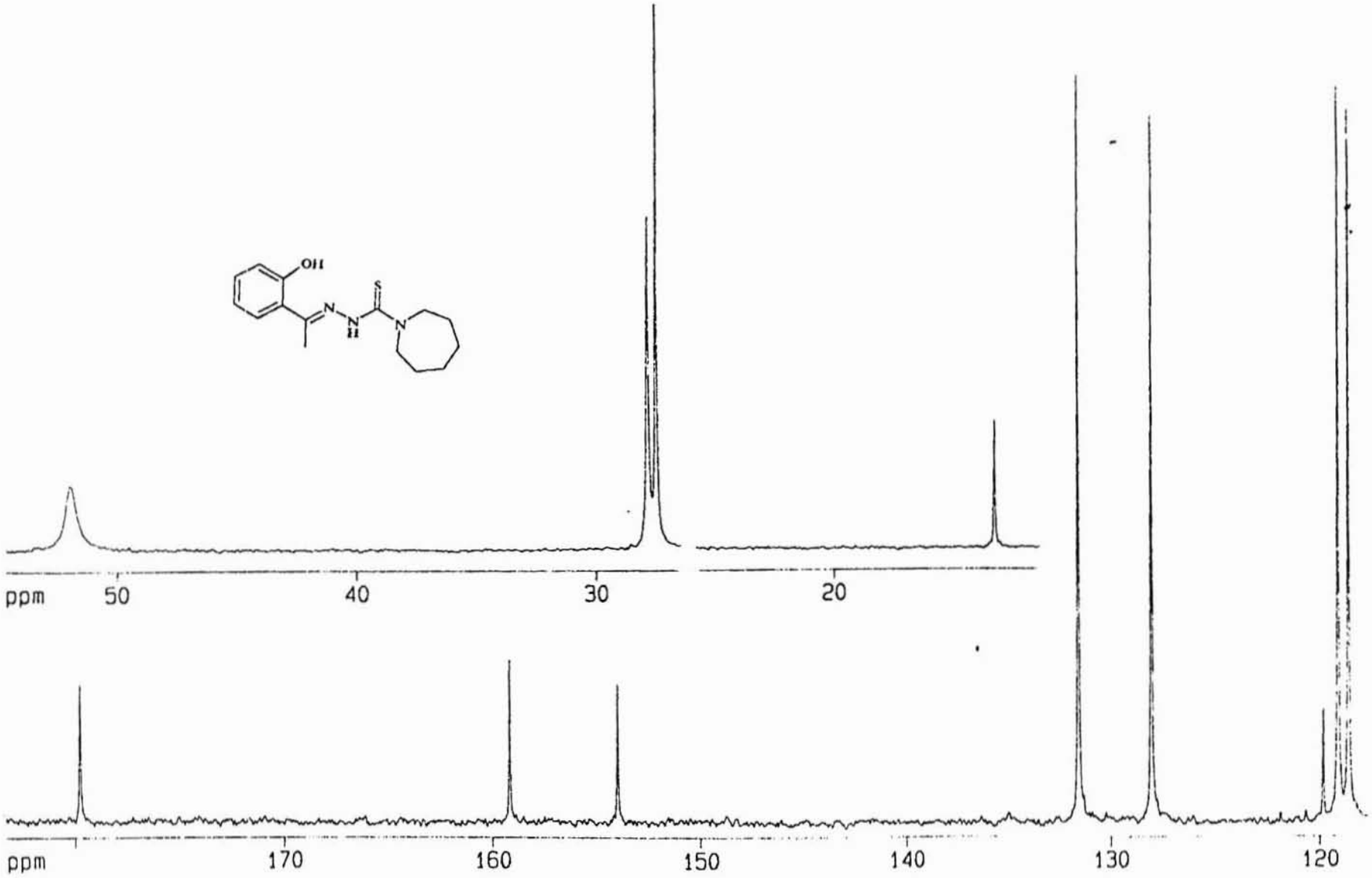

Figure 2a.7c. ^{13}C NMR spectrum of 2-hydroxyacetophenone hexamethyleneimine-3-thiosemicarbazone (H_2L^3).

References

1. E. J. Blanz Jr., F. A. French, *Cancer Res.*, 1968.
2. J. C. Logan, M.P.Fox, J. H. Morgan, A. M. Makohon, C. J. Pfau , *J. Gen. Virol.*, 1975, **28**, 271.
3. D. L. Klayman, J. E. Bartosevic, T. S. Griffin, C. J. Mason, J. P. Scovill, *J. Med. Chem.*, 1979, **22**, 855 and references therein
4. A. S. Dobek, D. L. Klayman, E. J. Dickson Jr., J. P. Scovill, E. C. Tramont, *Antimicrob. Agents Chemother.*, 1980, **18**, 27 and references therein
5. S. P. Mittal, S. K. Sharma, R.V. Singh, J. P. Tandon, *Curr. Sci.*, 1981, **50**, 483 and the references therein
6. A. B. DeMilo, R. E. Redfurn, A. B. Borkovec, *J. Agri. Food Chem.*, 1983, **31**, 713.; D. L. Klayman, J. P. Scovill, C. Ambros, G. E. Child, J. D. Notsch, *J. Med. Chem.*, 1984, **27**, 87; R. W. Brockman, R. W. Sidwell, G. Arnett, S. Shaddix, *Proc. Soc. Expt. Biol. Med.*, 1970, **133**, 609
7. E. C. Moore, M. S. Zedek, K. C. Agrawal, A. C. Sartorelli, *Biochemistry*, 1970, **9**, 4492
8. E.E. Ebenso, U.J. Ekpe, B.I. Ita, O.E. Offiong, U.J. Ibok, *Mat. Chem. Phy.*, 1999, **60**, 79.
9. J. E. J. C. Graudo, C. A. L. Filgueiras, A. Marques-Netto, A. A. Batista, *J. Braz. Chem. Soc.*, 2000, **11** (3), 237.
10. X. C. Tang, D. Z. Jia, L. Kai, X. G. Zhang, X. Xi, Z. Y. Zhou, *J. Photochem. Photobiol., A. Chem.*, 2000, **134**(1-2), 23
11. B. Holmber and B. Psilanderhielm, *J. Pract. Chem.* 1910, **82**, 440.
12. J. P. Scovill, *Phosphorus Sulphur Silicon*, 1991, **60**, 15.
13. K. R. Koch, *J. Coord. Chem.*, 1991, **22**, 289.
14. (a) D. X. West, C. E. Ooms, J. S. Saleda, H. Gebremethin and A. E. Liberta, *Trans. Met. Chem.*, 1994, **19**, 553; (b) D. X. West, D. L. Mokijewiski, H. Gebremethin and T. J. Romack, *Trans. Met. Chem.*, 1992, **17**, 384
15. P. Bindu and M. R. P. Kurup, *Ind. J. Chem.*, 1997, **36A**, 1094.
16. J. P. Scovill, *Phosphorus Sulphur Silicon*, 1991, **60**, 15.
17. S. Jayasree and K. K. Aravindakshan, *Trans. Met. Chem.*, 1993, **18**, 85.
18. S. K. Jain, B. S. Garg, Y. K. Bhoon, D. L. Klayman, J. P. Scovill, *Spectrochim. Acta*, 1985, **41A**, 407.

STRUCTURAL, SPECTROSCOPIC, BIOLOGICAL AND ELECTROCHEMICAL STUDIES OF COPPER(II) COMPLEXES

2b.1 INTRODUCTION

Among the transition metal elements copper and its complexes are outstanding as reagents or catalysts in the reaction of organic compounds. The importance of copper(II) species in oxygenation reactions has been reviewed [1]. The question of copper promoted reactions in aromatic chemistry and the role of organometallic complexes in organic reactions has been widely investigated. In general the role of copper is intimately involved and related to the presence of copper(I) and copper(II) oxidation states, although there is little or no information on the stereochemistry of various copper(I) and copper(II) complexes or of their mechanism of involvement. Copper is the third most abundant transition metal element in biological systems, with an occurrence of 80-120 mg in human body. The function [2] of copper in biological systems is primarily in redox reactions associated with the reduction of oxygen to water with the transfer of oxygen to the substrate. Super oxide dismutase has the specific, but important role of removing the highly reactive super oxide anion and in these oxygenation reactions copper is acting as a biological catalyst. The other role of copper in human body is in the transport of copper around the body, controlling its uptake and excretion. In attempts to model the physical and chemical behaviour of the biological copper system an extensive effort was made to synthesize and characterize a plethora of coordination complexes [3]. The interesting biological properties of copper has aroused the curiosity of inorganic chemists thus giving a spurt in research linking the widely tested thiosemicarbazones with the copper metal.

The chemistry of metal complexes of thiosemicarbazone has gained considerable attention due to their significant biological activity and medicinal properties [4]. Spectral and structural investigations of a series of metal complexes of biologically active 2-acetylpyridine ^4N-substituted thiosemicarbazones [5] and those of base adducts of copper(II) complexes of thiosemicarbazones [6] were widely studied. The base adducts of copper(II) with NNS donors have also been investigated [7]. There are some recent reports of copper(II) complexes of salicylaldehyde thiosemicarbazones and bases [42]. In this chapter we have attempted to explore into the structural aspect of the copper complexes of some ONS donor ligands especially that of thiosemicarbazones of 2-hydroxyacetophenone. The principal ligands we have chosen for the study are:

i) 2-hydroxyacetophenone ^4N-cyclohexyl thiosemicarbazone (H_2L^1)

ii) 2-hydroxyacetophenone-3-hexamethyleneiminyl thiosemicarbazone (H_2L^2)

iii) 2-hydroxyacetophenone-3-morpholyl thiosemicarbazone (H_2L^3)

iv) 2-hydroxyacetophenone ^4N-methyl-^4N-phenyl thiosemicarbazone (H_2L^4)

Bidentate bases such as bipyridine or phenanthroline are used as auxiliary ligands for coordination with copper metal. We have exploited the various spectral techniques to arrive at the stereochemistry of the prepared compounds and were also able to carry out the single crystal X-ray diffraction of one of the compounds. In this

chapter, we have discussed our attempts to investigate the redox behaviour and biological studies of all the eight complexes against some commonly found bacterial and fungal cultures.

2b.2. EXPERIMENTAL

2b.2.1. Materials and methods

The ligands H_2L^1, H_2L^2, H_2L^3 and H_2L^4 were prepared as described in the previous chapter. Copper(II) acetate monohydrate (Reagent grade, Qualigen's Fine Chemicals) was purified by standard methods; the bases, such as phenanthroline (Merck) and bipyridine (Merck) were used as received. The solvents were purified by standard procedures before use.

2b.2.2. Physical Measurements

The carbon, nitrogen and hydrogen analyses were carried out using a Heraeus Elemental Analyser, at CDRI, Lucknow. Copper was estimated by Atomic Absorption Spectroscopy in a Perkin-Elmer AAnalyst 700 spectrometer, after decomposing the compounds by standard methods. Magnetic measurements were made in the polycrystalline state in a simple Gouy balance using cobaltmercurichiocyanate, $Hg[Co(SCN)_4]$, as the reference substance, as suggested by Figgis and Nyholm [8]. Infrared spectra were recorded on a Shimadzu DR 8001 series FTIR instrument as KBr pellets and electronic spectra were recorded on Shimadzu 160A UV-visible Spectrophotometer from a solution in CH_2Cl_2/DMF The EPR spectra were recorded in a Varian E-112 Spectrometer using TCNE as the standard at RSIC, IIT, Bombay. The cyclic voltammetric measurements were made in a computer controlled Solartran SI 1280B electrochemical measurement unit at CECRI, Karaikudi. The CV measurements were made on degassed (N_2 bubbling for 15 min.) solutions in DMF (10^{-3} M) containing 0.1 M tetraethyl ammonium perchlorate (TEAP) as supporting electrolyte. The three-electrode system consisted of platinum foil (working), platinum wire (counter) and calomel (reference) electrodes. Molar conductance of the complexes was measured in a Century CC-601 Digital Conductivity meter using 10^{-3} M solution in DMF.

2b.2.3. Preparation of the complexes

The general method of synthesis of the copper complexes (**1-8**) is as described below:

To a hot solution (20 mL) of the thiosemicarbazone (0.5 mmol) in ethanol was added 10 mL methanolic solution of the base (0.5 mmol), bipyridine or phenanthroline with stirring. This was followed by a drop wise addition of about 10 mL of copper(II) acetate monohydrate (0.5 mmol) in methanol. The solution was refluxed for about 2-3 hours, allowed to cool, when microcrystals of the respective compounds crystallized out. The compounds were filtered off, washed with ethanol, water and ether respectively and dried *in vacuo*.

2b.2.4. Crystal structure determination of complex [CuL^{4}bipy] (7)

A dark brown crystal of the copper(II) complex having approximate dimensions 0.44 × 0.38 × 0.16 mm was sealed in a glass capillary, and intensity data were measured at room temperature (293 K) on an Enraf-Nonius [9] CAD4 diffractometer equipped with graphite-monochromated Mo Kα (λ = 0.71073 Å) radiation a variable-speed $\omega/2\theta$ scan technique. Cell dimensions and an orientation matrix for data collection were obtained from 25 high-angle reflections in the range $1.80 < \theta < 28.32°$. The octant measured was ***hkl*** (-26 → 28, -13 → 12, -30 → 25). Three standard intensity-control reflections were recorded during every 60 min of X-ray exposure time. During the data collection, the intensity of standard reflections decreased by 0.1%. A total of 5886 unique reflections were collected; of these, 2136 reflections had $F_o > 2.0$ and were used in the structure analysis. Data were corrected for Lorentz-polarization and absorption effects but not for extinction. The linear absorption coefficient, μ, for Mo Kα radiation was 15.6 cm^{-1}.

The trial structure was obtained by direct methods using SHELXS 97 [10] and refined by full-matrix least-squares on F^2 (SHELXL 97) [11]. The best E map revealed the positions of all the non-hydrogen atoms. Non-hydrogen atoms were refined anisotropically. Hydrogen atoms were located from successive Fourier maps and refined anisotropically. The final R-factor converged to 0.0699. Neutral-atom scattering factors were taken from Cromer and Waber [12]. During refinement, the function minimized was $\Sigma w(|F_o| - |F_c|)^2$ with $w = 4F_o^2/[(\alpha(F_o^2)^2 + (0.04F_o^2)^2]$. The final Fourier map was featureless with residual electron density values of ±0.49 e A^{-3}. Anomalous dispersion effects were included in the final calculations [13]; the atomic scattering factors were taken from ref 2b.12, and the mass attenuation coefficients were taken from ref 2b.13. All calculations were performed on a Micro Vax 3100 computer using CAD4 software. Data collection parameters and details of the structure solution and refinement are given in Table 2b. 2.

2b.3. RESULTS AND DISCUSSION

2b.3.1. Preparation of compounds

The compounds were found to form readily in ethanol-methanol mixture. The base added acts as the auxiliary ligand, which promotes the enolisation of the principal ligand and also provides the basicity for the medium. The thiosemicarbazones in solution undergo double deprotonation (L^{2-}) and coordinate in the thiolate form. The elemental analyses data (Table 2b.1) of the complexes are in agreement with the general formula [MLB]. X-Ray quality single crystals of compounds **2, 3, 4, 6** and **7** were isolated from DMF by slow evaporation over a period of 8 days. The structure of the compound **7** was determined by single crystal X-ray diffraction.

All the compounds **1-8** were soluble in dichloromethane and DMF. However, the bipyridine containing compounds dissolved rather slowly in either solvent. But dichloromethane was found to be a better solvent for all the complexes, since the colour of the compound remains stable in its solution. The dissolution of the compounds in DMF is assumed to initiate by the coordination of the solvent.

Since the thiosemicarbazones bind to the metal as a dianion, it neutralises +2 oxidation state of the copper(II) ion. The values of conductance measurements were in agreement with that for non-electrolytes. This rules out the possibility of an anionic species outside the coordination sphere of copper(II). This is in conformity with the stoichiometry established by elemental analysis data in the solid state. The magnetic moment values of the complexes (Table 2b.1) were in agreement with the spin only values of 1.73 -2.2 BM reported for mononuclear copper(II) complexes.

2b.3.2.X-Ray diffraction studies

The molecular structure of the compound 4 along with atomic numbering scheme is given in Figure 2b.1 and selected bond lengths and bond angles are summarised in Tables 2b.3 and 2b.4 respectively. The copper in the mononuclear complex is five coordinated and is having an approximate square planar (**SP**) geometry. The basal coordination positions are occupied by the phenolato oxygen, O(1), azomethine nitrogen, N(1), and thiolate sulfur, S(1), of the thiosemicarbazone and the pyridine nitrogen, N(5), of bipyridine. The Cu-N and Cu-O bond length vary in the range 1.9116 to 2.0474 A°. The apical position is occupied by second nitrogen of bipyridine, N(4), at a larger distance (2.2278 A°). This value is larger than the normal Cu-N bond lengths reported [7]. The four basal atoms are coplanar showing a slight but significant tetrahedral distortion. The central copper atom is slightly displaced from the basal plane in the direction of the axial nitrogen, which is evident from the bond angles of N(1)-Cu-N(5), 176.94°, and O(1)-Cu-S(1), 161.32°. The distortion from **SP** geometry can be related to the O(1)-Cu-N(1) (93.63°), O(1)-Cu-N(5) (89.40°), N(1)-Cu-S(1) (85.91°) and S(1)-Cu-N(5) (91.36°) angles which are close to those expected for **SP** geometry (90°). One of the reasons for the deviation from an ideal stereochemistry is the restricted bite angle imposed by both the L^4 and bipy ligands. In other complexes involving HL or L coordinated to copper [14], the bite angles around the metal viz., N(1)-Cu-O(1) and N(1)-Cu-S(1) are limited to 80-85°. Similarly the bite angle N(5)-Cu-N(4) of 76.86° may be considered normal, when compared with an average value of 77° cited in the literature.[15a,b]. The O(1)-Cu-N(4) bond angle, 95.52°, and S(1)-Cu-N(4) bond angle, 102.83°, indicate a slight tilting of the axial Cu-N(4) bond in the direction of the O(1)-Cu bond and away from S(1)-Cu bond. The variation in Cu-N bond distances, Cu-N(1) (1.9606 A°), Cu-N(5) (2.0474 A°) and Cu-N(4) (2.2278 A°) indicate difference in the strength of the bond formed by each of the coordinating nitrogen atoms. The azomethine nitrogen coordinates rather strongly, than that of the bipyridine nitrogen, which indicates that the thiosemicarbazone moiety dominates the equatorial bonding. The difference in bond lengths can be attributed to the difference in the extent of π-back-bonding between the bipyridine and thiosemicarbazone moiety. However the large bond distance of the axial Cu-N(4) supports the lack of significant out-of-plane π-bonding. This fact is in accordance with the EPR studies.

The Cu-N bond lengths are longer than those reported for mononuclear copper(II) complexes [16] indicating a weaker binding of the base and the thiosemicarbazone, while, there is no significant variation in the Cu-S bond lengths reported. The comparison of the thiosemicarbazone moiety bond distances of the compound 4 to those of the uncoordinated thiosemicarbazone [17] shows that coordination lengthens the $^{7}C=^{1}N$ bond slightly [1.307 A° and 1.297 A° respectively] and the $^{9}C=S$ bond length substantially [1.740 A° and 1.692 A° respectively], as would

be expected on coordination of the azomethine nitrogen and thiol sulfur. It should be noted that there is no change in the ^{1}N-^{2}N bond length of the thiosemicarbazone moiety (1.392 A°) upon complexation. The other bond distances of the thiosemicarbazones moiety are found to decrease by 0.010 to 0.040 A° upon coordination.

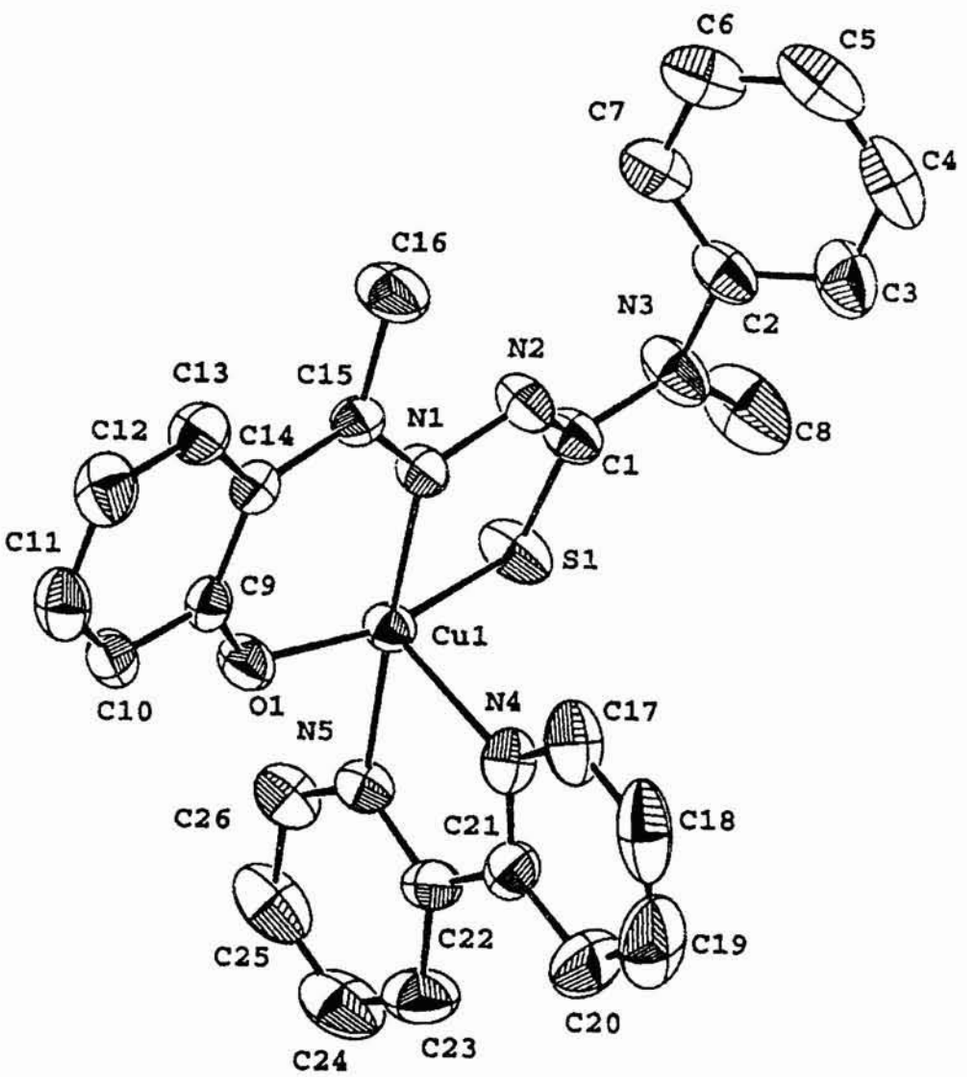

Figure 2b.1.: **ORTEP drawing and atomic labelings for compound 4, Hydrogen atoms are omitted for clarity**

Table 2b.2. Crystal data and structure refinement for **[CuL^{3}bipy]**

Empirical formula	$C_{26}H_{23}CuN_5OS$
Formula weight (M)	517.09
Temperature (T), K	293(2)
Wavelength (λ, Mo Kα), A°	0.71073
Crystal system	Orthorhombic
Space group	*Pbcn*
Unit cell dimensions	
a, A°	21.285(3)
b, A°	9.8755(8)
c, A°	22.609(2)
α, deg	90.0
β, deg	90.0
γ, deg	90.0
Volume (V), A° ^{3}	4752.5(8)
Z	8
	0.71073
Calculated density (ρ), g /cm^3	1.445
Absorption coefficient (μ), cm^{-1}	10.36
F(000)	2136
Crystal size	0.44 x 0.38 x 0.16 mm
θ range for data collection	1.80 – 28.32 deg.
Limiting indices	$-26 \leq h \leq 28$, $-13 \leq k \leq 12$, $-30 \leq l \leq 25$
Reflections collected	31541
Unique reflections	5886 [R (int) = 0.0699]
Completeness to θ	= 28.32 99.4 %
Max. and min. transmission	0.8517 and 0.6585
Refinement method	Full-matrix least-squares on F^2
Data / restraints / parameters	5886 / 0 / 307
Goodness-of-fit on F^2	0.986
Final R indices [$I > 2\sigma(I)$]	R_1 = 0.0389, $Rw2$ = 0.0975
R indices (all data)	R_1 = 0.0701, $Rw2$ = 0.1117
Largest diff. peak and hole	0.378 and -0.671 e • A^{-3}

Table 2b.3. Selected Bond lengths (A°) in compound 4, **[CuL^{4}bipy]**

Atoms	Bond distance	Atoms	Bond distance
Cu(1)-O(1)	1.9116(15)	C(4)-C(5)	1.367(4)
Cu(1)-N(1)	1.9606(16)	C(3)-C(4)	1.392(4)
Cu(1)-N(5)	2.0474(16)	C(5)-C(6)	1.368(4)
Cu(1)-N(4)	2.2278(18)	C(6)-C(7)	1.373(3)
Cu(1)-S(1)	2.2729(7)	C(9)-C(10)	1.416(3)
S(1)-C(1)	1.740(2)	C(9)-C(14)	1.419(3)
O(1)-C(9)	1.308(2)	C(10)-C(11)	1.364(3)
N(1)-C(15)	1.307(2)	C(11)-C(12)	1.386(3)
N(1)-N(2)	1.392(2)	C(12)-C(13)	1.365(3)
N(2)-C(1)	1.302(2)	C(13)-C(14)	1.413(3)
N(3)-C(1)	1.379(3)	C(14)-C(15)	1.467(3)
N(3)-C(2)	1.434(3)	C(15)-C(16)	1.514(3)
N(3)-C(8)	1.459(3)	C(17)-C(18)	1.364(4)
N(4)-C(21)	1.334(3)	C(18)-C(19)	1.355(5)
N(4)-C(17)	1.334(3)	C(19)-C(20)	1.371(4)
N(3)-C(2)	1.434(3)	C(20)-C(21)	1.391(3)
N(5)-C(26)	1.332(3)	C(21)-C(22)	1.478(3)
N(5)-C(22)	1.353(3)	C(22)-C(23)	1.388(3)
C(2)-C(7)	1.382(3)	C(23)-C(24)	1.358(4)
C(2)-C(3)	1.385(4)	C(24)-C(25)	1.373(4)
		C(25)-C(26)	1.385(3)

Table 2b.4. Selected Bond angles (°) in compound **4, [CuL^{4}bipy]**

Atoms	Bond angles	Atoms	Bond angles
O(1)-Cu(1)-N(1)	93.63(6)	C(1)-S(1)-Cu(1)	92.48(7)
O(1)-Cu(1)-N(5)	89.40(6)	C(15)-N(1)-Cu(1)	127.31(13)
N(1)-Cu(1)-N(5)	176.94(6)	N(2)-N(1)-Cu(1)	117.66(12)
O(1)-Cu(1)-N(4)	95.52(7)	C(21)-N(4)-Cu(1)	112.80(15)
N(1)-Cu(1)-N(4)	102.39(7)	C(17)-N(4)-Cu(1)	128.08(17)
N(5)-Cu(1)-N(4)	76.86(7)	C(26)-N(5)-Cu(1)	123.17(15)
O(1)-Cu(1)-S(1)	161.32(5)	C(22)-N(5)-Cu(1)	117.83(14)
N(1)-Cu(1)-S(1)	85.91(5)	C(9)-O(1)-Cu(1	126.47(13)
N(5)-Cu(1)-S(1)	91.36(5)	C(9)-O(1)-Cu(1	126.47(13)
N(4)-Cu(1)-S(1)	102.83(5)	N(4)-C(17)-C(18)	123.30(3)
C(1)-N(2)-N(1)	114.57(16)	N(4)-C(21)-C(20)	120.3(2)
C(1)-N(3)-C(2)	120.90(18)	N(4)-C(21)-C(22)	115.84(19)
C(1)-N(3)-C(8)	121.60(2)	N(5)-C(22)-C(23)	120.40(2)
C(2)-N(3)-C(8)	117.12(19)	N(5)-C(22)-C(21)	116.41(18)
C(15)-N(1)-N(2)	115.03(16)	N(5)-C(26)-C(25)	122.90(2)
C(21)-N(4)-C(17)	119.10(2)	C(10)-C(9)-C(14)	117.88(18)
C(26)-N(5)-C(22)	118.99(19)	C(11)-C(10)-C(9)	122.60(2)
N(2)-C(1)-N(3)	116.21(18)	C(10)-C(11)-C(12)	119.80(2)
N(2)-C(1)-S(1)	125.46(16)	C(13)-C(12)-C(11)	119.10(2)
N(3)-C(1)-S(1)	118.31(15)	C(12)-C(13)-C(14)	123.30(2)
C(7)-C(2)-N(3)	120.70(2)	C(13)-C(14)-C(9)	117.24(18)
C(3)-C(2)-N(3)	120.10(2)	C(13)-C(14)-C(15)	118.25(17)
N(1)-C(15)-C(14)	121.94(17)	C(9)-C(14)-C(15)	124.49(17)
N(1)-C(15)-C(16)	118.76(18)	C(14)-C(15)-C(16)	119.29(17)
O(1)-C(9)-C(10)	117.21(18)	C(19)-C(18)-C(17)	117.70(3)
O(1)-C(9)-C(14)	124.89(18)	C(19)-C(20)-C(21)	119.00(3)
C(20)-C(21)-C(22)	123.90(2)	C(23)-C(22)-C(21)	123.20(2)
C(24)-C(25)-C(26)	117.60(2)	C(23)-C(24)-C(25)	120.30(2)
C(24)-C(23)-C(22)	119.80(3)	C(24)-C(25)-C(26)	117.60(2)

2b.3.3. Electronic and IR spectra

The electronic absorptions of the complexes are presented in Table 2b.5. The thiosemicarbazone ligands and their copper(II) complexes have π-π^* at *ca.* 41000 cm^{-1} and an n-π^* band at *ca.* 32000 cm^{-1}. There is a slight shift in the energy of these bands on complexation. A second n-π^* band found below 30,000 cm^{-1} in the spectrum of uncomplexed thiosemicarbazones was found at *ca.* 31,000 cm^{-1} in the spectra of copper(II) complexes. Two metal-to-ligand charge transfer bands are found at *ca.* 27,000 and 21,000 - 23,000 cm^{-1}. In accordance with studies of previous copper(II) complexes [18] the higher energy bands are assignable to $S\rightarrow Cu^{II}$ LMCT transitions [19], tailing into the visible region, and the band in 21,000 – 23,000 cm^{-1} is assignable to phenoxy $O\rightarrow Cu^{II}$ LMCT transitions [20]. The position of S→Cu CT band is determined by the steric requirements of the ^4N substituents such that thiosemicarbazones with bulkier ^4N substituents have this band at somewhat higher energies. The d-d bands of copper(II) complexes are at *ca.* 14,000 and 17,000 cm^{-1}, the later being seen as a very weak shoulder in the tail of the CT bands (Figure 2b.2). These spectra are similar to copper(II) complexes of S-N donor ligands having a square pyramidal geometry [21].

The infrared spectral data of the complexes **1-8** are reported in Table 2b.6, with their tentative assignments. The peak at *ca.* 1605 cm^{-1} in the uncomplexed thiosemicarbazone gets shifted to *ca.* 1560 cm^{-1}, a shift of 45 cm^{-1}, upon complexation. It is assigned to $\nu_{(C=N}$ that has got weakened due to the coordination of the azomethine nitrogen with copper(II). The appearance of a new medium sharp peak at *ca.* 1595 cm^{-1} is due to stretching vibration of the newly formed $^2N=^9C$ bond as a result of enolisation of the principal thiosemicarbazone ligand. Further proof for the coordination of the azomethine nitrogen is obtained from the appearance of new bands in the range 420-470 cm^{-1}, assignable to $\nu_{(Cu\text{-}N)}$ for the complexes [43]. The disappearance of the $\nu_{N\text{-}H}$ band also supports the enolisation of the ligand before complexation. It is learnt that the enolisation is thermodynamically most favoured due to the additional stability conferred on the resulting complex upon complexation. The enolisation and the electron delocalisation in the thiosemicarbazone moiety are supported by the increase in the stretching frequency of the N-N bond of the principal ligand. The decrease in the stretching frequency from *ca.* 830 cm^{-1} in the uncomplexed thiosemicarbazones by 60-80 cm^{-1} upon complexation supports the coordination via the thiolate sulphur of the thiosemicarbazone. The coordination of the phenoxy group gives rise to peaks in the range 405-435 cm^{-1}, assignable due to $\nu_{(Cu\text{-}O)}$ stretching vibrations, and shifting of the $\nu_{(C\text{-}O)}$ vibrations to lower frequencies. The coordination of the bases is indicated by the appearance of characteristic peaks of bipyridine and phenanthroline in the fingerprint region of 600-1400 cm^{-1} in the complexes [44].

2b.3.4. EPR spectra

The EPR spectra of compounds **1-8** (Figure 2b.3.) in the polycrystalline state at 298 K display different type of geometrical species. Compounds **1** and **7** show typical axial spectra with clearly defined $g_{\parallel}$ and $g_{\perp}$ features. Compounds **2, 6** and **8** give signals corresponding to axial symmetry, but the $g_{\parallel}$ features cannot be clearly defined because of the broadening resulting from smaller spin lattice relaxation time and large spin-orbit

coupling [22]. All the above compounds have their *g* values (Table 2b.7.) in conformity with that of a copper(II) species (d^9 system) with a $d_{x^2-y^2}$ ground state. Spectra of compounds **3**, **4** and **5** give three *g* values viz., g_1, g_2, g_3 which indicate rhombic distortions in their geometry. The values g_1 and g_2 are very close to each other, in **3** and **4**, which mean that the rhombic distortion is very small. Comparing the rhombic distortions the bipyridine derivatives are found to have more distortion. We were able to observe such small distortions in their geometry as the spin lattice relaxation time is very large and the spin orbit coupling remains comparatively small in these compounds. The polycrystalline spectrum of the compound **2** is very broad compared to all other spectra (nearly isotropic). It can be inferred that the dipolar interactions are the greatest in compound **2**. The variation in $g_{\|}$ and $g_{\perp}$ values indicates that the geometry of the compounds in the solid state is affected by the nature of the ^{4}N substituents. The value increases with the bulkiness of the substituents. The geometric parameter *G* was calculated for all compounds and *R* was calculated for compounds **3**, **4** and **5** that show rhombic solid-state spectra (Table 2b.7). The *G* values obtained are in the range of 3.5 to 5.0, indicating that the *g* values obtained in the polycrystalline sample are near to the molecular *g* values and hence the unit cell of the compounds contain magnetically equivalent sites [23].

The solution spectra at 298 K were recorded in DMF (Figure 2b.4). All the recorded spectra clearly show four well resolved hyperfine lines (^{65}Cu, I = 3/2) corresponding to M_I = -3/2, -1/2, 1/2, 3/2 transitions ($\Delta M_I = \pm 1$). The signal corresponding to M_I = +3/2 splits clearly into three peaks with a superhyperfine coupling (**shf**) constant $A_N \approx$ 18 G. This is characteristic of the compounds bound through azomethine nitrogen and an indication that the bonding in solution state is dominated by the thiosemicarbazone moiety, compared to the base. The small variation in the g_{av} value of the complexes in DMF solution from the g_{av} value calculated in the solid state can be attributed to the variation in the geometric environment of the compounds upon dissolution.

The EPR spectra of the compounds in frozen DMF (77 K) (Figure 2b.5) show well resolved four hyperfine lines corresponding to monomeric copper(II) complexes. The $g_{\|} > g_{\perp}$ values suggest a distorted square pyramidal geometry rather than a bipyramidal geometry that is expected to have $g_{\|} < g_{\perp}$. The clearly resolved five **shf** lines in the $g_{\|}$ features (M_I= -3/2, or M_I =-1/2) of compounds **2**, **3**, **4**, **5**, **6**, and **8** show that the coordination of two nitrogens are coplanar [24] i.e., one of azomethine nitrogen and that of one nitrogen of the coordinated bases, whereas the apical nitrogen of the heterocyclic base does not make a significant contribution to the superhyperfine splitting. All the spectra were simulated to get accurate values of various magnetic parameters (Figure 2b.6). The EPR parameters $g_{\|}$, $g_{\perp}$, g_{av}, $A_{\|}$ (Cu) and $A_{\perp}$ (Cu) and energies of d-d transitions were used to evaluate the bonding parameters α^2, β^2 and γ^2 which may be regarded as measures of covalency of the in-plane σ bonds, in-plane π bonds and out-of-plane π bonds, respectively. The $g_{\|}$ values (2.190 to 2.201) are almost the same for all the compounds, which indicate a more or less axial geometry for all the complexes in solution but are different from that in the solid state. It can be inferred that the geometry of the compounds undergoes changes upon dissolution in polar coordinating solvents. Though it can be assumed that the polar solvents that coordinates via oxygen or sulfur does not occupy the equatorial position, but more or less helps to create an average **SP** geometric environment around copper [25], the probability of occupation of a permanent coordination position around copper can be

ruled out as the single crystal isolated from DMF lacks the solvent in its coordination sphere. The $g_{\parallel}$ values of the complexes are nearly the same ($\approx$ 2.198) indicating that the bonding is dominated by the thiosemicarbazone moiety. Since the values of $g_{\parallel}$ are much smaller than 2.3, significant covalency can be assumed in bonding [26a,b]. The g_{av} values of compounds **1**, **4** and **5** does not vary much (Table 2b. 8), while the value increases for compound **3**, **6** and **8**, and decreases for **2** and **7**, from the g_{av} values observed in the solid state. This variation can be attributed to the variation in the overall geometry and resulting change in the covalency of the bonds, which decreases with increase in covalency.

In all the compounds $g_{\parallel} > g_{\perp} > 2.00$ and $G = (g_{\parallel} - 2)/ (g_{\perp}-2)$ values are less than 4.4 which are consistent with a $d_{x^2-y^2}$ ground state with small exchange coupling [27]. The value of in-plane π bonding parameter α^2 can be estimated from the expression [23a, 2b.25].

$$\alpha^2 = A_{\parallel}/0.036 + (g_{\parallel} - 2.0023) + 3/7(g_{\perp} - 2.0023) + 0.04$$

The orbital reduction factors, $K_{\parallel} = \alpha^2 \beta^2$ and $K_{\perp} = \alpha^2 \gamma^2$ were calculated using the following expressions [28a,b]

$$K_{\parallel}^2 = (g_{\parallel}-2.0023)\ \Delta E(d_{xy} \rightarrow d_{x^2-y^2})/8\lambda_o$$
$$K_{\perp}^2 = (g_{\perp}-2.0023)\ \Delta E(d_{xz,yz} \rightarrow d_{x^2-y^2})/2\lambda_o$$

Where λ_o = is the spin-orbit coupling constant and is of a value of -828 cm^{-1} for copper(II) d^9 system.

According to Hathaway [29b], for pure σ bonding $K_{\parallel} \approx K_{\perp} \approx 0.77$, for in-plane π bonding $K_{\parallel} < K_{\perp}$, while for out-of-plane π bonding $K_{\parallel} > K_{\perp}$. It is seen that in all the complexes $K_{\parallel} < K_{\perp}$, which suggests stronger in-plane π bonding. This is further supported by the values of the bonding parameters $\alpha^2(\approx 0.74)$, β^2 ($\approx$ 0.89) and $\gamma^2(\approx$ 0.94) having values less than 1.0, which also indicate that there is significant covalent bonding. This is because the value 1.0 is expected for 100% ionic character, and decreases on increasing the covalent character of the bonding. The α^2 value is closer to that found for N-S donor ligand adducts. This observation supports the argument that there is significant in-plane π- bonding and in-plane σ bonding.

The Fermi contact hyperfine interaction term, which is a measure of the contribution of the s electrons to the hyperfine interaction, can be estimated from the expression:

$$K_{\parallel} = A_{iso}/P\beta^2 + (g_{av}-2.0023)/\beta^2$$

This is a dimensionless quantity and is generally found to have a value of 0.3. The values calculated are in the range of 0.3 for all the complexes (Table 2b.8). The empirical factor $f = g_{\parallel}/A_{\parallel}$ (cm) is an index of tetrahedral distortion [30]. The value may vary from 105 to 135 for small to extreme distortion. It is seen that for all of our compounds the f value is *ca.* 126 cm, which indicate medium distortion from planarity.

2b.3.5. Cyclic voltammetry

The electrochemical properties of metal complexes, particularly with sulfur donor atoms have been studied in order to monitor spectral and structural changes accompanying electron transfer [31]. In the positive range, +1.0 to 0.0 V, the oxidation processes Cu(III)/Cu(II) can be observed, while scanning in the negative range, between 0.0 V and –1.5 V, permits the study of copper reduction centred process and the ligand reductions; the potential reduction of the Cu(II)/Cu(I) process is related to potential Super Oxide Dismutase mimetic activity. Cyclic voltammetric measurements of all the compounds (**1-8**) were carried out. The results are tabulated in Table 2b.9.

A representative cyclic voltammogram of compound **5** is shown in Figure 2b. 7. The peak at -0.38 V, -0.95 V corresponds to successive copper(II) reduction processes The peak at –0.38 V corresponds to $Cu^{II/I}$ redox couple (denoted by A) and the one at –0.95 V (denoted by B) corresponds to copper(I)/copper(0) reduction process [32]. The earlier reports suggests that the copper(II) to copper(I) redox process is a completely reversible or quasi-reversible one-electron process [33, 106b]. This variation could be due to a series of coupled processes that immediately follows the reduction process. It has been shown that copper(II)/copper(I) redox process is influenced by coordination, stereochemistry, and the hard/soft character of the ligand donor atoms. However, due to inherent difficulties in relating coordination number and stereochemistry of the species present in solution, the redox process is generally described in terms of the nature of the ligands present [34]. Patterson and Holm [35] have shown that softer ligands tend to give more positive E° values, while hard acids give rise to more negative E° values. The observed values for these thiosemicarbazone complexes indicate considerable "hard acid" character, comparable to ligands like ethylenediamine (E° = -0.35 V), which is likely to be due to phenolato oxygen, azomethine nitrogen and thiolate sulfur atoms. It has also been observed earlier that with the increase in basicity of the coordinating atom, the metal ligand σ-bond strength increases and as a result the metal centred reduction potential decreases [36]. The changes in ^{4}N alkyl moiety is not affecting the E° values appreciably and is comparable to other copper(II)/copper(I) couples [37]. The irreversible peak at –1.30 V (denoted by point C) may correspond to the reduction of the conjugated portion of the thiosemicarbazone ligand [38], and its value, -1.15 to –1.3 V, which is comparable with the values observed for many thiosemicarbazone ligands (i.e., -1.31 V) [39]. An anodic peak at +0.68 V associated with the cathodic peak at +0.625 V is due to a quasi-reversible one electron transfer of copper(III)/copper(II) redox couple [40]. The ΔE_p values fall in the range 50-70 mV for scan rates 100-500 mV/s, which also supports the above conclusion.

2b.3.6. Biological activity

All copper complexes (**1-8**) along with their parent thiosemicarbazone ligands were screened against two bacterial cultures viz., *E. Coli* and *Staphylococass Aureus*, and two fungal cultures viz., *Candida Albicans* and *Asperigillus Flavus*. The 'well method' [41] was adopted for the activity measurements. The bacteria and fungi were grown in Nutrient and Sabouraud dextrose agar slants and the viable bacterial cells and fungal spores were swabbed onto Nutrient agar and Sabouraud dextrose agar plates, respectively. The compounds to be tested were dissolved in DMF to a final

concentration of 0.1%. 0.5 cm diameter well was cut in a medium inoculated with the respective cultures, and the solutions of the compounds in different concentrations (5 μg and 1 μg for bacterial cultures and 50 μg and 20 μg for fungal cultures) were allowed to stay in the wells. The petri-plates were incubated for 36 hours for bacteria and 76 hours for the fungal culture respectively. All the compounds were screened against a standard viz., Flucanazole for fungal cultures and Gentamycin for bacteria cultures, in their standard concentration(200μg/well). The activity of the compounds was counted by measuring the inhibition zone around the respective wells. The results are tabulated in Table 2b. 10.

The copper complexes were found to be more active than uncomplexed thiosemicarbazones, and the concentration is not having significant effect on the inhibitory activity of the compounds. The compounds are having potential inhibitory activity to a concentration as low as 1μg/well for bacterial cultures and 20μg/well for fungal cultures. The 2-hydroxyacetophenone morpholine-3-thiosemicarbazone (H_2L^3) and its copper-phenanthroline base adduct (Compound **6**), is found to be more active against bacteria *E. Coli*, followed by compound **5**, **4**, **3**, **2** respectively. However, compounds **2**, **4** and **6** are more active against bacteria *Staphylococcus Aureus* among complexes, while H_2L^3 showed better activity among uncomplexed thiosemicarbazones. Though the complexes are less effective against the fungal culture *Asp. Flavus* compounds **3**, **4** and **5** are found to have better growth inhibitory activity. Compound **2** shows potential growth inhibitory activity against culture *Candida Albicans*, followed by compounds **5** and **6**.

Compound **1, [CuL1bipy]**:

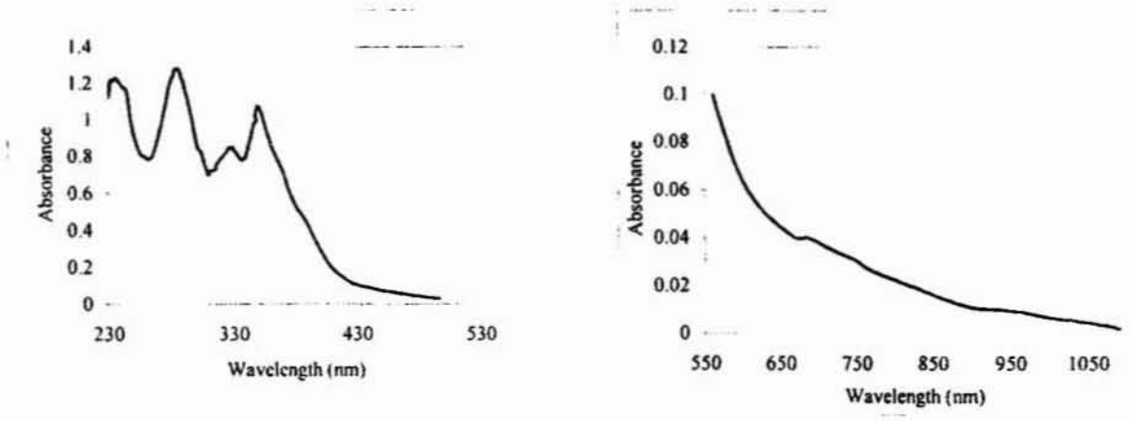

Compound **4, [CuL^{2}phen]**:

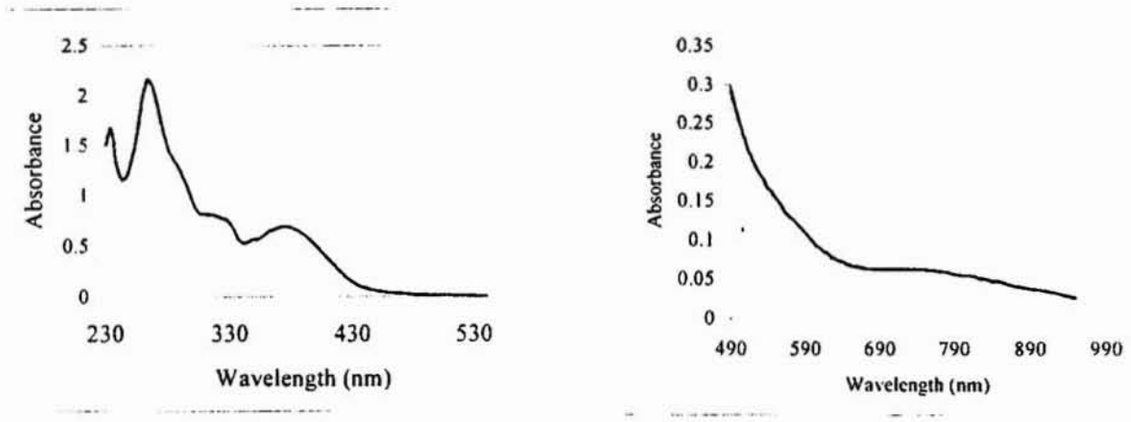

Compound **8, [CuL^{4}phen]**:

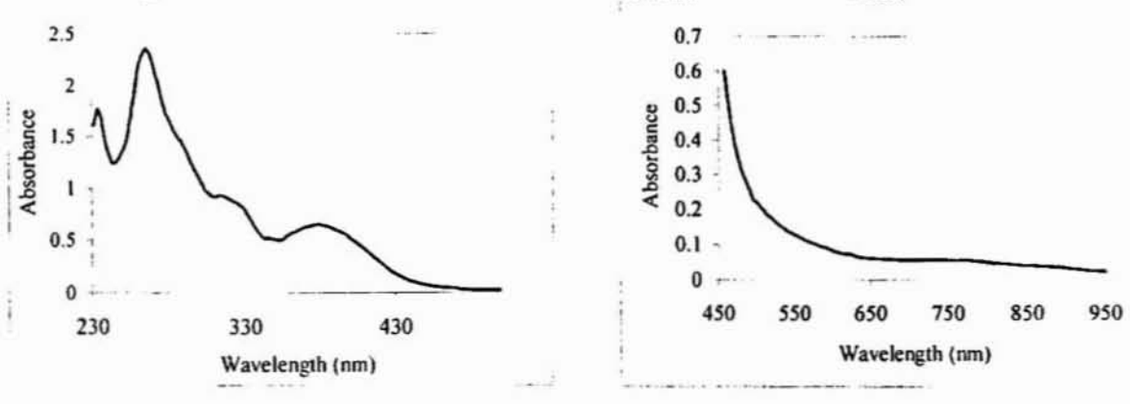

Figure 2b. 2: Electronic spectra of the compounds **1, 4** and **8.**

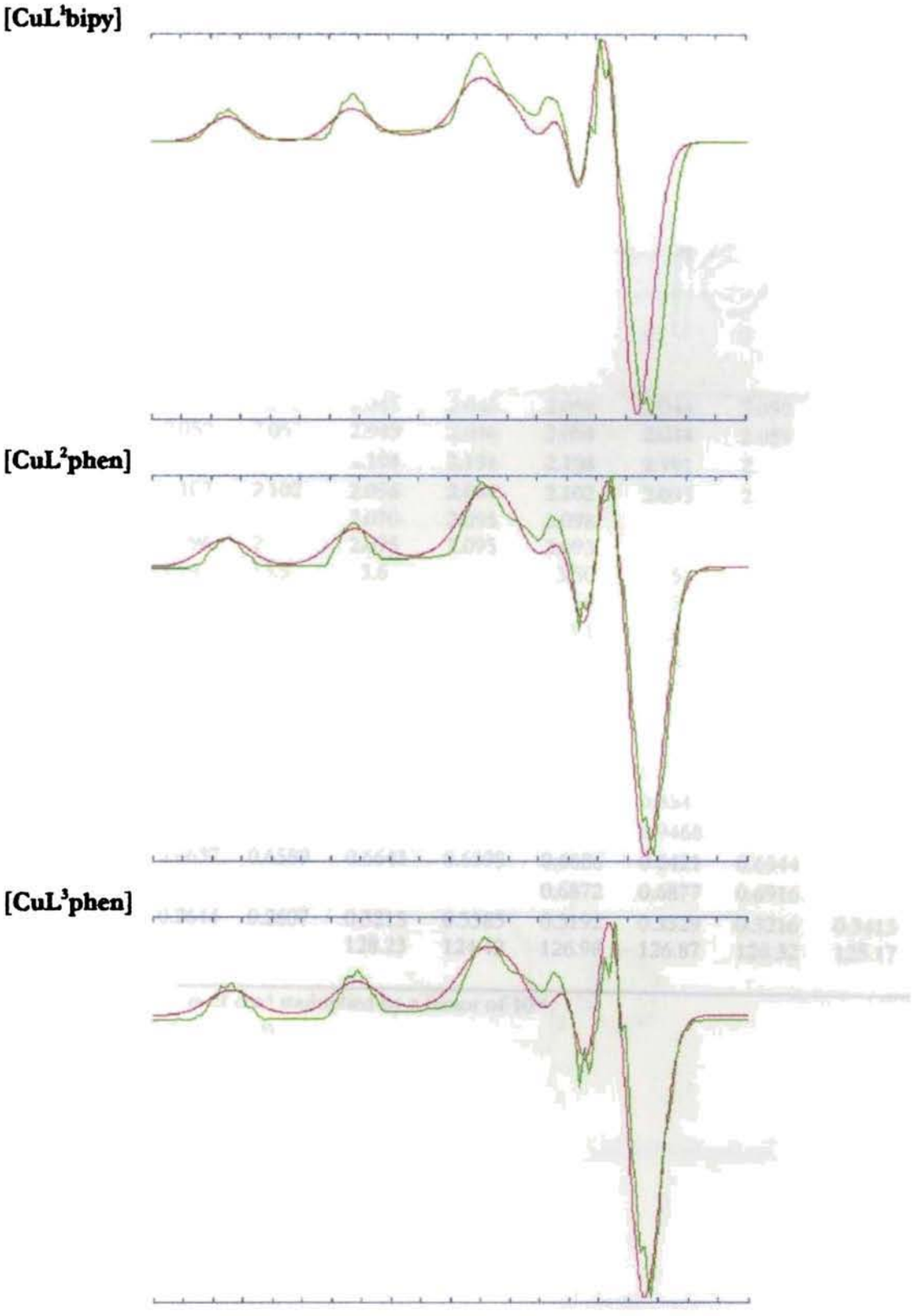

Figure 2b. 6: Simulated best fits superimposed over the experimental spectra for Compounds **1, 4** and **5**

Table 2b.8: Molecular magnetic and bonding parameters for compounds **1-8**

Compound	**1**	**2**	**3**	**4**	**5**	**6**	**7**	**8**
g_{xx}	2.054	2.053	2.045	2.046	2.054	2.044	2.059	2.053
$g_{\perp}$/ g_{yy}	2.052	2.053	2.049	2.046	2.054	2.044	2.059	2.053
$g_{\parallel}$ / g_{zz}	2.201	2.201	2.194	2.191	2.198	2.191	2.198	2.198
g_{av} (77 K)	2.102	2.102	2.096	2.094	2.102	2.093	2.105	2.101
g_{av} (solid)	2.095	2.125	2.070	2.095	2.098	2.067	2.123	2.067
g_{av} (DMF)	2.096	2.096	2.095	2.095	2.093	2.095	2.098	2.093
$A_{xx}{}^{a}$	13.4	13.5	13.6	13.81	13.50	14.5	13.5	13.5
$A_{\perp}{}^{a}$/ $A_{yy}{}^{a}$	13.0	13.5	13.0	13.81	13.50	14.5	13.5	13.5
$A_{\parallel}{}^{a}$ / $A_{zz}{}^{a}$	173.6	171.6	171.1	176.1	173.1	172.7	171.4	175.6
$A_{iso}{}^{a}$	49.64	50.14	70.90	71.79	69.66	71.80	68.57	71.80
G (77 K)	3.92	3.92	4.29	4.32	3.79	4.53	3.45	3.86
G (solid)	3.18	----	2.76	4.28	4.02	----	3.02	----
R^{c}	----	----	0.326	0.134	0.161	----	----	----
α^2	0.7426	0.7371	0.7265	0.7365	0.7387	0.7263	0.7352	0.7452
β^2	0.8937	0.8939	0.9143	0.8687	0.9051	0.8841	0.8901	0.9006
γ^2	0.9588	0.9765	0.9506	0.9409	0.9303	0.9468	0.9409	0.9889
$K_{\parallel}$	0.6637	0.6589	0.6643	0.6398	0.6686	0.6421	0.6544	0.6711
$K_{\perp}$	0.7120	0.7198	0.6906	0.6871	0.6872	0.6877	0.6916	0.7369
K_0	0.2644	0.2607	0.3215	0.3385	0.3192	0.3329	0.3216	0.3413
f^{b} (cm)	126.78	128.26	128.23	124.42	126.98	126.87	128.32	125.17

[a] expressed in units of cm^{-1} multiplied by a factor of 10^{-4}

[b] parameter $f = g_{11}/ A_{11}$ cm.

[c] parameter $R = (g_2-g_1)/(g_3-g_2)$

Table 2b.9: Cyclic Voltammetric data[a]

Compound	Oxidation $E_{1/2}$/V	Reduction -$E_{1/2}$ /V
[CuL^1bipy]	0.64[b]	0.70[c], 1.05[b], 1.20[b]
[CuL^1phen]	0.41[b]	0.38[b], 0.95[b], 1.30[b]
[CuL^2bipy]	0.62[c]	0.38[b], 0.91[c], 1.30[b]
[CuL^2phen]	0.64[c]	0.41[b], 0.95[c], 1.30[b]
[CuL^3bipy]	0.64[c]	0.36[c], 0.91[c], 1.31[c]
[CuL^3phen]	0.38, 0.61[b]	0.38[b], 0.94[c], 1.31[b]
[CuL^4bipy]	0.32	0.51[c], 0.91, 1.15
[CuL^4phen]	---	0.76

[a] The reported data corresponds to a scan rate of 200 mV/s
[b] irreversible redox response
[c] quasi-reversible $i_{pa}>i_{pc}$
Table 2b.8: Molecular magnetic and bonding parameters for

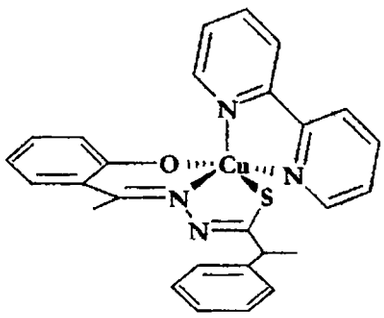

Figure 2b.1.: The approximate structure proposed for compound 4 based on EPR and electronic data.

Table 2b.1: Elemental analysis data of copper(II) complexes

Compound	Color	Found (calcd.) (%)								Magnetic moment BM
		C		H		N		Cu		
CuL^1bip (**1**)	Greenish brown	59.62	(58.98)	5.50	(5.35)	14.26	(13.76)	13.05	(12.48)	1.95
CuL^1phen (**2**)	Brown	60.91	(60.83)	5.11	(5.10)	12.74	(13.14)	11.53	(11.92)	1.75
CuL^2bip (**3**)	Greenish brown	59.01	(58.98)	5.42	(5.35)	13.07	(13.76)	11.90	(12.48)	1.88
CuL^2phen (**4**)	Greenish brown	60.96	(60.83)	5.14	(5.10)	12.49	(13.14)	12.00	(11.92)	1.95
CuL^3bip (**5**)	Olive green	55.92	(55.58)	4.74	(4.66)	13.55	(14.09)	13.17	(12.78)	1.73
CuL^3phen (**6**)	Greenish brown	57.79	(57.62)	4.48	(4.45)	13.10	(13.44)	11.65	(12.19)	1.72
CuL^4bip (**7**)	Pale brown	61.20	(60.39)	4.53	(4.48)	13.16	(13.54)	11.77	(12.29)	1.93
CuL^4phen (**8**)	Olive green	62.78	(62.15)	4.22	(4.28)	13.10	(12.94)	11.06	(11.74)	1.87

Table 2b.5: Electronic spectral assignments, $\lambda/cm^{-1}(\log\varepsilon^a)$ for compound **1-8**

Compound	d-d	LMCT	n→π*	π→π*
CuL^1bipy (**1**)	14705(2.03), 16920(2.43)	28531 (3.87) 27100 sh (3.62)	35273 (4.13), 30902 sh (3.96)	42283 (4.11)
CuL^1phen (**2**)	14492(1.84), 16750(2.14)	28571 (3.41) 27972 sh (3.38)	32414 (3.92)	43103 (4.22), 37313 sh (4.24)
CuL^2bipy (**3**)	15267(2.18), 17699(2.49)	22727 sh (3.19), 27932 (4.24)	35335 (4.34)	41067 (4.37)
CuL^2phen (**4**)	14388(2.07), 17921(2.43)	26560 (4.20)	30581 sh (4.25), 34722 sh (4.46)	38095 (4.66), 42553 (4.54)
CuL^3bipy (**5**)	15151(2.11), 17699(2.46)	22624 (3.29), 28129 sh (4.20)	34843 sh (4.49)	41068 (4.43), 37665 (4.43)
CuL^3phen (**6**)	14492(2.11), 17544(2.38)	21739 sh (2.99), 26560 (4.06)	34843 sh (4.43), 31250 sh (4.19)	42644 (4.49), 37665 (4.62)
CuL^4bipy (**7**)	14514(2.04), 17361(2.48)	22222 sh (2.90), 28530 (4.16)	30534 (4.06), 35149 sh (4.32)	42105 (4.23), 37879 (4.03)
CuL^4phen (**8**)	15267(2.14), 17241(2.37)	21265 (3.02), 26525 (4.20)	31746 sh (4.36), 35026 (4.56)	42735 (4.74), 37807 (4.63)

[a] = ε is expressed in ($l\ mol^{-1}cm^{-1}$)

Table 2b.6: IR spectral assignments for 4 ligands and their copper complexes[1](All absorptions are given in units of cm^{-1})

Compound	ν ($^{7}C=N^{1}$)	ν ($^{2}N=C^{9}$)	ν ($^{1}N-N^{2}$)	ν (Cu-N)	ν/ δ (C=S)	ν (C-O)	Bands due to heterocyclic base
H_2L^1	1599s	-	988 m	-	1365 m, 826 m	1219 s	-
CuL^1bipy (1)	1566 m	1592 s	1022 m	432 w	1337 s, 768 m	1152 s	1439m, 735m, 747w
CuL^1phen (2)	1565 m	1590 s	1028 m	424 w	1329 s, 764 m	1150 s	1431 m, 725 w, 763 m, 845 m
H_2L^2	1603 s	-	997 m	-	1383 s, 839 m	1252 s	-
CuL^2bipy (3)	1557 m	1592 s	1024 m	426 w	1337 m, 742 m	1204 s	1437 m, 1424 m, 650 w, 623 w
CuL^2phen (4)	1557 m	1588 s	1026 m	430 w	1333 m, 750 m	1194 s	1485m, 1460m, 845 m, 725 m, 636 w
H_2L^3	1605 s	-	1017 m	-	1374, 835 m	1219 s	-
CuL^3bipy (5)	1559 m	1592 s	1022 m	426 w	1341s, 803 m	1132 s	1439 m, 735 m, 650 w, 762 w
CuL^3phen. (6)	1559 m	1593 s	1028 m	430 w	1341 s, 803 m	1138 s	1482 m, 1450 m, 727 m, 845 m
H_2L^4	1601 s	-	995 m	-	1375 s, 808 m	1222 s	-
CuL^4bipy (7)	1559 m	1593 s	1019 m	432 w	1345 m, 766 m	1142 s	756 m, 745 w
CuL^4phen (8)	1563 m	1593 s	1022 m	430 w	1340 m, 750 m	1134 s	727 m, 638 w

Table 2b.7: EPR spectral assignments of copper complexes (experimentally determined)

Compound	Solid (298 K)		DMF soln. (298 K)			DMF (77 K)				
	g_0/ $g_{\|\|}$ / g_3	$g_\perp$/g_1, g_2,	g_0	$A_0^{\#}$	$A_N^{\#}$	$g_{\|\|}$	$g_\perp$	g_{av}	$A_{\|\|}^{\#}$	$A_\perp^{\#}$ (N)
CuL^1bipy (1)	$g_{\|\|}$ 2.1730	$g_\perp$ 2.0560	2.0960	50.62	20.0	2.1937	2.0535	2.1002	170.0	13.1
CuL^1phen (2)	g_0 2.1249	----	2.0967	51.25	19.0	2.1907	2.0483	2.0957	172.0	14.0
CuL^2bipy (3)	g_3 2.1204	g_1 2.0346 g_2 2.0557	2.0948	72.33	18.5	2.1937	2.0521	2.0993	170.0	---
CuL^2phen (4)	g_3 2.1917	g_1 2.0375 g_2 2.0557	2.0953	73.33	20.0	2.1915	2.0496	2.0969	173.3	14.5
CuL^3bipy (5)	g_3 2.1936	g_1 2.0392 g_2 2.0606	2.0928	71.33	18.5	2.1900	2.0515	2.0977	170.0	14.2
CuL^3phen (6)	g_0 2.0671	----	2.0953	73.33	15.0	2.1899	2.0509	2.0972	171.7	14.2
CuL^4bipy (7)	$g_{\|\|}$ 2.2200	$g_\perp$ 2.0745	2.0934	70.00	----	2.1900	2.0522	2.0981	166.7	---
CuL^4phen (8)	$g_{\|\|}$ 2.2091	$g_\perp$ 2.0672	2.1064	73.33	19.2	2.1739	2.0587	2.0971	173.3	13.0

[#] All '*A*' values are reported in units of Gauss.

[1]All IR spectral measurements were done as KBr disc.

Table 2b.10: Biological activity measurements of copper(II) complexes*

Complex/ligand	*E.Coli*		*Staphylococus*		*Asp. Flavus*		*C. Albicans*	
	5μg	1μg	5μg	1μg	50μg	20μg	50μg	20μg
H_2L^1	17.2 ± 0.3	15.2 ± 0.5	19.2 ± 0.5	18.0 ± 0.2	09.5± 0.3	09.5 ± 0.3	11.1± 0.2	10.0 ± 0.4
CuL^1bip.(**1**)	18.0 ± 0.7	16.0 ± 0.3	19.4 ± 0.3	18.2 ± 0.4	11.2 ± 0.5	11.0 ± 0.5	12.0 ± 0.5	11.0 ± 0.3
CuL^1phen (**2**)	18.2 ± 0.5	17.4 ± 0.7	23.0 ± 0.4	22.3 ± 0.2	14.0 ± 0.2	13.0 ± 0.4	26.2 ± 0.3	27.0 ± 0.5
H_2L^2	18.0 ± 0.5	17.2 ± 0.2	17.0 ± 0.3	16.0 ± 0.2	15.0 ± 0.3	13.2 ± 0.3	11.0 ± 0.4	12.0 ± 0.3
CuL^2bip (**3**)	19.2 ± 0.3	17.5 ± 0.3	17.2 ± 0.4	16.3 ± 0.3	18.1 ± 0.4	18.0 ± 0.4	15.0 ± 0.5	13.0 ± 0.4
CuL^2phen (**4**)	18.5 ± 0.4	18.1 ± 0.4	23.0 ± 0.5	22.2 ± 0.4	19.0 ± 0.5	19.0 ± 0.5	18.0 ± 0.2	15.0 ± 0.2
H_2L^3	19.1 ± 0.2	16.0 ± 0.5	24.2 ± 0.4	22.0 ± 0.3	10.0 ± 0.3	10.0 ± 0.4	11.0 ± 0.3	11.0 ± 0.4
CuL^3bip (**5**)	19.5 ± 0.7	17.2 ± 0.3	19.1 ± 0.3	18.3 ± 0.4	19.0 ± 0.4	17.0 ± 0.2	23.0 ± 0.5	22.0 ± 0.3
CuL^3phen (**6**)	20.3 ± 0.3	19.4 ± 0.3	23.2 ± 0.2	22.5 ± 0.3	15.2 ± 0.4	14.0 ± 0.4	24.0 ± 0.2	25.0 ± 0.4
H_2L^4	15.2 ± 0.2	15.2 ± 0.5	17.0± 0.3	16.0 ± 0.5	09.5 ± 0.3	09.5 ± 0.3	10.0 ± 0.3	10.0 ± 0.5
CuL^4bip (**7**)	15.5 ± 0.5	14.0 ± 0.7	19.2 ± 0.5	17.2 ± 0.3	13.0 ± 0.2	12.2 ± 0.4	22.0 ± 0.4	21.0 ± 0.2
CuL^4phen (**8**)	14.4 ± 0.7	13.0 ± 0.5	18.6 ± 0.6	16.5 ± 0.4	16.0 ± 0.3	14.0 ± 0.3	17.0 ± 0.3	16.0 ± 0.4
Gentamycin/ Flucanazole #	26.0 ± 2.0	26.0 ± 2.0	30.0 ± 2.0	30.0 ± 0.2	20.0 ± 0.5	20.0 ± 0.5	22.0 ± 0.2	22.0 ± 0.2

* All measurements are in mm diameter of the inhibition zone (9.0 mm indicates no inhibition)

\# Commercially available anti-microbial agents

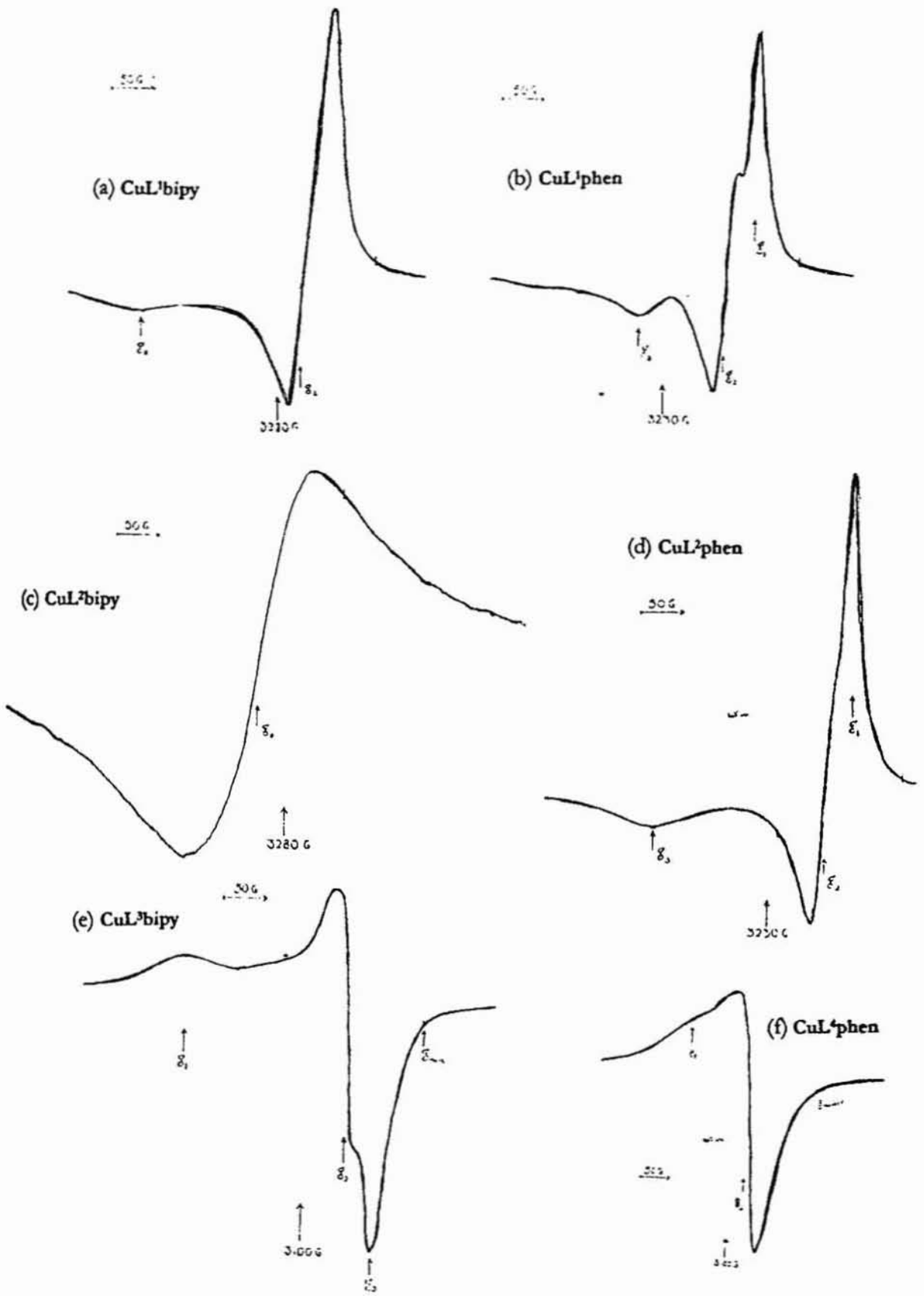

Figure 2b. 3· EPR spectra of copper(II) complexes in polycrystalline state at 298 K.
a) compound **1**, b) compound **2**, c) compound **3**, d) compound **4**,
e) compound **5**, f) compound **8**.

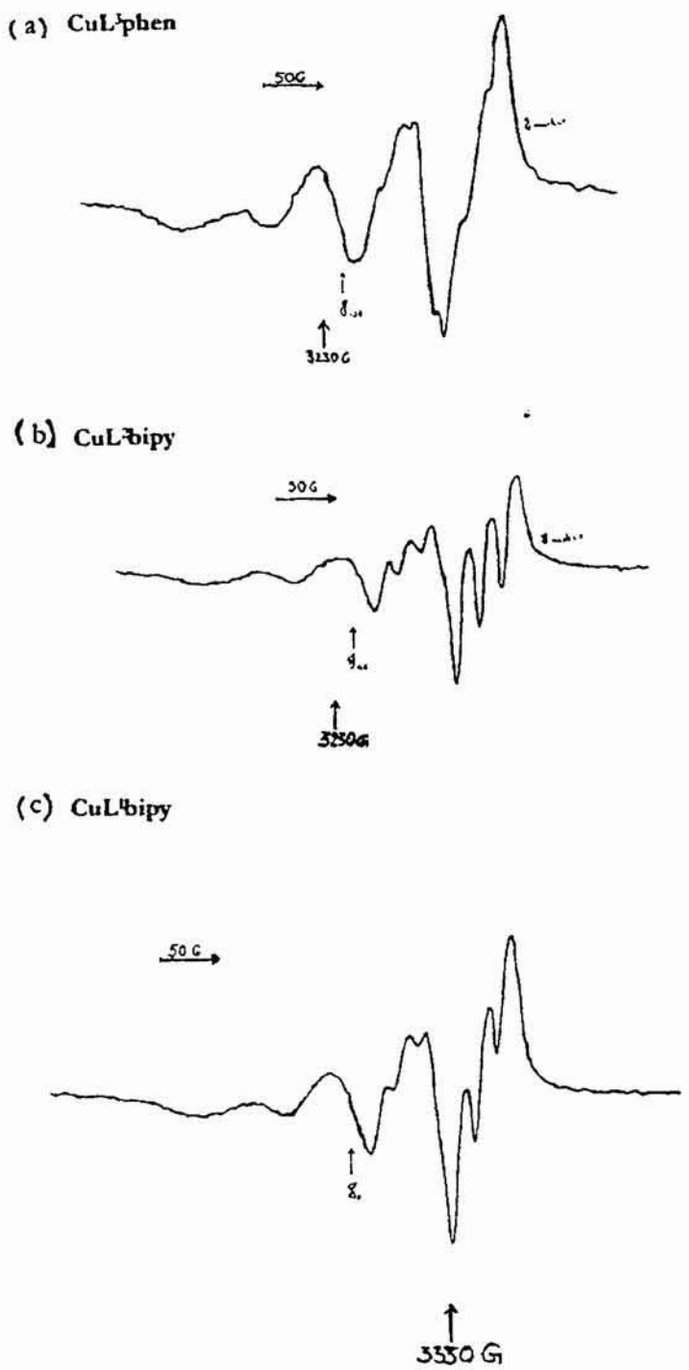

Figure 2b. 4. EPR spectra of copper(II) complexes in DMF at 298 K. a) compound **6**, b) compound **3**, c) compound **1**

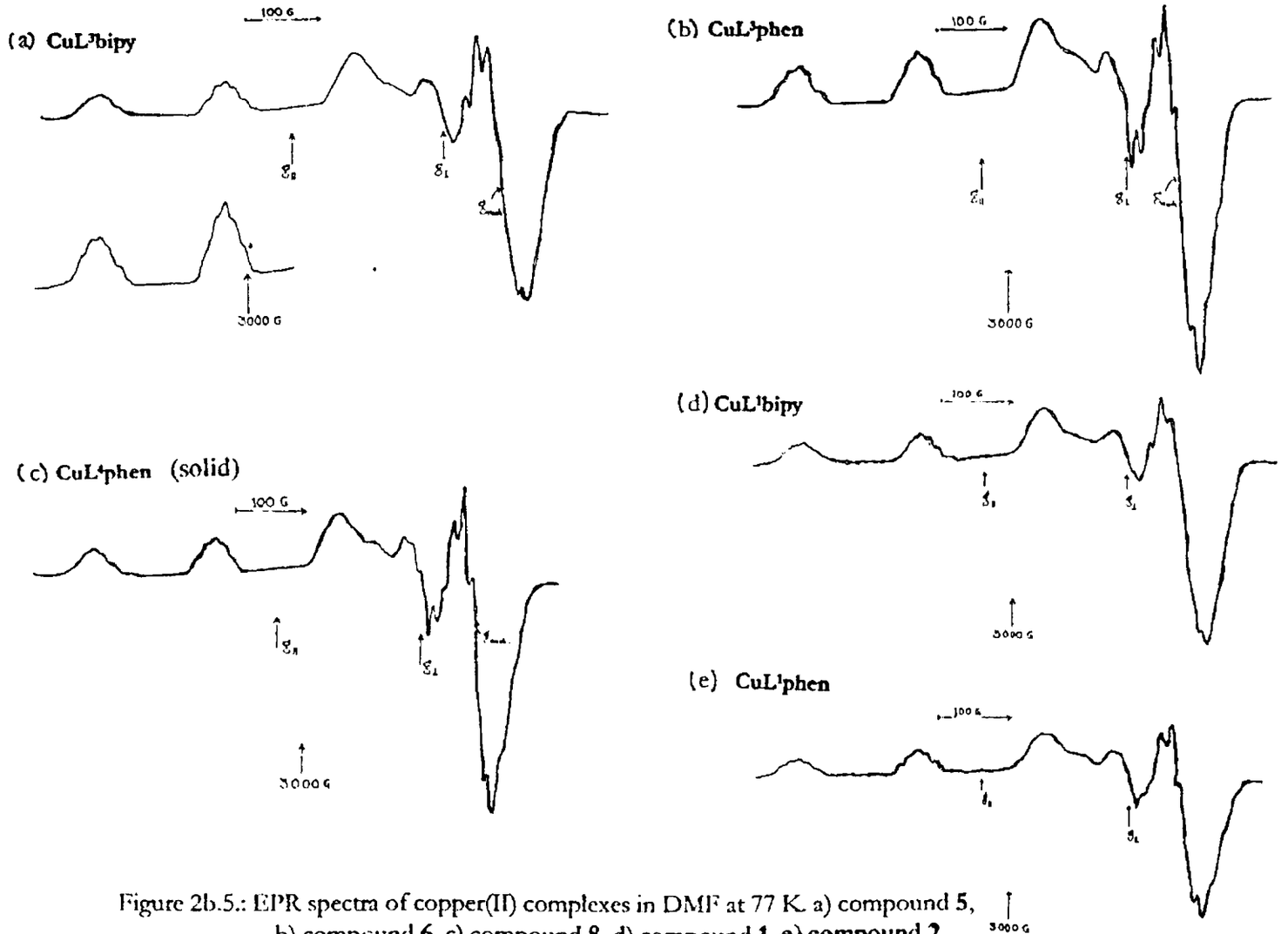

Figure 2b.5.: EPR spectra of copper(II) complexes in DMF at 77 K. a) compound **5**, b) compound **6**, c) compound **8**, d) compound **1**, e) compound **2**

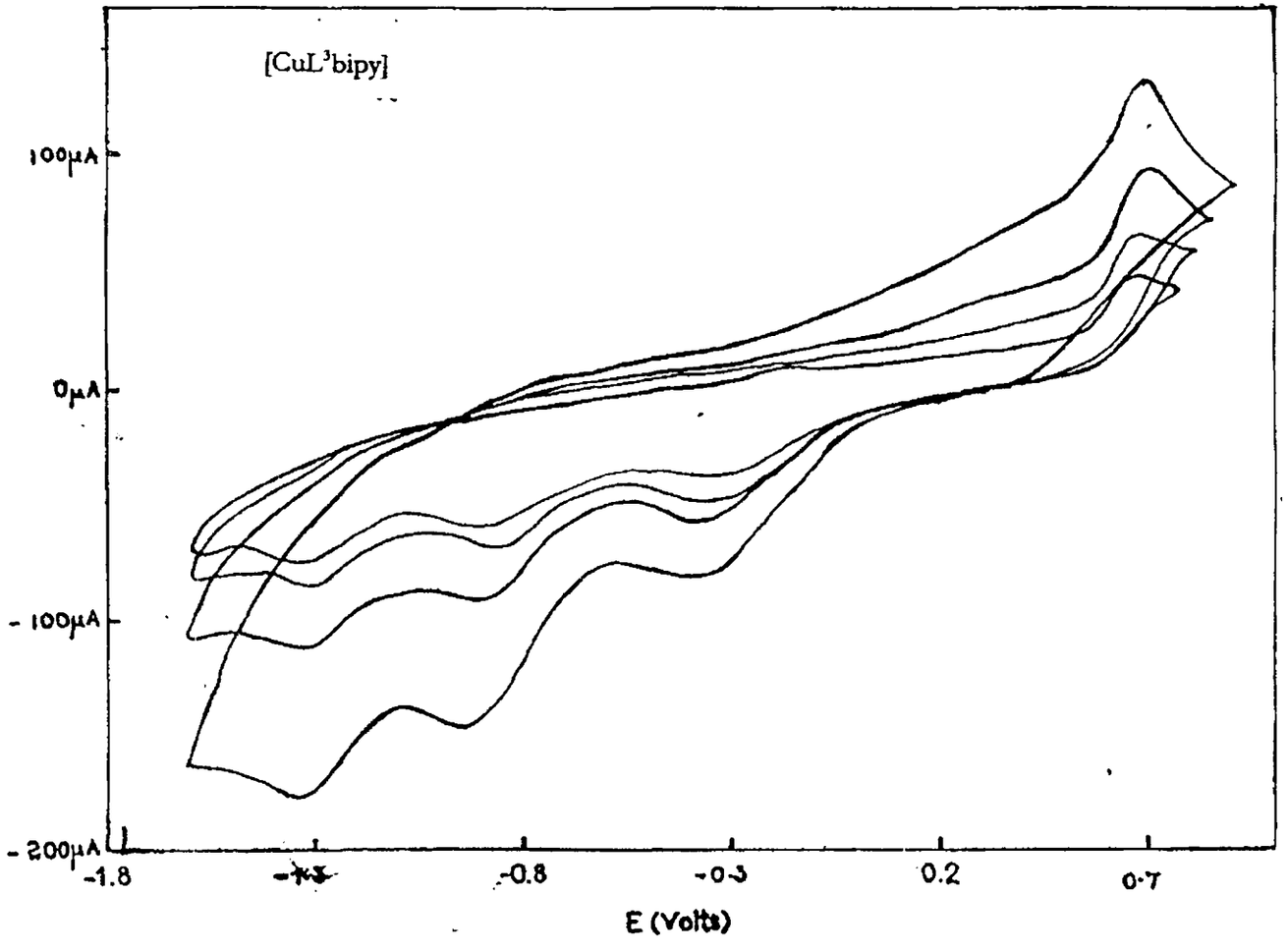

Figure 2b.7.; Cyclic voltammogram of compound 5

REFERENCES

2b.1 K. D. Karlin, and J. Zubieta (ed.), (a) 'Copper Coordination Chemistry: Biological and Inorganic Perspectives'. Adenine Press, NY, 1983; (b) 'Biological and Inorganic Copper Chemistry', Adenine Press, NY, 1986.

2b.2 E. Ochiai, 'Bioinorganic Chemistry, An Introduction', Allyn and Bacon, Boston, 1977.

2b.3 (a) K. Seff, *Acc. Chem. Res.*, 1976, **9**, 121; H. S. Lee and K. Seff, *J. Phys. Chem.*, 1981, **85**, 397; H. S. Lee, W.V. Cruz and K. Seff, *J. Phy. Chem.*, 1982, **86**, 3562; (b) R. Osterberg, *Coord. Chem. Rev.*, 1974, **12**, 309; (c) E. I. Solomon, K.W. Penfield and D. E. Wilcox, *Struct. Bonding (Berlin)*, 1983, **53**, 1.

2b.4 J. P. Scovill, D. L. Klayman and C. F. Franchino, *J. Med. Chem.*, 1982, 25, 1261.

2b.5 B. S. Garg, M. R. P. Kurup, S. K. Jain and Y. K. Bhoon, *Transition Met. Chem.*, 1988, 13, 309; D. X. West, D. A. Bain, R. J. Butcher, J. P. Jasinski, R. Y. Pozdniakiv, R. A. Toscano and S. H. Ortega, Polyhedron, 1996, **15**, 665.

2b.6 M. A. Ali, D. A. Chowdhary and M. Nazimuddin, *Polyhedron*, 1984, **3**, 595.

2b.7 E. W. Ainscough, A. M. Brodie, J. D. Ranford and J. M. Waters, *J. Chem. Soc., Dalton Trans.*, 1991, 1737.

2b.8 B. N. Figgis and R. S. Nyholm, *J. Chem. Soc.*, 1958, 4190.

2b.9 *CAD4 Software*, Version 5.0, Delft, The Netherlands, 1989.

2b.10 G. M. Sheldrick, SHELXS 97, Program for the Solution of Crystal Structures, University of Göttingen: Göttingen, Germany, 1997.

2b.11 G. M. Sheldrick, SHELXS 97, Program for Crystal Structure Refinement, University of Göttingen, 1997.

2b.12 D. T. Cromer and J. T. Waber, International Tables for X-ray crystallography, Kynoch Press: Birmingham, U.K., 1974, Vol. 4.

2b.13 D. C. Creagh, W. J. McAuley, International Tables for X-ray Crystallography; A. J. C. Wilson, Ed., Kluwer, Boston, MA, 1992, p 219.

2b.14 A. G. Bingham, H. Bögge, A. MCller, E. W. Ainscough and A. M. Brodie, *J. Chem. Soc., Dalton Trans.*, 1987, 493.

2b.15 a) C. B. Castellani, G. Gatti and R. Millini, *Inorg. Chem.*, 1983, **23**, 4004; b) N. J. Ray and B. J. Hathaway, *Acta Crystallogr., Sect. B*, 1978, **34**, 3224; G. Druhan and B. J. Hathaway, *Acta Crystallogr., Sect. B*, 1979, **35**, 344.

2b.16 D. X. West, R. J. Butcher, *Trans. Met. Chem.*, 1993, **18**, 449; D. X. West, H. Gebremethin, R. J. Butcher, J. P. Jasinski and A. E. Liberta, *Polyhedron*, 1993, **12**, 2489.

2b.17 a) M. Soriano-Garcia, J. Valdez-Martinez and R. A. Toscano, *Acta Cryst.*, 1988, **C44**, 1247; b) D. X. West, A. Castineiras, E. Bermejo, *J. Mol. Struct.*, 2000, **120**, 503; c) H. Beraldo, R. Lima, L. R. Teixeira, A. A. Moura, D. X. West, *J. Mol. Struct.*, 2001, **559**, 99

2b.18 D.X. West, M. M. Salberg, G.A. Bain, A.E. Liberta, J. Valdez-Martinez, S. Hernandez-Ortega, *Trans. Met. Chem.*, 1996, **21**, 206; P. Bindu and M. R. P. Kurup, *Transition Met. Chem.*, 1997, **22**, 578.

2b.19 M. Mikuriya, H. Okawa and S. Kida, *Inorg. Chim. Acta*, 1979, **34**, 13; E. W. Ainscough, A. M. Brodie and N. G. Larsen, *Inorg. Chim. Acta*, 1982, **60**, 25.

2b.20 M. Mikuriya, H. Okawa and S. Kida, *Bull. Chem. Soc. Japan*, 1980, 53, 3717.

2b.21 A. A.G. Tomilson and B. J. Hathaway, *J. Chem. Soc.*, 1968, 1685; D. M. L. Goodgame, M. Goodgame, G. W. Canham Rayner, *J. Chem. Soc. A*, 1971, 1923.

2b.22 B. J. Hathaway and D. E. Billing, *Coord. Chem. Rev.*, 1970, **5**, 143; B. J. Hathaway, *Essays Chem.*, 1971, **2**, 61.

2b.23 I. M. Proctor, B. J. Hathaway and P. Nicholis, *J. Chem. Soc., A*, 1968, 1678;

M. J. Beu, B. J. Hathaway and R. J. Fereday, *J. Chem. Soc., A*, 1972, 1229; A. A. G. Tomlinson and B. J. Hathaway, *J. Chem. Soc. A*, 1968, 1905; B. J. Hathaway, *J. Chem. Soc., Dalton Trans.*, 1972, 1196.

2b.24 J. Jezierska, *Asian J. Chem.*, 1992, **4**, 189.

2b.25 J. Jezierska, B. Jezowska-Trzebiatowska and G. Petrova, *Inorg. Chim. Acta*, 1981, **50**, 153; J. Jezierska, A. Jezierski, B. Jezowska-Trzebiatowska and A. Ozarovski, *Inorg. Chim. Acta* 1983, **68**, 7; J. Jezierska, *Polyhedron*, 1987, **6**, 1669.

2b.26 a) A. H. Maki and B. R. McGarvey, *J. Chem. Phys.*, 1958, **29**, 35;
b) J. R. Wasson and C. Trapp, *J. Phys. Chem.*, 1969, **73**, 3763.

2b.27 M. J. Bew, B.J. Hathaway, R.R. Faraday, *J. Chem. Soc. Dalton Trans.*, 1972, 1229.

2b.28 D. Kivelson and R. Neiman, *J. Chem. Soc. Dalton Trans.*, 1961, **35**, 149.

2b.29 a) B. N. Figgis, *Introduction to ligand fields*, Interscience, NY, 1966, p 295;
b) D. X. West, *Inorg. Nucl. Chem.*, 1984, 73, 3169.

2b.30 U. Sakaguchi and A.W. Addison, *J. Chem. Soc., Dalton Trans.*, 1979, 600.

2b.31 A. M. Bond and R. L. Martin, *Coord. Chem. Rev.*, 1984, **54**, 23.

2b.32 D.X. West, A. E. liberta, S. B. Padhye, R. C. Chikate, P. B. Sonawane, A. S. Kumbhar and R. S. Yeranda, Coord. Chem. Rev. 1993, 123, 49 and references there in.

2b.33 A. S. Kumbhar, S. B. Padhye, D. X. West and A. E. Liberta, *Transition Met. Chem.*, 1991, **16**, 276.

2b.34 B. J. Hathaway in G. Wilkinson, R. D. Gillard and J. A. McCleverty (Eds.) *Comprehensive Coordination Chemistry*, Vol. 5, Pergamon, Oxford, 1987.

2b.35 G. S. Patterson, and R. H. Holm, J. Bioinorg. Chem., 1975, **4**, 257.

2b.36 S. Dutta, P. Basu, A. Chakravorthy, Inorg. Chem., 1991, **30**, 4031.

2b.37 H. B. Gray, *Transition Met. Chem.*, 1965, **1**, 239; G. N. Schrauzer, *Trans. Met. Chem.*, 1968, **4**, 299.

2b.38 Yu. P. Kitaev, G. K. Budnikov and A. E. Arbuzov, *Izv. Akad. Nauk SSR, Otd. Khim. Nauk.*, 1962, **2**, 244; 1965, **5**, 824.

2b.39 V. Eisner and E. Karowa-Eisner, in A. J. Bard and H. Lund (Eds.) *Encyclopedia of Electrochemistry of the Elements*, Marcel Dekker, NY, 1979, Vol.13, p 348.

2b.40 E. Franco, E. Lopez-Torres, M. A. Mendiola, M. T. Sevilla, Polyhedron, 2000, 19, 441.

2b.41 C. H. Collins, P. M. Lyne, Microbiological Methods, University Park Press, Baltimore, 1970, 422.

2b.42 (a) P. Bindu and M. R.P. Kurup, *Trans. Met. Chem.*, 1997, **22**, 578; (b) P. Bindu, M. R. P. Kurup and T. R. Satyakeerthy, *Polyhedron*, 1998, **18**, 321.

2b.43 K. Nakamoto, *Infrared and Raman Spectra of Raman and Coordination Compounds*, 3rd edn, John Wiley and Sons, NY, 1978.

2b.44 P. Bindu and M. R. P. Kurup, *Ind. J. Chem.*, 1997, **36A**, 1094.

CHAPTER 3

SYNTHESIS, SPECTRAL CHARACTERISATION AND ELECTROCHEMICAL STUDIES OF OXOVANADYL (IV) COMPLEXES

3.1. INTRODUCTION

Vanadium is an important trace element for different organisms. Oxovanadium(IV) and vanadate(V) are the main species present in solution under physiological conditions. The physiological effects are in many cases a consequence of good complexation behaviour of VO^{2+} ion, and the chemical similarity of phosphate and vanadate. The coordination chemistry of vanadium has received considerable attention since the discovery of vanadium in enzymes like bromoperoxidases and azotobacter vinelandii [1]. Its biological significance is further exemplified by its incorporation in natural product (amavadin in mushroom), in the blood of sessile marine organisms (*A. Museama-tunicates*) and in enzymes of potent inhibitor of phosphoryl transfer [2]. The recent investigations also support the fact that vanadium is involved in biological system in more than one way [3, 3.4]. The attempts to learn more of the coordination chemistry of vanadium in the blood of ascidians, various living specimen and sometimes the whole blood, were exposed to saline solution of a number of ligands including 2,2'-bipyridine. In some 'applousobranch' and 'phlebobranch' species that are known to concentrate vanadium in their blood cells [5], it was noted that an intense purple colouration was noted within the compartmental cells, and in some species unpigmented morula cells [6]. Some vanadium dependant bromoperoxidases (VBrPO) enzymes were isolated from marine algae [7] and terresterial lichen [8]. Vanadium bromoperoxidase catalyses peroxide dependant halogenation of organic compounds in the presence of halide ions. Thus vanadium has gained importance as an important element by catalysing both oxidative (peroxidase) and reductive (nitrogenase) catalytic processes in biological systems. A few vanadium compounds seems to have therapeutic effects [9]. But it has been established that vanadium compounds have insulin-mimetic properties [10]. A compound, bis(picolinato) oxovanadium(IV) [$VO(pic)_2$] has proved to be an orally active and long-acting insulin-mimetic compound with which insulin-dependant diabetes mellitus (IDDM) may be treated in rats [11]. In an effort to model these compounds an attempt was made to synthesise oxovanadium complexes of 2-hydroxyacetophenone N(4)-substituted thiosemicarbazones of our interest, and bidentate bases as bipyridine and phenanthroline, which is discussed in this chapter along with their spectral, and redox properties.

3.2. EXPERIMENTAL

3.2.1. Materials and Methods:

The ligands H_2L^1, H_2L^2, H_2L^3, and H_2L^4 were prepared as described in chapter 2b. $VO(acac)_2$ (Merck) was used as such; the bases, such as phenanthroline (Merck) and bipyridine (Merck) were used as received. The solvents were purified by standard procedures before use.

3.2.2. Physical measurements

The various physical measurements, such as elemental analysis, IR, electronic and EPR spectral measurement, magnetic moment, conductance and cyclic voltammetric techniques are described in Chapter 2b. The metal content was estimated by "peaceful pyrolisis" technique by converting a known quantity of the compound into its stable oxide as V_2O_5. The MALDI (Matrix Assisted Laser Desorption Ionisation) measurements of some selected compounds were carried out using a matrix of α-cyano-4-hydroxy cinnamic acid in 1:1 acetone-water mixture, on a Kartos PC Kompact MALDI VI 0.3 spectrometer at IISc., Bangalore. FAB mass spectra were recorded in Joel SX-120 FAB spectrometer at CDRI, Lucknow.

3.2.3 Preparation of the complexes

The syntheses of all vandyl complexes (**9-16**) were carried out under dinitrogen atmosphere employing standard Schlenk glassware and techniques.

To a stirred solution of the thiosemicarbazone (0.5 mmol) in dichloromethane (20 mL), under nitrogen atmosphere, was added vanadyl acetylacetonate {$VO(acac)_2$}(0.5 mmol). When the solution turned into a homogeneous brown solution, was added (0.5 mmol) of the base, bipyridine or phenanthroline, in 5 mL of a dichloromethane. The stirring was continued with mild refluxing for about an hour. The solution was then layered with hexane when micro crystals of the respective compounds crystallize out. The compounds were filtered off, washed with 1:5 mixture of dichloromethane-hexane, followed by ether and dried *in vacuo*.

Compound **9** [$C_{25}H_{27}N_5O_2SV$] F.W. 512.52: Analytical data: elemental. Found: C 58.87, H 5.35, N 13.41, V 9.28; Calcd C 58.59, H 5.31, N 13.66, V 9.98.
Compound **10** [$C_{27}H_{27}N_5O_2SV$] F.W. 536.54: Analytical data: elemental. Found: C 60.68, H 5.18, N 13.39, V 9.39; Calcd C 60.44, H 5.07, N 13.05, V 9.49; MALDI M^+(m/z) 537.1 (70), M^+-(16+1) (m/z) 521.1 (100).
Compound **11** [$C_{25}H_{27}N_5O_2SV$] F.W. 512.52: Analytical data: elemental Found: C 59.06, H 5.42, N 13.85, V 9.99; Calcd C 58.59, H 5.31, N 13.66, V 9.98; MALDI M^+-16 (m/z) 497.9 (100).
Compound **12** [$C_{27}H_{27}N_5O_2SV$] F.W. 536.54: Analytical data: elemental. Found: C 60.99, H 5.16, N 13.46, V 9.00; Calcd C 60.44, H 5.07, N 13.05, V 9.49; MALDI M^+-(16) (m/z) 521.1 (100).
Compound **13** [$C_{23}H_{23}N_5O_2SV$] F.W. 500.47: Analytical data: elemental Found: C 59.06, H 5.42, N 13.85, V 9.99; Calcd C 58.59, H 5.31, N 13.66, V 9.98.
Compound **14** [$C_{25}H_{23}N_5O_3SV$] F.W. 524.49: Analytical data: elemental. Found: C 57.36, H 4.37, N 13.42, V 9.50; Calcd C 57.25, H 4.42, N 13.35, V 9.71; FAB M^+-(16) (m/z) 524.1 (100), M^+-(16+1) 509 (70).
Compound **15** [$C_{26}H_{23}N_5O_2SV$] F.W. 520.50: Analytical data: elemental. Found C 59.58, H 4.39, N 13.42, V 9.50. Calcd C 60.00, H 4.45, N 13.46, V 9.71
Compound **16** [$C_{28}H_{23}N_5O_2SV$] F.W. 544.52: Analytical data: elemental. Found C 61.38, H 4.27, N 12.73, V 9.34, Calcd C 51.75, H 4.26, N 12.86, V 9.36

3.3. RESULTS AND DISCUSSION

3.3.1. Preparation of compounds

All the complexes prepared (compounds **9-16**) are of the general formula [VOLB] as indicated by their elemental analysis (Table 3.1). While the compounds 9 and **11** were obtained as solid isolable products upon stirring itself, the rest of the compounds were got upon layering with hexane as microcrystalline powders, or bulky solids. Compounds **10, 14** and **16** were obtained as microcrystalline powders, compound **12** was found to form as fine feathery needles, compound **13** as feathery flakes and compound **15** as bulky lumps. The time for crystallisation of the compounds vary from 2 hrs up to 3 days. While the compounds **10, 12, 14** and **16** starts crystallising within 4-5 hours of layering with hexane, compounds **13** and **15** takes 2-3 days for compound formation. Efforts to recrystallize compounds from different solvents, mixed as well as pure were unsuccessful as oxidation of the compound takes place on standing with methanol, acetonitrile etc. However, we were able to isolate single crystals of the compound **14** in 3 days by diffusion of hexane into a solution of dichloromethane near the freezing temperatures. All the compounds are soluble in dichloromethane, DMF and DMSO. The solubility varies for different compounds. Dichloromethane is suggested as a better solvent than DMF for optical measurements as the colour of the solution is stable for reasonable period. However, in the case of DMF coordination of the solvents brings changes in the optical features of the compounds (Figure 3.1) – refer discussion of electronic spectra. Compounds containing bipyridine as the auxiliary ligand are less readily soluble than their phenanthroline counter parts. The attempts to crystallise compounds from DMF resulted in isolation of a few yellow cubic crystals of compound **11** over a period of 3 weeks. However, the crystal was not stable as it decomposed due to loss of solvent on exposure to air. This impaired the prospects of crystal structure investigations. The dissolution and the subsequent growth of the crystal is initiated and facilitated by the coordination of the solvent with the central vanadyl atom.

The molar conductances of *ca.* 10^{-3} M solutions of complexes in DMF lie in the range 20-35 Ω^{-1} cm^{-1} mol^{-1}, indicating their non-electrolytic nature in solution. The elemental data also supports the formulation [VOLB] that lacks any ionisable component in solution. The magnetic moment values are in the range of 1.71 - 1.91 BM consistent with the spin only values for mononuclear oxovanadium(IV) in d^1 configuration(Table 3.1) with low orbital contribution[12]. The FAB mass spectrum of compound **14** was obtained and indicates the existence of the compound as [VOL^3B]. The MALDI measurements of the compounds were in conformity with a species that has lost its oxygen. The EPR spectra were recorded in DMF since other solvents do not yield glassy formation at 77 K

3.3.2. IR and electronic spectra

The disappearance of the peaks at *ca.* 3300 cm^{-1} (Table 3.2) indicates the loss of imine nitrogen (^{2}N-H) inferred to be due to the enolisation and the consequent binding of the thiosemicarbazone in the thiol form. This is further supported by the appearance of a new band near 1595 cm^{-1} due to the formation of a new $^2N=^9C$ bond. The shifting of the $^7C=^1N$ band *ca.* 1601 cm^{-1} to a band *ca.* 1559 cm^{-1} is a result of the coordination of the imine nitrogen to vanadium. The disappearance of the band *ca.* 3350 cm^{-1} and the shifting of band *ca.* 1220 cm^{-1} to *ca.* 1138 cm^{-1} is an evidence for the deprotonation of the

phenolic –OH, and its subsequent strong coordination [13]. The band *ca.* 1370 cm^{-1} due to $\nu_{C=S}$ shifts by 50 – 70 cm^{-1} and the band due to $\delta_{C=S}$ by about 30 - 60 cm^{-1} can be assumed is an evidence for the coordination of the C=S bond as thiolate [14]. The strong band *ca.* 960 cm^{-1} is an evidence for the presence of the V=O bond which stays in tact [15, 16], but is also characteristic of the coordination of vanadium in the sixth position [17, 18]. The low frequency range observed in the complexes indicates that the V=O bond is weakened by strong σ and π electron donation by the thiolate and phenoxy groups to the anti-bonding orbital of the V=O group [19]. The variation in the frequency suggests that the $d\pi$-$p\pi$ overlap between vanadium and the oxygen atoms is influenced by the substituents and the coligands [20]. The presence of a band in the region *ca.* 530 cm^{-1} is an evidence for the V-O coordination [21].

The visible spectra of the complexes **9-16** in dichloromethane show the characteristic series of absorption bands common to vanadyl systems [22-24]. In terms of the Ballhausen and Gray model [25], accordingly, the first absorption band occurring in the 13000 – 14000 cm^{-1} region can be assigned to the electronic transition $^2B_2 \rightarrow {}^2E$ ($d_{xy} \rightarrow d_{xz}$, d_{yz}), the second broad intense band ca. 19000 cm^{-1} is due to closely lying bands that corresponds to two transitions $^2B_2 \rightarrow {}^2B_1$ ($d_{xy} \rightarrow d_{x^2-y^2}$) and $^2B_2 \rightarrow {}^2A_1$ ($d_{xy} \rightarrow d_{z^2}$). This closely lying states $d_{x^2-y^2}$ and d_{z^2} are indicative of the small tetragonal distortion to the vanadyl environment.

The optical property of the vanadyl complexes in two different solvents, viz, dichloromethane and DMF were found to vary significantly. The band *ca.* 19000 cm^{-1} was found to shift to higher energies and disappear into the tail of the charge transfer band for all the complexes. The rate at which it happens is different for complexes containing bipyridine and phenanthroline. For bipyridine containing complexes the dissolution in DMF is taking place with coordination of the solvent. The resulting DMSO coordinated species does not have optical absorption in the 19000 cm^{-1} region. The dissolution of the complexes is also followed by a shift in the CT bands to higher energy region (Figure 3.4). The overall changes can be taken to mean the gradual replacement of the coordinated ligands, first being initiated with removal of the base. EPR spectroscopic measurements also these observations.

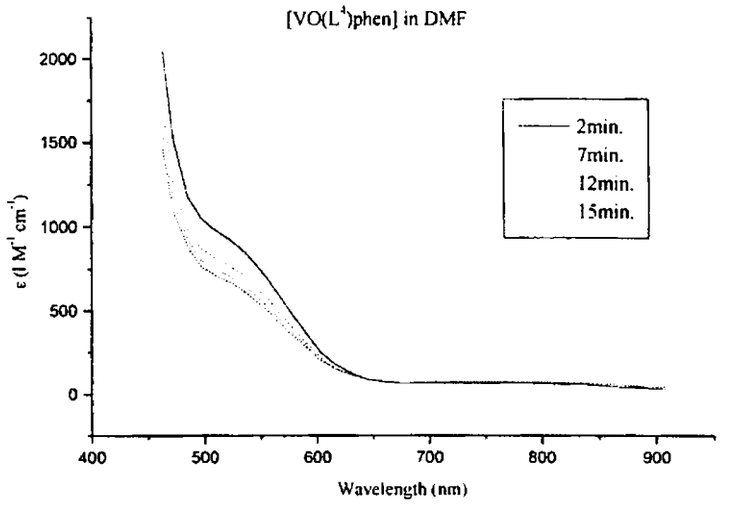

Figure 3.1.: The variation in the optical absorption of compound **16**

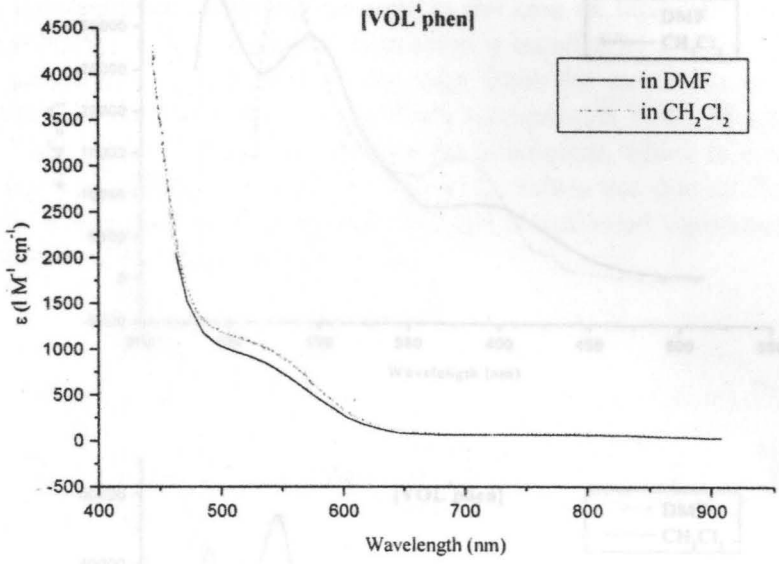

Figure 3.2.: Optical absorption feature of compound **16** in two different solvents, viz. dichloromethane and DMF

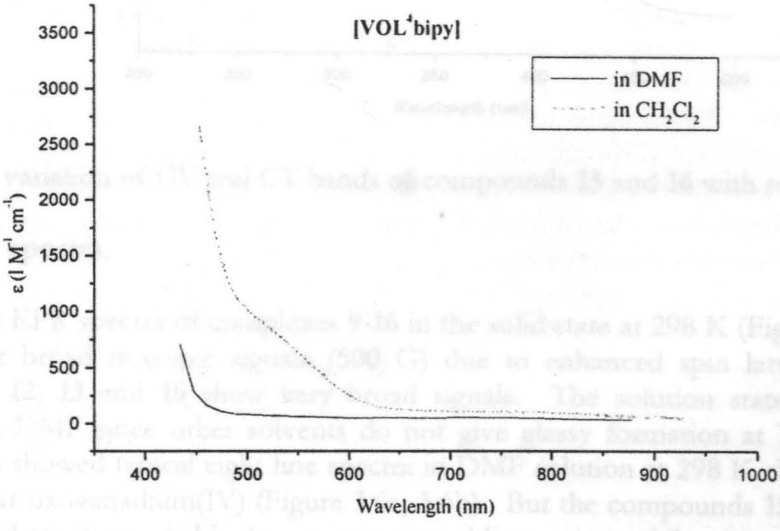

Figure 3.3.: The optical spectrum of compound **15** on dissolution of the respective solvents.

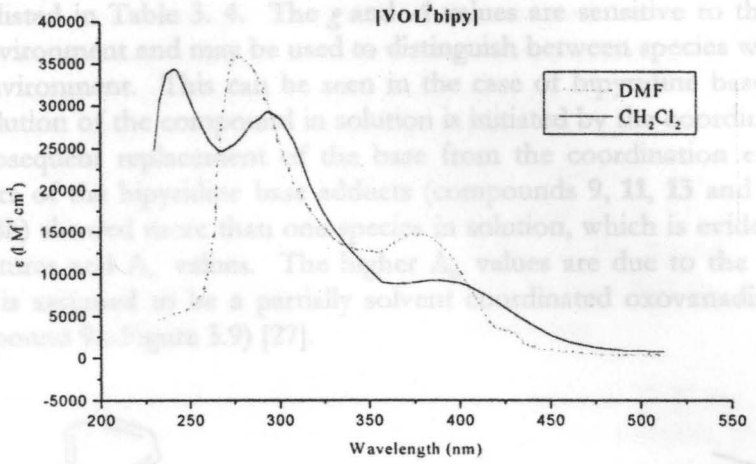

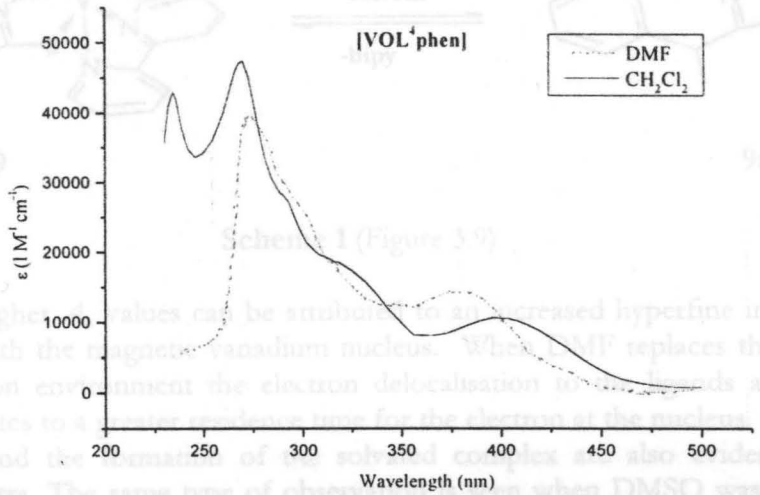

Figure 3.4.: variation of UV and CT bands of compounds **15** and **16** with solvents.

3.3.3. EPR spectra

The EPR spectra of complexes **9-16** in the solid state at 298 K (Figure 3.5a, 3.5b) gives rather broad isotropic signals (500 G) due to enhanced spin lattice relaxation. Complexes **12**, **13** and **16** show very broad signals. The solution state spectra were recorded in DMF since other solvents do not give glassy formation at 77 K. All the compounds showed typical eight line spectra in DMF solution at 298 K characteristic of mononuclear oxovanadium(IV) (Figure 3.6a, 3.6b). But the compounds **15** failed to give well-resolved spectra probably due to greater tumbling action, while compounds **9** and **11** gave well-resolved eight lines.

The EPR spectra in frozen DMF (77 K) differ for bipyridine and phenanthroline containing complexes, though they are typical of five- and six-coordinate vanadyl complexes having axial geometry [26]. Figure 3. 7 shows a typical axial spectrum exhibited by all phenanthroline base adducts of oxovanadium(IV). The absence of any ligand nitrogen super hyperfine lines in the g_o features of the complexes is an explicit indication of the sole electron lying in the d_{xy} orbital -$^2B_2$ ground state. The axial spectrum is characterised by two sets of eight lines, which result from the coupling of

electron spin to magnetic moment of ^{51}V nucleus (I = 7/2). The magnetic and spectral parameters are listed in Table 3. 4. The g and A values are sensitive to the vanadium coordination environment and may be used to distinguish between species with different coordination environment. This can be seen in the case of bipyridine base adducts in which the dissolution of the compound in solution is initiated by the coordination of the solvent and subsequent replacement of the base from the coordination environment. The EPR spectra of the bipyridine base adducts (compounds **9, 11, 13** and **15**) at 77 K (Figure 3.8a, 3.8b) showed more than one species in solution, which is evident from the different g_o features and A_o values. The higher A_o values are due to the new species formed, which is assumed to be a partially solvent coordinated oxovanadium(IV) ion-scheme 1 (compound **9a**-Figure 3.9) [27].

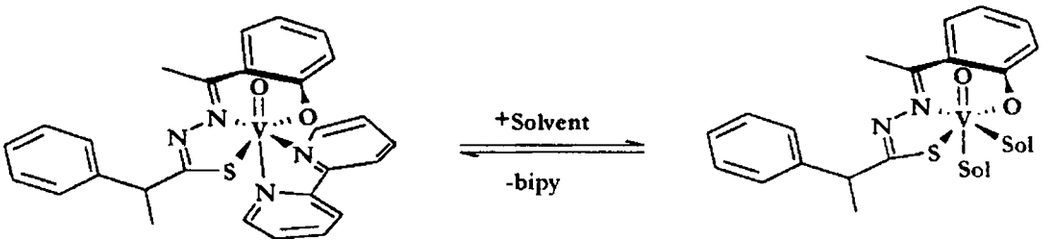

9 **9a**

Scheme 1 (Figure 3.9)

The higher A_o values can be attributed to an increased hyperfine interaction of the electron with the magnetic vanadium nucleus. When DMF replaces the base from the coordination environment the electron delocalisation to the ligands are restricted which contributes to a greater residence time for the electron at the nucleus. The solvent coordination and the formation of the solvated complex are also evident from the electronic spectra. The same type of observation is seen when DMSO was used as the solvent. The magnetic parameters are found out from the EPR best-fits (Figure 3.10). In all the cases the dominant species in solution is the solvent coordinated one, which is evident from the higher intensity corresponding to the solvent coordinated species. The coordination of the solvent in all the bipyridine base adducts is assumed to be initiated by the restricted bite angle offered by the bipyridine [28], leading to a distorted octahedral geometry with small tetragonal distortions. The coordination at the sixth position is assumed to be the first step in the process. The more room offered by the bipyridine adducts attracts the polar coordinating solvents such as DMF and DMSO, *trans* to position driven by the electron withdrawing influence of the *trans* coordinated oxygen of V=O group. The equilibrium of the solvent coordination is far to the solvent side, driven by the stronger σ bonding influence offered by the coordinated solvent. This is supported by the lower values of the in-plane σ bonding parameters (α^2). The in-plane π-bonding parameters (β^2) [29] observed, are consistent with those observed by McGarvey [30] and Kivelson [31] for vanadyl complexes of acetylacetonate, phenanthroline and bipyridine. The bonding parameters α^2 and β^2 can be calculated from equations (1) and (2).

$$\beta^2 = 7/4[(-A/P) + (g_o - 2.0023) + 3/7(g - 2.0023) - K] \quad (1)$$

$$\alpha^2 = \Delta_o (\Delta g_o / g_o)/4\lambda\beta^2 \quad (2)$$

Where K, isotropic contact term, is taken as 0.71, P is assigned a value of 128 x 10^{-4} cm^{-1} and the spin-orbit coupling constant λ is assumed to have a value of 170 cm^{-1}. Δ_o is the energy corresponding to the optical transition $d_{xy} \rightarrow d_{x^2-y^2}$ ($^2B_2 \rightarrow {}^2B_1$). The hyperfine coupling constant is taken as having negative value during the calculation. A lowering in the value of α^2 is an indication of increasing covalency, while that of β^2 does not found to vary significantly, from the most often observed value of $\approx$ 1.0 for most of the complexes. This is expected as the π-bonding ability of the ligand decreases with increasing distortion from the planar geometry. It can be seen that the phenanthroline adducts show smaller β values, i.e., greater in-plane π-bonding.

The EPR spectra at of the phenanthroline base adducts 77 K are, however, not influenced by the solvent and are reasonably stable in the polar solvents, probably due to the lack of proper room at the sixth coordination site of these compounds. The slow fading of the band in their optical spectra also supports this conclusion.

3.3.4. Cyclic voltammetry

The irreversible peak at –0.5 V and quasi reversible peak at -0.85 V are due to the successive $V^{IV/III}$ and $V^{III/II}$ redox couples, the one at –1.15 to -1.3 is due to the ligand moiety reductions [2b.38]. The irreversible peak at +0.95 in the reverse sweep can be assigned to the $V^{IV/V}$ oxidation (Figure 3.11). The small variation in the peak potentials is due to the effect of the substituents in the thiosemicarbazone ligand moiety. The details of cyclic voltammetry are listed in Table 3. 5.

Table 3.5.: Cyclic Voltammetric data[a]

Compound	Oxidation potential (V)	Reduction Potential (V)
[VOL^{1}bipy] (**9**)	0.41, 0.89	0.85, 1.31
[VOL^{3}bipy] (**13**)	0.91	0.59, 0.87,1.18
[VOL^{3}phen] (**14**)	0.91	0.49, 0.82, 1.28
[VOL^{4}bipy] (**15**)	0.87	0.79, 1.28
[VOL^{4}phen] (**16**)	0.64, 0.91	0.49, 0.82, 1.28

[a] = all data are reported for a scan rate of 200/100 mVs^{-1}

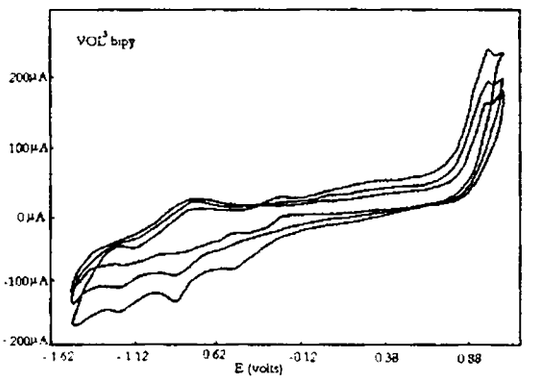

Figure 3.11: Cyclic voltammogram of compound **13** [VOL^{3}bipy]

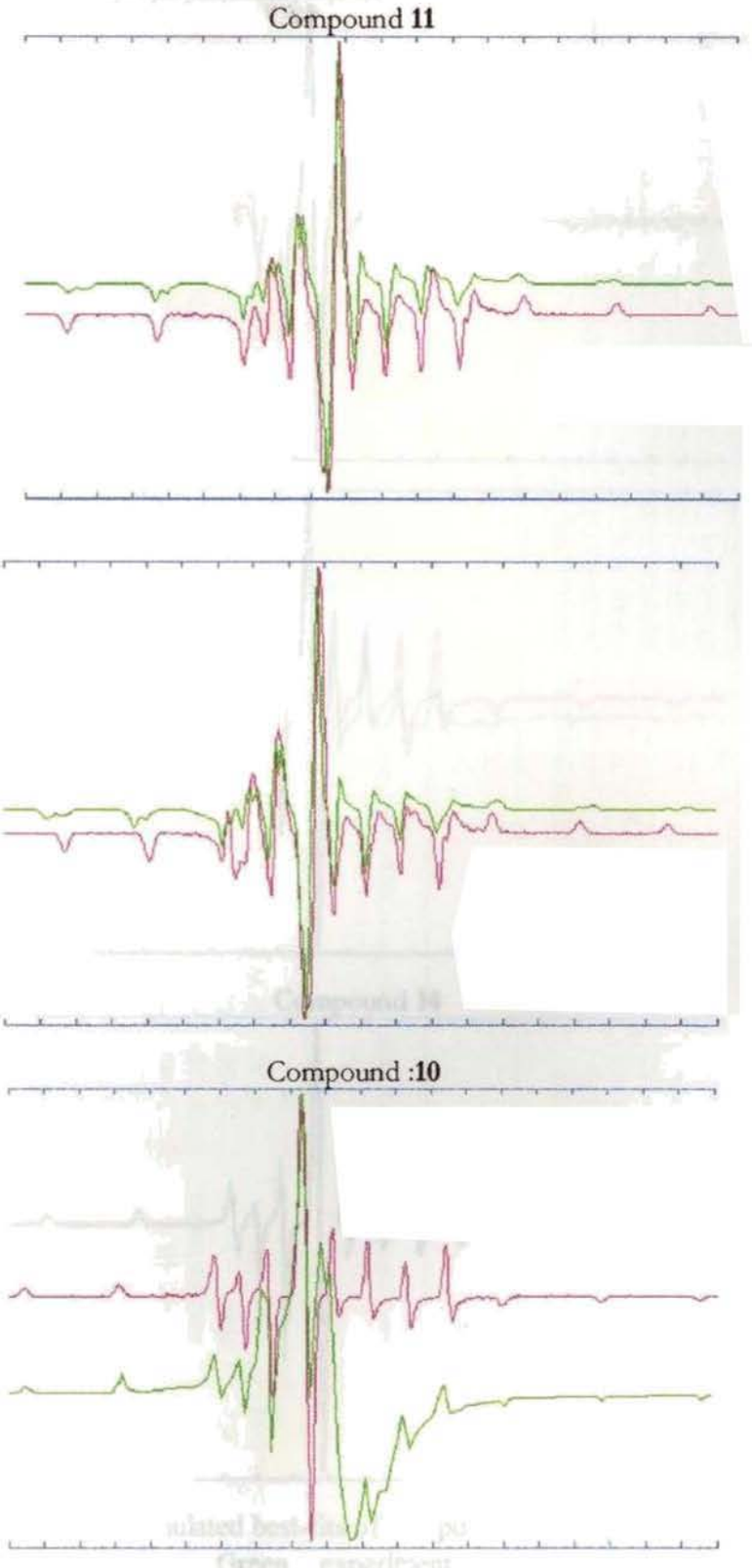

Figure 3.10a.: Simulated best-fits of Compound **10** (c) and **11** (a, b).

- Green = experimental spectrum
- Red = simulated best-fit

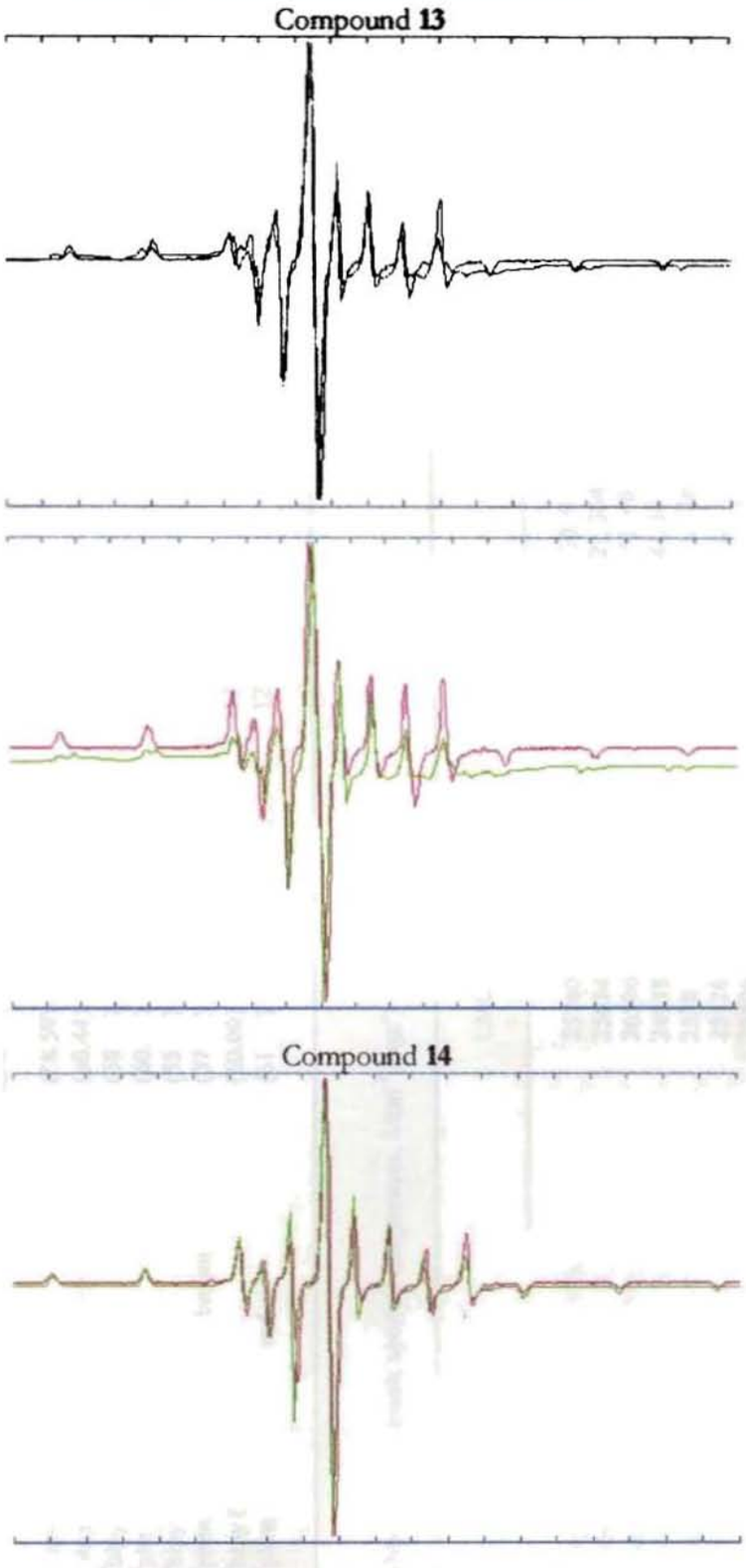

Figure 3.10.: Simulated best-fits of compound **13**(a, b) and **14 (c)**

- Green = experimental spectrum
- Red = simulated best-fit

Table 3.1: Elemental analysis data of oxovanadium (IV) complexes (**9-16**)

Compound	Color	Found (Calcd.) (%)				Magnetic moment BM
		C	H	N	V	
VOL^1bipy (**9**)	Orange red	58.87 (58.59)	5.35 (5.31)	13.41 (13.66)	9.28 (9.98)	1.74
VOL^1phen (**10**)	Deep orange red	60.68 (60.44)	5.18 (5.07)	13.39 (13.05)	9.39 (9.49)	1.89
VOL^2bipy (**11**)	Bright red	59.06 (58.59)	5.42 (5.31)	13.85 (13.66)	9.99 (9.98)	1.88
VOL^2phen (**12**)	Blood red	60.99 (60.44)	5.16 (5.07)	13.46 (13.05)	9.00 (9.49)	1.75
VOL^3bipy (**13**)	Blood red	54.40 (55.20)	4.62 (4.63)	13.92 (13.99)	9.49 (10.18)	1.92
VOL^3phen (**14**)	Reddish brown	57.36 (57.25)	4.37 (4.42)	13.20 (13.35)	10.05 (9.79)	1.79
VOL^4bipy (**15**)	Red	59.58 (60.00)	4.39 (4.45)	13.42 (13.46)	9.50 (9.71)	1.77
VOL^4phen (**16**)	Deep red	61.38 (61.76)	4.27 (4.26)	12.73 (12.86)	9.34 (9.36)	1.79

Table 3. 3: Electronic spectral assignments, $\lambda/cm^{-1}(\log\varepsilon^a)$ for compound **9-16**

Compound	d-d	LMCT	n→π*	π→π*
VOL^1bipy (**9**)	13282 (1.98), 19476 (2.86)	25740 (3.90), 26596 sh (4.12)	34014 (4.50), 30395 sh (4.14)	41237 (4.56)
VOL^1phen (**10**)	13812 (1.91), 20080 (2.94)	25674 sh (3.96)	34483 sh (4.42), 30488 sh (4.10)	42553 (4.55), 37736 (4.63)
VOL^2bipy (**11**)	13280 (1.98), 19231 (2.51)	26596 (4.24)	34483 (4.46), 31746 sh (4.27)	37453 (4.60)
VOL^2phen (**12**)	13140 (1.87), 19476 (2.98)	24938 (3.78)	31153 sh (3.98), 34188 sh (4.23)	37037 (4.49)
VOL^3bipy (**13**)	13321 (1.89), 19531 (2.96)	25381 (3.95)	33134 sh (4.43), 32680 sh (4.23)	41753 (4.54)
VOL^3phen (**14**)	12886 (2.02), 19685 (2.92)	25126 (3.49)	34364 sh (4.41), 31056 sh (4.20)	42644 (4.61), 37106 (4.65)
VOL^4bipy (**15**)	13072 (2.01), 19531 (2.96)	25806 (3.97)	31025 sh (4.28), 34014 sh (4.47)	41322 (4.53)
VOL^4phen (**16**)	13315 (1.90), 19607 (2.90)	25221 (4.02)	31546 sh (4.27), 34483 (4.45)	42644 (4.63), 37037 (4.68)

[a] = ε is expressed in ($l\ mol^{-1}cm^{-1}$)

Table 3.2: IR spectral assignments for thiosemicarbazones and their vanadyl complexes (All absorptions are given in units of cm^{-1})

Compound	ν ($^{7}C=N^{1}$)	ν ($^{2}N=C^{9}$)	ν ($^{1}N-N^{2}$)	ν (V-N)	ν/ δ (C=S)	ν (C-O)	ν (V=O)	ν (V-O)	Bands due to heterocyclic base
H_2L^1	1599s	-	988 m	-	1365s 826 m	1219 s	-		-
VOL^1bipy (9)	1561m	1595s	1022m	453 m, 436 w	1329s 766m	1223 s	957s	530w	1435m, 735m, 757w
VOL^1phen (10)	1564m	1593s	1030m	451 m 432w	1317s	1231s	953s	528w	1429m, 725 w, 745m, 848m
H_2L^2	1603s	-	997m	-	1383s 839m	1252s	--		-
VOL^2bipy (11)	1563m	1595s	1018m	453 m, 420 w	1369s 810m	1204 s	959s	510w	1423m, 1445m, 735m, 654w, 615w
VOL^2phen (12)	1565m	1593s	1015m	451m 436w	1369s 810 m	1190s	955s	512w	1489m, 1450m, 623w, 851 m, 727w,
H_2L^3	1605s	-	1017m	-	1374s 835m	1219s	-		-
VOL^3bipy (13)	1561m	1597s	1030m	451m, 438w	1327s 808 m	1118s	948s	527w	735 m, 652 w, 618 w
VOL^3phen (14)	1563m	1593s	1032 m	451m 436w 424w	1323s 808m	1115s	961s	529w	727 m, 848 m
H_2L^4	1601s	-	995 m	-	1375s 808m	1222s	-		-
VOL^4bipy (15)	1559m	1593s	1020 m	455 m 440w 418w	1327s 776m	1159s	968s	511w	615w, 735 w, 758 m
VOL^4phen (16)	1555m	1593s	1021 m	451 m 430w	1333s 764 m	1128s	961s	510w	727 m, 640 w

Table 3.4: EPR spectral assignments of vanadyl complexes **(9-16)**

Compound	Solid (298 K)	DMF (298 K)		DMF (77 K)[a]				α^2	β^2
		g_{iso}	A_{iso}[b]	$g_{\parallel}/g_{zz}$	$g_{\perp}/g_{xx},g_{yy}$	$A_{\parallel}/A_{zz}$[b]	$A_{\perp}/A_{xx},A_{yy}$[b]		
9/DMF	1.982	1.979	94.28	1.952	1.983 1.981	157.1 149.4	53.17 54.23	0.7180 0.7971	1.0078 0.9025
9/DMSO	--	--	--	1.957	1.987	156.6	56.46	0.6682	0.9910
10/DMF	1.981	1.977	90.00	1.949	1.976	149.2	51.80	0.7860	0.9103
11/DMF	1.980	1.976	91.04	1.959	1.994 1.986	154.9 149.3	53.64 54.32	0.6330 0.6115	0.9655 0.8867
11/DMSO	--	--	--	1.952	1.983	154.4	59.14	0.9709	0.7317
12/DMF	1.992	1.975	84.29	1.960	1.988	149.0	51.00	0.6881	0.8792
13/DMF	1.986	1.977	95.71	1.952	1.981	157.6 149.5	53.10	0.7101 0.7970	1.0161 0.9053
13/DMSO	--		--	1.952	1.984 1.983	156.5 149.7	53.70	0.7224 0.7967	0.9987 0.9057
14/DMF	1.992	1.974	90.74	1.956	1.984	149.6	54.26	0.6556	1.0210
15/DMF	1.992	1.979	96.57	--	--	--	--	--	--
15/DMSO	--	--	--	1.946	1.979	156.8	51.74 54.11	0.7939	1.0172
16/DMF	1.986	1.976	89.43	1.962	1.988	149.0	51.00	0.7032	0.8805

[a] = All values are obtained from the simulated best-fits

[b] = All Hyperfine values are reported in units of cm^{-1} multiplied by 10^{-4}

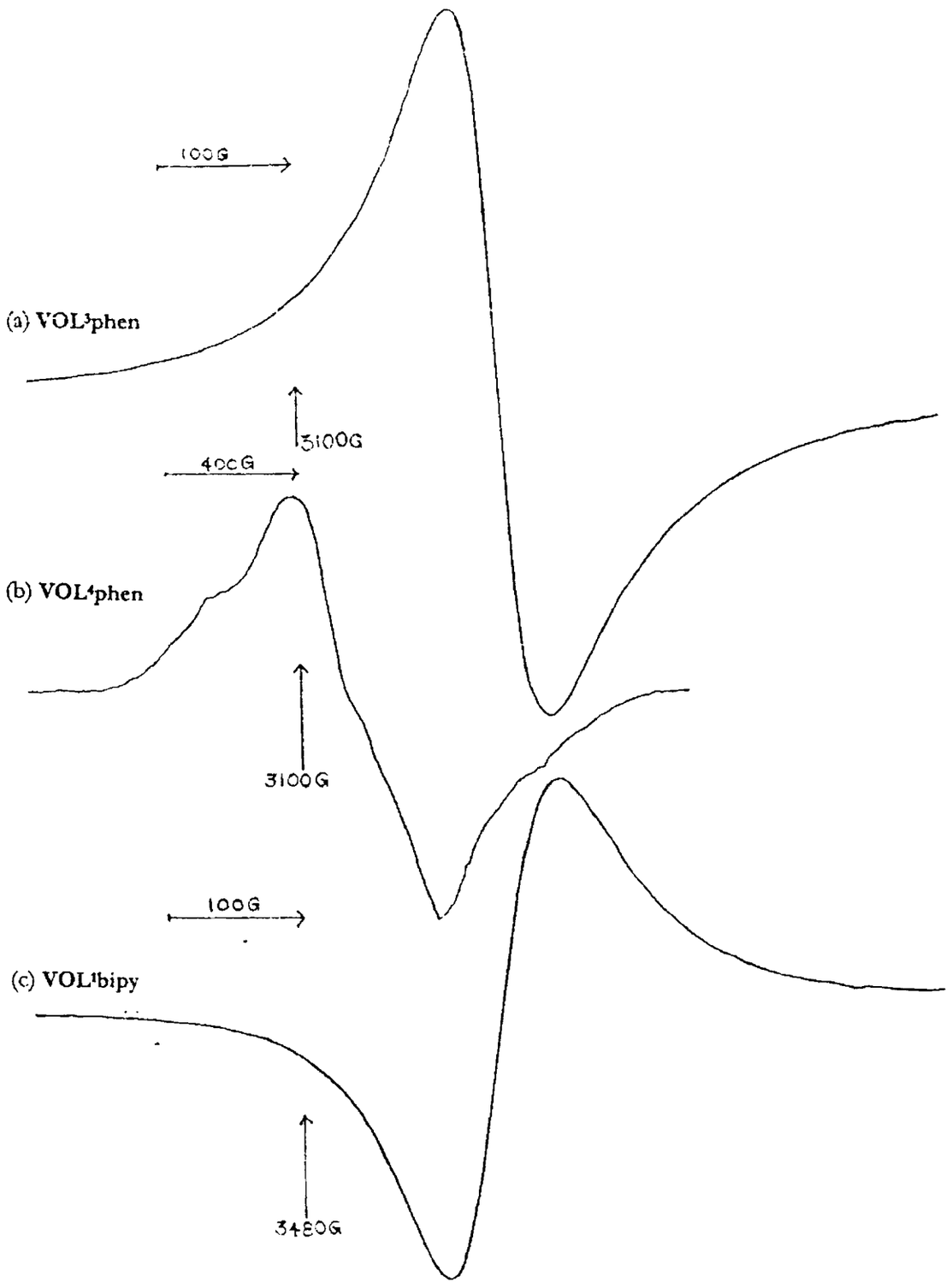

Figure 3.5a.: EPR spectra of vanadyl complexes in polycrystalline state at 298 K.
a) compound **14**, b) compound **16**, c) compound **9**

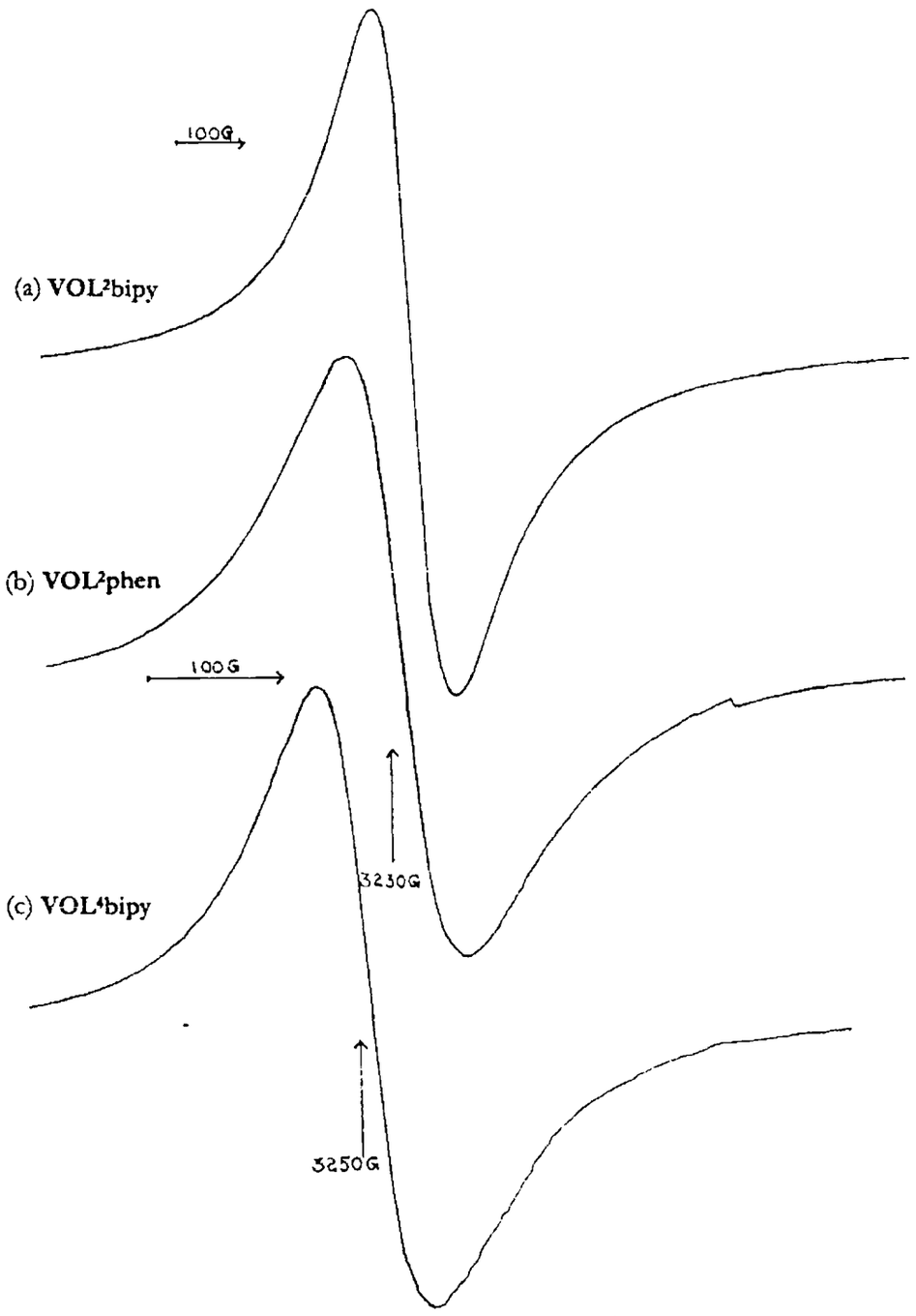

Figure 3.5b.: EPR spectra of vanadyl complexes in polycrystalline state at 298 K.
a) compound **11**, b) compound **12**, c) compound **15.**

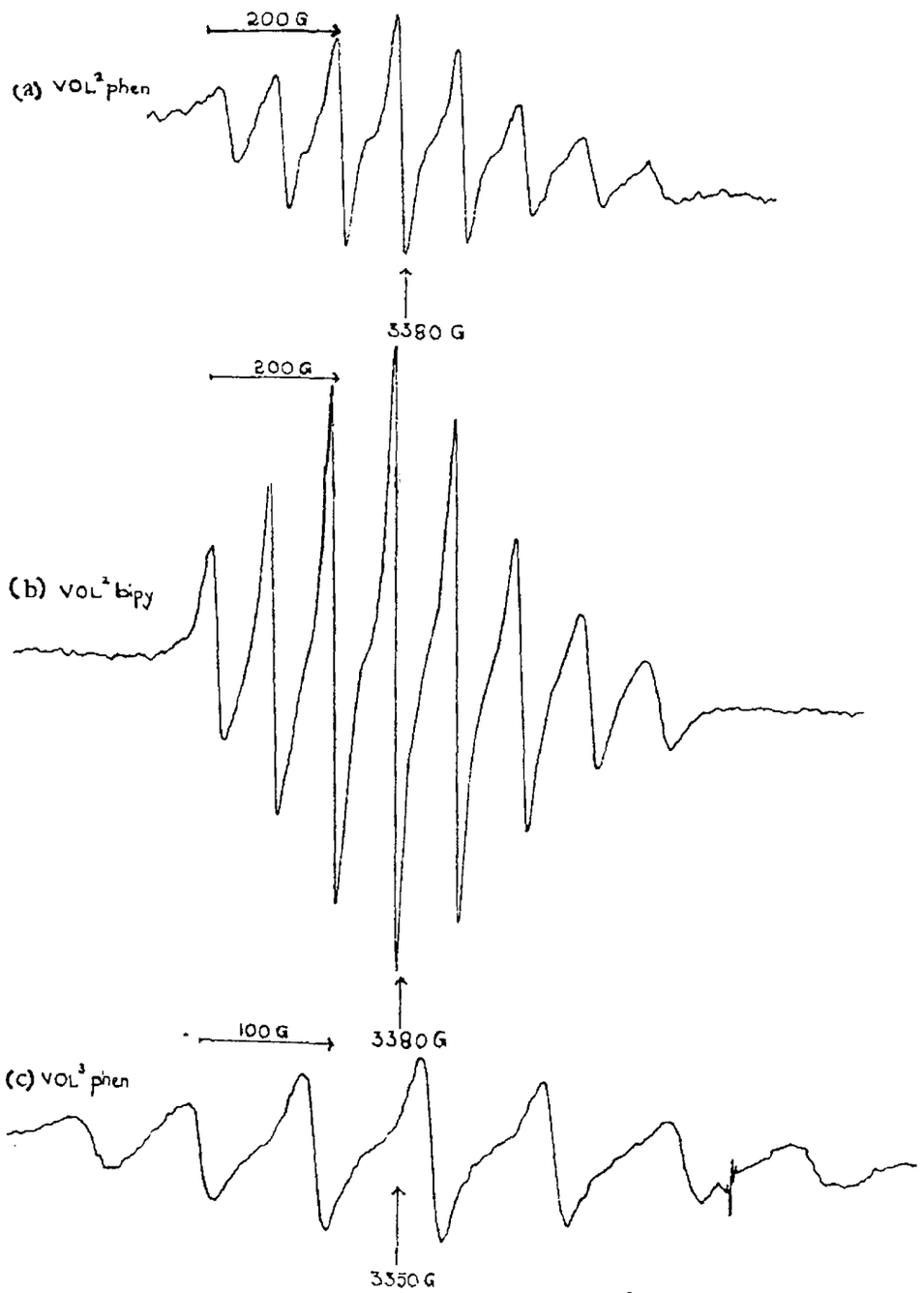

Figure 3.6a.: EPR spectra of vanadyl complexes in DMF at 298 K. a) compound **12**, b) compound **11**, c) compound **14**.

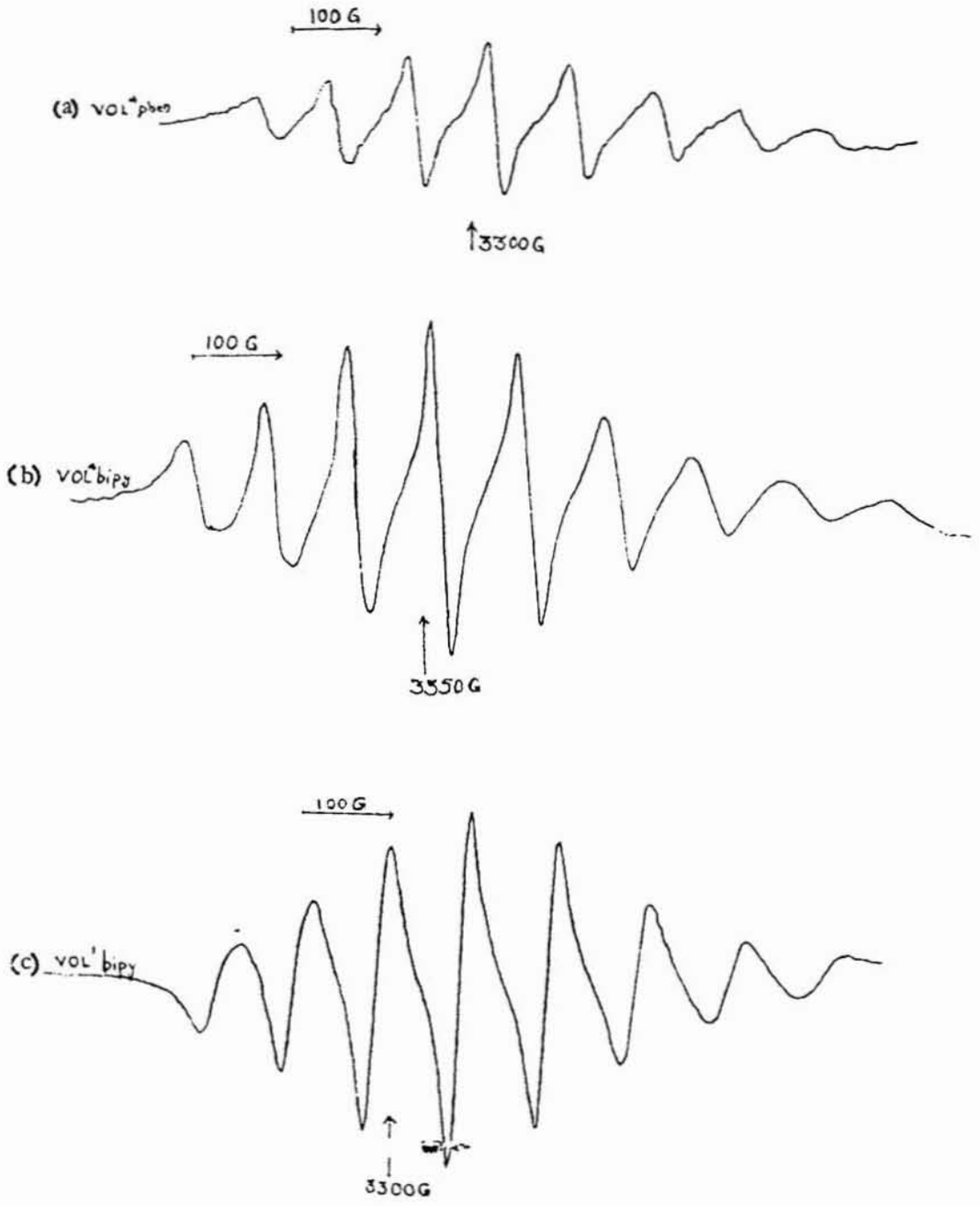

Figure 3.6b.: EPR spectra of vanadyl complexes in DMF at 298 K. a) compound **16**, b) compound **15**, c) compound **9**.

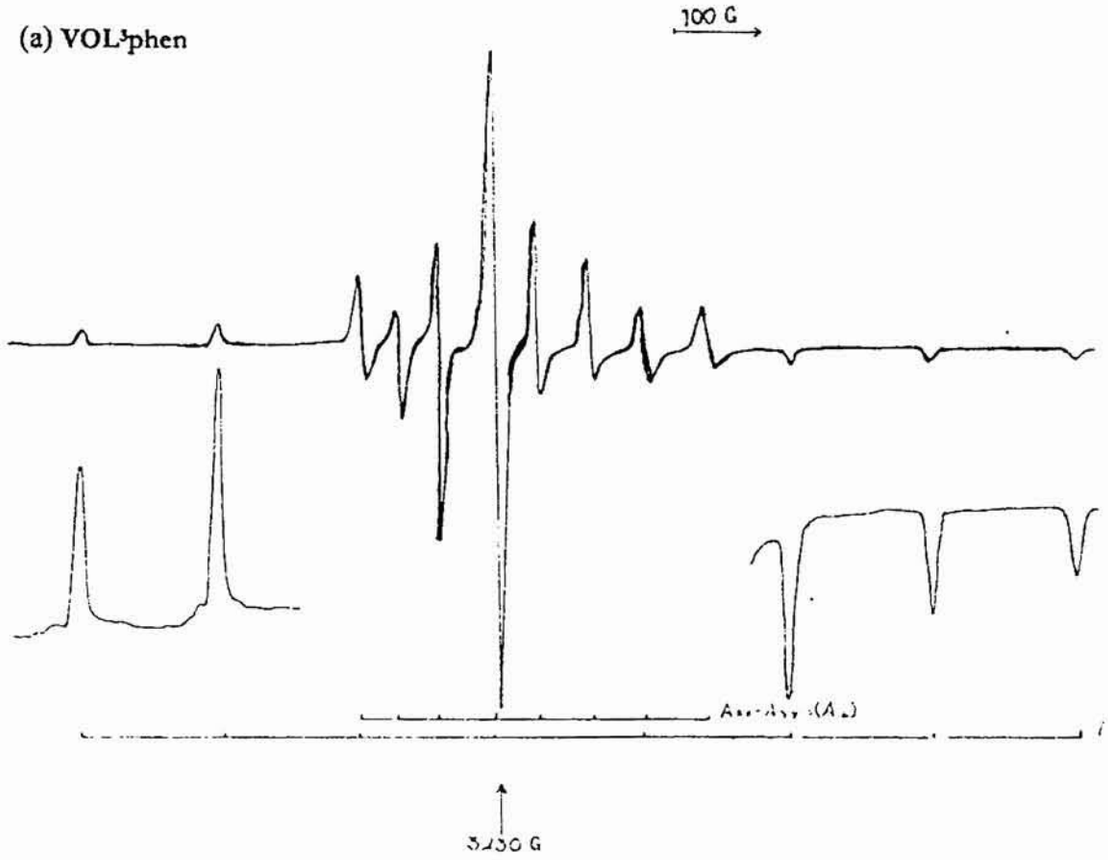

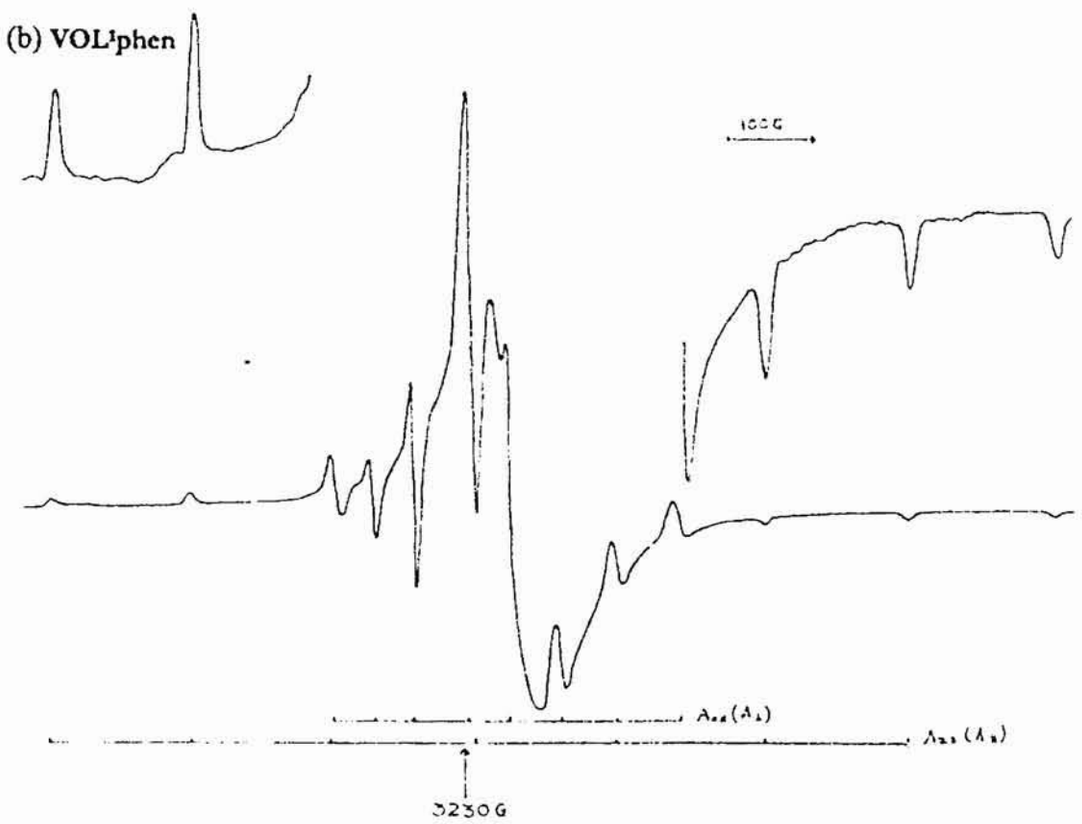

Figure 3.7: EPR spectra of phenanthroline base adducts of oxovanadium(IV) in DMF at 77K. a) compound **14**, b) compound **10**.

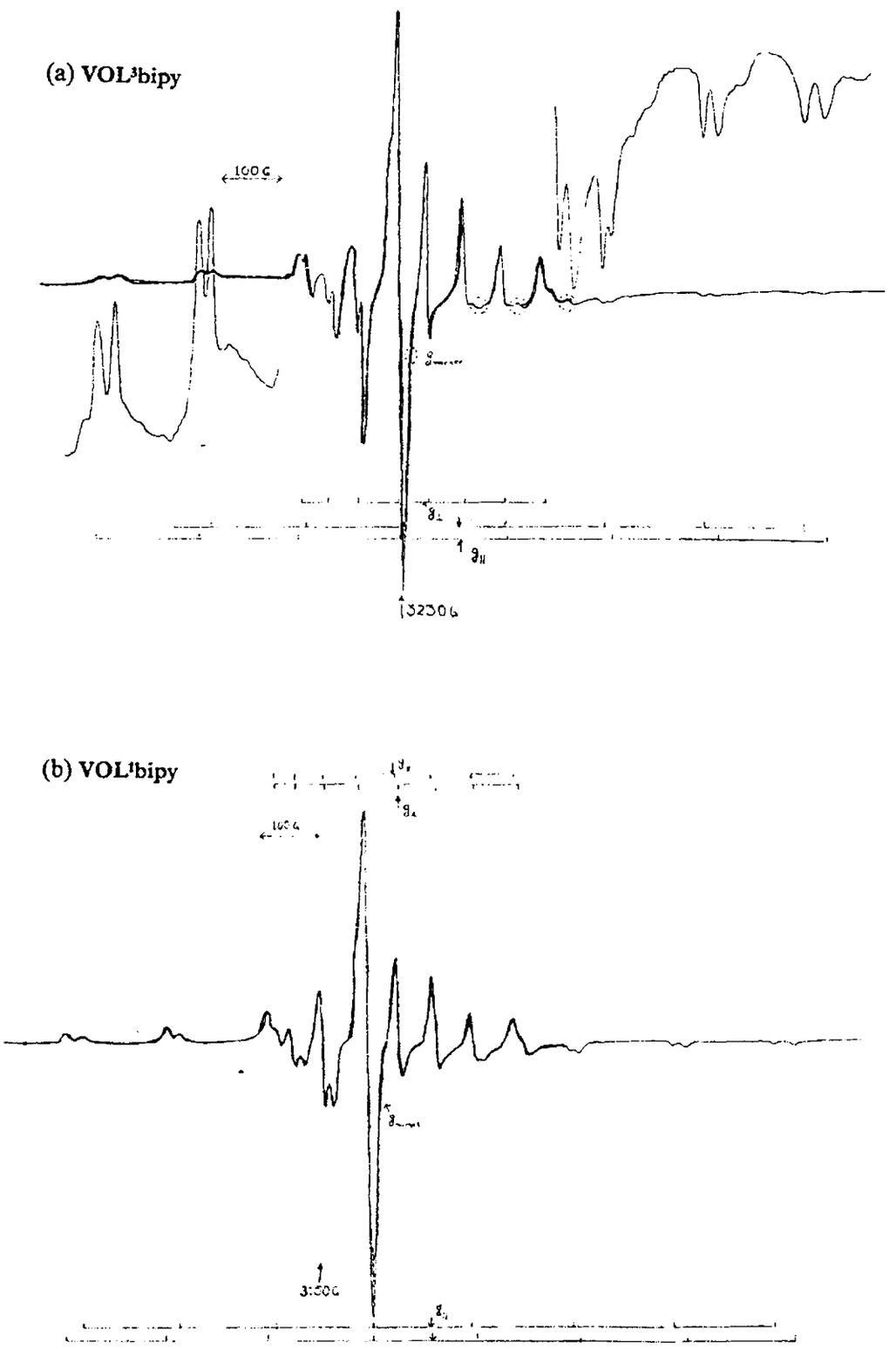

Figure 3.8a.: EPR spectra of bipyridine base adducts of oxovanadium(IV) in solution at 77K. a) compound **13** in DMF, b) compound **9** in DMF.

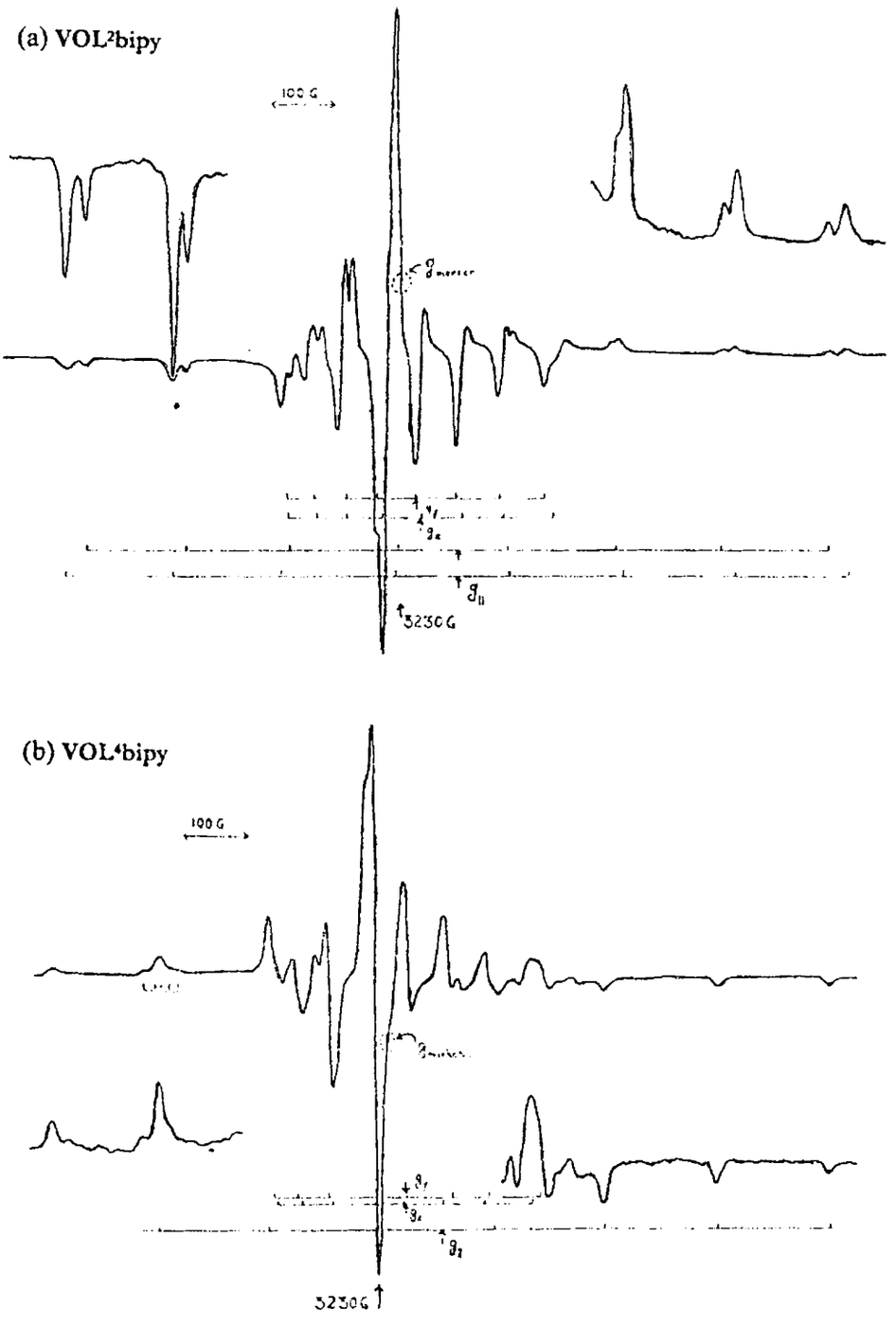

Figure 3.8b.: EPR spectra of bipyridine base adducts of oxovanadium(IV) in solution at 77K. a) compound **11** in DMF, b) compound **15** in DMSO.

REFERENCES:

1. C. J. Carrano, C. M. Nunn, R. Quan, J. A. Bonadies and V. L. Pecoraro, *Inorg. Chem.*, 1990, **29**, 941.
2. X. Li, M. S. Lah and V. L. Pecoraro, *Inorg. Ch*em., 1988, **27**, 465.
3. R. P. Ferrari, E. Laurenti, S. Poli and Casella, *J. Inorg. Biochem.*, 1992, **45**, 21.
4. A. Buttler, C. J. Carrano, Coord. Chem. Rev., 1991, **109**, 61; A. Buttler, Walker V. J. *Chem. Rev.*, 1993, **93**, 1937.
5. C. J. Hawkins, P. Kott, D. L. Parry, J. H. Swinehart, *Comp. Biochem. Physiol.*, 1983, **76B**, 555.
6. S. G. Brand, C. J. Hawkins, A. L. Marshall, G. W. Nette, D. L. Parry, *Comp. Biochem. Physiol.*, 1989, **93B**, 425.
7. H. S. Soedjak, A. Butler, *Inorg. Chem.*, 1990, **29**, 5015.
8. H. Plat, B. E. Krenn, R. Wever, *J. Biochem.*, 1987, **248**, 277.
9. D. Rehder, *Met. Ions Biol. Syst.*, 1995, **31**, 1.
10. C. Orvig, K. H. Thompson, M. Battell, J. H. McNeill, *Met. Ions Biol. Syst.*, 1995, **31**, 575.
11. H. Sakurai, K. Fujii, H. Watanabe, H. Tamura, *Biochem. Biophys. Res. Commun.*, 1995, **214**, 1095.
12. R. L. Dutta and G. P. Senguptha, *J. Indian Chem. Soc.*, 1972, 49, 919; A. Pasini, and M. Gullotti, *J. Coord. Chem.*, 1974, 3, 319.
13. M. Akbar Ali, D. A. Chowdhary, I. and M. Nazim Uddin, *Inorg. Chim. Acta.*, 1973, **7**, 179.
14. R. Mukhopadhyay, S. Bhattarjee and R. Bhattacharya, *J. Chem. Soc. Dalton Trans.*, 1994, 2799.
15. E. Sinn, C. M. Harris, *Coord. Chem. Rev.*, 1969, **4**, 39.
16. N. Choudhary, D. L. Hughes, U. Kleinkes, L. F. Larkworthy, G. J. Leigh, M. Maiwald, C. J. Marmion, J. R. Sanders, G. W. Smith, C. Sudbrake, *Polyhedron*, 1997, **16**, 1517.
17. C. J. Carrano and J. A. Bonadies, *J. Am. Chem. Soc.*, 1986, **108**, 4088.
18. J. Chakravarty, S. Dutta, A. Dey and A. Chakravorty, *J. Chem. Dalton. Trans.*, 1994, 557.
19. T. Ma, T. Kojima and Y. Matsuda, *Polyhedron*, 2000, **19**, 1167.
20. C. Tsiamis, B. Voulgaropoulos, D. Christos, G. P. Voustas and C. A. kavounis, *Polyhedron*, 2000, **19**, 2003.
21. P. A. Wicklund and D. G. Brown, *Inorg. Chem.*, 1976, 15, 396.
22. L. J. Boucher and T. F. Yen, *Inorg. Chem.*, 1968, **7**, 2665; H. A. Kuska and M. T. Rogers, *Inorg. Chem.*, 1966, **5**, 313.
23. C. J. Ballhausen and H. B. gray, Inorg. Chem., 1962, **1**, 111; H. A. Kuska, Y. P. Yang, *Inorg. Chem.*, 1974, **13**, 1090.
24. J. C. Donini, B. R. Hollebone, G. London, A. B. P, Lever and J. C. Hampel, *Inorg. Chem.*, 1975, **14**, 455.
25. J. Slebin, *Chem. Rev.*, 1965, **65**, 153.
26. N. D. Chasteen In *Biological Magnetic Resonance*, L. J. Berliner, J. Reuben, Eds., Plenum Press: NY, 1981, Vol. 3, p 53-119.
27. C. R. Cornman, J. Kampf, M. S. Lah and V. L. Pecoraro, *Inorg. Chem.*, 1992, **31**, 2035.
28. S. G. Brand, N. Edelstein, C. J. Hawkins, G. Shalimoff, M. R. Snow and E. R. T. Tiekink, *Inorg. Chem.*, 1990, **29**, 434.
29. J. M. Assour, J. Goldmacher and S. E. Harrison, J. Chem. Phys., 1965, 43, 159.
30. B. R. McGarvey, *J. Phys. Chem.*, 1967, **71**, 51.
31. D. Kivelson and S-K. Lee, *J. Chem. Phys.*, 1964, **41**, 1896.

CHAPTER 4

SPECTRAL AND BIOLOGICAL STUDIES OF ZINC(II) COMPLEXES

4.1 INTRODUCTION

In several proteins the zinc atom has either a structural or analytical role which seems to be connected with the following features: i) the ready formation of low coordination number sites which are more strongly acidic than high-coordination number sites; ii) the easy deformation of geometry of the ligands in the coordination sphere with subsequent change in coordination number from four to five to six; iii) relatively rapid exchange of the ligands in the complexes; iv) absence of redox chemistry [1]; and v) the suggestion that zinc fingers may be a common feature in many protein-(DNA-RNA) interactions. Further research in this field has revealed that the efficient modeling of metal sites in enzymes requires the designing of polydentate ligands having nitrogen and sulfur donors, as histidine and cysteine/ methionine are the most common donor units for metal ions in protein environment. This is specifically so for zinc enzymes [2] and there is quite a number of such zinc enzymes, as exemplified by liver alcohol dehydrogenase [3], spinach carbonic anhydrase [4] or bovine aminolaevulinate dehydratase [5] in which the catalytic zinc enzyme is coordinated to the protein solely by a N_xS_y donor set. The quest to model such a donor set requires a design of an N,S-donor ligand which has the right number of N and S donors. It uses all these donors for monodentate functions and encapsulates the zinc ion, so that there is room for one co-ligand representing the enzymatic substrate. Besides, copper(II) and zinc(II) complexes have substantial inhibitory effects against tumor cells [6, 7].

Guided by the above observations and considering the growing interest in the chemistry and the pharmacological properties of thiosemicarbazones [8] we have prepared and characterized some novel ternary five-coordinate zinc complexes of 2-hydroxyacetophenone thiosemicarbazones and bidentate heterocyclic bases.

4.2 EXPERIMENTAL

4.2.1 Materials

The reagents used for the synthesis of the ligands are discussed in the Chapter 2a. Zinc acetate-dihydrate (E. Merck) was purified by recrystallisation before it was used for the synthesis of complexes. The bipyridine and phenanthroline were obtained from E. Merck and were purified by standard methods. The ligands were recrystallised from ethanol and dried *in vacuo* before complexation.

4.2.2 Preparation of the complexes

The general method of preparation of zinc(II) complexes (**17-24**) of the thiosemicarbazones are as follows.

To a 0.5 mmol solution of the ligand in ethanol (20 mL), was added 10mL of 0.5 mmol methanolic solution of zinc acetate with constant stirring. This was followed by the addition of the respective base, bipyridine or phenanthroline (0.5 mmol) in the solid form. The stirring was continued for about an hour when fine crystals began to separate. This was filtered washed with ethanol, water and ether successively and dried *in vacuo* over P_4O_{10}.

Compound **17**: $[C_{25}H_{27}N_5OSZn]$ F.W. 510.97; Anal. Elemental: Found C 58.46, H 5.35, N 13.80, Zn 12.90; Calcd C 58.77, H 5.33, N 13.71, Zn 12.80; IR (KBr) 3432 b, 3297 b, 1595 s, 1567 m, 1475 s, 1441 s, 1315 m, 1221 s, 1153 m, 769 m, 739 m, 822 w, 482 w, 416 w cm^{-1}; NMR ($CDCl_3$) δ 8.60 (s, 2H, H^1-bipy), 8.06 (s, 2H, H^4-bipy) 7.93 (t, 2H, H^3-bipy), 7.46 (s, 2H, H^2-bipy), 7.39 (d, 1H, H^6-Ph) 6.89 (t, 1H, H^4-Ph) 6.51 (d, 1H, H^3-Ph) 6.46 (t, 1H, H^5-Ph) 4.74 (s, 1H, Ha^2) 3.94 (s, 1H, ^{4}NH) 2.66 (s, 3H, Methyl), 1.14 - 2.11 (m, 10H, Cyclohexyl)

Compound **18**: $[C_{27}H_{27}N_5OSZn]$ F.W. 534.99; Anal. Elemental: Found C 60.86, H 5.15, N 13.29, Zn 12.35; Calcd C 60.62, H 5.09, N 13.09, Zn 12.22; IR (KBr) 3434 b, 3210 sh, 1590 s, 1569 m, 1478, 1432, 1315, 1227 s, 1151 m, 1092 m, 1030 m, 850 m, 821 m, 727 m, 424 w cm^{-1}. ^{1}H-NMR ($CDCl_3$) δ 8.93 (d, 2H, H^1-phen), 8.42 (d, 2H, H^3-phen), 7.90 (s, 2H, H^4-phen), 7.78 (dd, 2H, H^2-phen), 7.45 (d, 1H, H^6-ph), 6.87 (t, 1H, H^4-ph), 6.46 (m, 2H, H^3&H^2-ph), 4.73 (d 1H, Ha^2), 3.96 (m, ^{1}H, ^{4}NH), 2.73 (s, 3H, Methyl), 1.12-2.13 (m, 10H, Cyclohexyl).

Compound **19**: $[C_{25}H_{27}N_5OSZn]$ F.W. 510.97; Anal. Elemental: Found C 59.10, H 5.43, N 13.80 Zn 12.84; Calcd C 58.77, H 5.33, N 13.71, Zn 12.80; IR (KBr) 1595 s, 1571 m, 1482 s, 1441 s, 1369 m, 1317 m, 1253 m, 1165 m, 1021 m, 859 m, 797 m, 721 m, 527 w, 415 w cm^{-1}; ^{1}H-NMR ($CDCl_3$) δ 8.61 (s, 2H, H^1-bipy), 8.07 (d, 2H, H^4-bipy), 7.94 (t, 2H, H^3-bipy), 7.46 (m, 2H, H^2-bipy), 7.37 (d, 1H, H^6-Ph), 6.85 (t, 1H, H^4-Ph), 6.5 (t, 2H, H^3&H^5-Ph), 3.82 (s, 4H, Ha), 2.66 (s, 3H, methyl), 1.79 (s, 4H, H_b), 1.53 (m, 4H, H_c).

Compound **20**: $[C_{27}H_{27}N_5OSZn]$ F.W. 534.99; Found C 59.98, H 5.18, N 12.97, Zn 12.10; Calcd. C 60.62, H 5.09, N 13.09, Zn 12.22; IR (KBr) 1591 m, 1564 m, 1484 s, 1419 s, 1390 m, 1359 m, 1313 m, 1193 m, 1162 m, 1031 m, 851 m, 866 m, 779 m, 764 m, 422 w cm^{-1}; ^{1}H-NMR ($CDCl_3$) δ 8.93 (d, 2H, H^1-phen), 8.39 (d, 2H, H^3-phen), 7.87 (s, 2H, H^4-phen), 7.75 (dd, 2H, H^2-phen), 7.44 (d, 1H, H^6-Ph), 6.80 (t, 1H, H^4-Ph), 6.45 (t, 2H, H^3 &H^5-phen), 3.62 (t, 4H, Ha), 2.72 (s, 3H, Methyl), 1.60 (s, 4H, H_b), 1.53 (m, 4H, H_c).

Compound **21**: $[C_{23}H_{23}N_5O_2SZn]$ F.W. 498.92; Anal. Elemental: Found C 55.01, H 5.82, N 13.84 Zn 12.93; Calcd C 55.37 H 4.65, N 14.04, Zn 13.11; IR (KBr) 1594 m, 1574 m, 1472 m, 1439 m, 1355 m, 1317 m, 1214 s, 1116 m, 1022 m, 886 m, 781 m, 764 m, 486 w, 427 w, 421 w cm^{-1}; ^{1}H-NMR ($CDCl_3$) δ 8.58 (s, 2H, H1-bipy), 8.05 (s, 2H, H4-bipy), 7.92 (t, 2H, H3-bipy), 7.45 (s, 2H, H2-bipy), 7.39 (d, 1H, H6-Ph), 6.89 (t, 1H, H4-Ph), 6.49 (t, 1H, H5-Ph), 6.45 (s, 1H, H3-Ph), 3.82 (s, 4H, Ha), 3.71 (t, 4H, H_b), 2.64 (s, 3H, Methyl); FAB

(m/z) 499 (80) [M^+], 500 (49) [M^++1] (501 (54) [M^++2], 497 (100) [M^+-2H], 343 (40) [M^+-bipy], 341 (51) [M^+-(2H+bipy)]

Compound **22**: [$C_{25}H_{23}N_5O_2SZn.H_2O$] F.W. 540.95; Anal. Elemental: Found C 55.73, H 4.59, N 12.99, Zn 12.05; Calcd. C 55.51, H 4.66, N 12.95, Zn 12.09; IR (KBr) 3423 b, 1593 m, 1564 m, 1469 s, 1436 s, 1356 m, 1318 m, 1211 s, 1115 m, 1030 m, 849 m, 761 m, 541 w, 485 w, 423 w cm^{-1}; ^{1}H-NMR ($CDCl_3$) δ 8.93 (d, 2H, H1-phen), 8.45 (d, 2H, H3-phen), 7.93 (s, 2H, H4-phen), 7.80 (dd, 2H, H2-phen), 7.45 (d, 1H, H6-Ph), 6.87 (t, 1H, H4-Ph), 7.46 (t, 2H, H3&H5-Ph), 3.85 (t, 4H, Ha), 3.70 (t, 4H, H_b), 2.72 (s, 3H, Methyl).

Compound **23**: [$C_{26}H_{23}N_5O_2SZn$] F.W. 518.95; Anal. Elemental: Found C 60.13, H 4.52, N 13.38, Zn 12.49 Calcd. C 60.18, H 4.47, N 13.50, Zn 12.60; IR (KBr) 1594 m, 1574 m, 1464 s, 1409 m, 1351 m, 1316 m, 1161 m, 1135 m, 1020 m, 856 m, 809 w, 705 m, 567 w, 422 w, 484 w cm^{-1}; ^{1}H-NMR ($CDCl_3$) δ 8.58 (d, 2H, H^1-bipy), 8.05 (d, 2H, H^4-bipy), 7.92 (t, 2H, H^3-bipy), 7.40 (t, 2H, H^2-bipy), 7.14-7.40 (m, 6H, peaks due to Aromatic groups), 6.86 (t, 1H, H^4-Ph), 6.44 (m, 2H, H^3& H^5-Ph), 3.54 (s, 3H, Ha1), 2.67 (s, 3H, Methyl).

Compound **24**: [$C_{28}H_{23}N_5O_2SZn$] F.W. 542.97; Anal. Elemental: Found C 61.73, H 4.31, N 12.79, Zn 11.92; Calcd. C 61.94, H 4.27, N 12.90, Zn12.04; IR (KBr) 1593 m, 1565 m, 1493 s, 1405 s, 1338 m, 1125 m, 1024 m, 848 m, 764 m, 727 m, 640 w cm^{-1}; ^{1}H-NMR ($CDCl_3$) δ, 8.90 (d, 2H, H^1-phen), 8.39 (d, 2H, H^3-phen), 7.87 (s, 2H, H^4-phen), 7.73 (dd, 2H, H^2-phen), 7.46 (d, 1H, H^6-Ph), 7.27 (m, 4H, Ar), 7.16 (m, 1H, Ar), 6.64 (t, 1H, H^4-Ph), 6.42 (m, 2H, H^3 & H^5-Ph).

4.2.3 Physical measurements

The experimental techniques used for the characterization of the compounds are described in chapter 2b. The IR spectra were recorded in a Perkin-Elmer, Spectrum GX FT IR Spectrometer at CVM, SICART, Gujarat. FAB mass spectrum was recorded in JEOL SX 102 FAB mass spectrometer at CDRI, Lucknow. The TGA of selected samples were carried out at the Catalysis division, IIT, Chennai.

4.3. RESULTS AND DISCUSSION

4.3.1 Preparation of the complexes

Refluxing instead of stirring can also be adopted for the preparation of the compounds. Compared to refluxing, stirring was found to be more effective in terms of time and yield of product complex. All the compounds are more or less yellow in color. The color is rather deep for complexes of H_2L^1, while, bright yellow for complexes of H_2L^3.

The elemental analysis data showed that all complexes are having a stochiometry formulated as [MLB], where L is the doubly deprotonated thiosemicarbazone ligand and B is the bidentate heterocyclic bases viz., phenanthroline and bipyridine. Small variation in the elemental data can be attributed to the small fraction of water of crystallization present in non-stochiometric proportions. The TGA of a representative compound (compound 21) showed that the compound starts decomposing at 220°C with the loss of small amount of lattice water, present in non-stochiometric proportion. Compound **20** and **22** also

contains lattice water, ≈0.7- 0.9% by composition. Isolation of X-ray quality single crystals had not been successful.

4.3.2. FAB Spectra

The FAB mass spectra of a representative compound, **21** gave the molecular ion (M^+) peak at m/z 499 (80). A peak at m/z 501 (60), may be due to isotope of zinc. The base peak is at m/z 497 (100) resulting from the loss of two weakly bound protons from the molecular ion. The region between the base peak and the m/z 343 do not have any significant features. The peak at m/z 343 (30) corresponds to the ML^+ species resulting from the loss of bipyridine. The peak at m/z 341 (48) corresponds to (ML^+-2H) species. It indicates that the weakest bond in the representative complex is $Zn\text{-}N_{(base)}$.

4.3.3. IR spectra

The Infrared spectra of the compounds show two strong to medium bands due to the imine coordinated $^7C{=}^1N$ bond, *ca.* 1575 cm^{-1} and the one due to the newly formed $^2N{=}^9C$ bond, ca. 1595 cm^{-1}[9*]. The shifting of bands near 1605 cm^{-1} in uncoordinated thiosemicarbazones, to lower frequencies *ca.* 25-30 cm^{-1} is an indication of the coordination of the azomethine nitrogen to the zinc metal. The presence of weak bands in the region 405 - 490 cm^{-1} is due to the Zn-N stretching frequencies. Compound **20**, **21** and **22** showed broad peaks centered around 3400 cm^{-1}, which is characteristic of lattice water [32]. The new peaks observed in the range 540 - 570 cm^{-1} are due to the $Zn\text{-}O_{(phenolic)}$ bond [10]. A small shift in the absorption bands due to the N-N stretching vibrations to higher region is an indication of the formation of the thiol tautomer before coordination. The presence of heterocyclic bases is indicated by their characteristic vibrational modes listed in Table 4.1.

4.3.4 NMR spectra

The NMR spectra of all the complexes lack the peaks corresponding to the acidic protons of the uncoordinated thiosemicarbazones, which is an evidence for the coordination of the ligand as doubly deprotonated anion. The downfield shift of proton peaks corresponding to phenolic ^3CH, ^8CH (methyl), H^1 of heterocyclic bases are the result of the withdrawal of electron density from the thiosemicarbazone moiety and the heterocyclic base, due to coordination with the metal atom [11]. The structure of the complexes is given along with their atom labeling in Figure 4.2 with respect to NMR assignments. Since the proton NMR signals of the heterocyclic bases are equivalent it can be inferred that the heterocyclic base is lying in a plane symmetrical with respect to the thiosemicarbazone moiety. This is possible if the compounds assume trigonal bipyramid geometry. The tentative structure is given in Figure 4. 1.

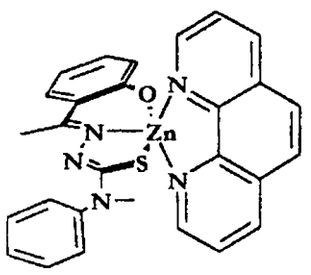

Compound 24

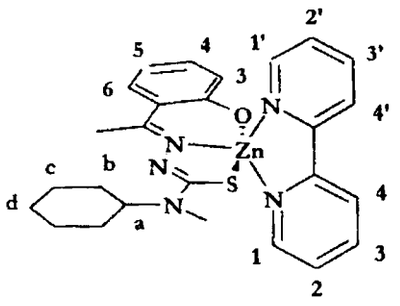

Compound 17

Figure 4.1.: Suggested trigonal bipyramid (TBP) structure of the compounds **17** and **24**

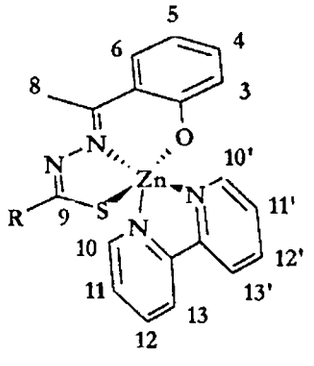

I

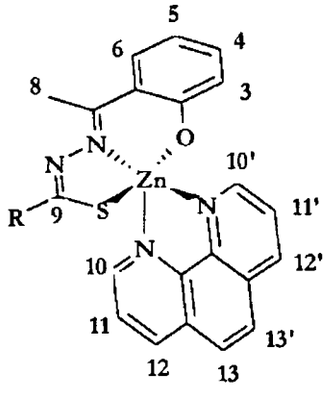

II

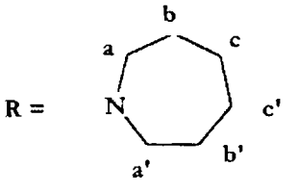

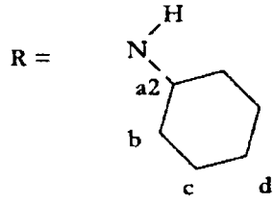

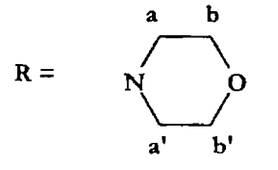

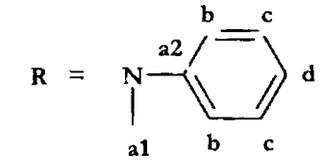

Figure 4.2.: The structures representative complexes are given along with their atom labeling

4.3.5. Biological studies

All the zinc complexes were screened against bacteria *E.Coli*, *Staphylococcus Aureus*, and fungal cultures *Candida Albicans* and *Asperigillus Flavus*. The method and the procedure are described in detail in chapter 2b. As in the case of copper complexes the screening was carried out at concentrations i.e., 5 μg and 1 μg for bacterial cultures and 50 μg and 20 μg for fungal cultures. In all cases of bacterial screening 50 μg of gentamycin and 50 μg of flucanazole for fungal cultures were used as the standard. The data are tabulated in Table 4.2.

The zinc complexes are found not to have significant activity against any of the cultures tested, compared to either its copper counterparts or its thiosemicarbazone compounds.

Table 4.1: IR spectral assignments for thiosemicarbazones and their zinc complexes *

Compound	ν (^{7}C=N^1)	ν (^{2}N=C^9)	ν (^{1}N-N^2)	ν (Zn-N)	ν/ δ (C=S)	ν (C-O)	ν (Zn-O)	Bands due to heterocyclic base
H_2L^1	1599s	-	988 m	-	1365s 864 m	1219 s	--	-
ZnL^1bip (**17**)[a]	1567m	1595s	1020m	482 w, 416 w	1316s 822 m	1153 s	571 w	1475 m, 1441s, 739 m, 757w
ZnL^1phen (**18**)	1569m	1591s	1030m	481 w, 424w	1315s 822 m	1151 s	575 w	1478 s, 1432 m, 728 w, 850 m
H_2L^2	1603s	-	997m	-	1383s 839 m	1252 s	--	-
ZnL^2bip (**19**)	1571m	1595s	1021m	415 w	1316s 797 m	1190 s	528 w	1482m, 1441m, 1367m, 721m
ZnL^2phen (**20**)	1565m	1593s	1031m	422w	1314s 791 m	1194 s	561 w	1484m, 1419m, 1359 m, 851 m
H_2L^3	1605s	-	1017m	-	1374s 835 m	1219 s	--	-
ZnL^3bip (**21**)	1574m	1594s	1062m	427m, 421w	1317s 791 m	1116 s	542 w	1472m, 1439m, 1355 m, 854m, 738m, 629 w
ZnL^3phen (**22**)	1564m	1593s	1030 m	485 w, 423w	1318s 797 m	1114 s	542 w	1469, 1436, 1356, 761 m, 849w, 642 m
H_2L^4	1601s	-	1001 m	-	1375s 791m	1222 s	--	-
ZnL^4bip (**23**)	1575m	1594s	1021 m	484w 422w	1316s 776m	1161 s	567 w	1463s, 1409 s, 1351m, 856 m, 705m
ZnL^4phen (**24**)	1565m	1593s	1027 m	484 m 423w	1338s 764 m	1125 s	563 w	1493m, 1405m, 848 m, 727 m, 640 w

- All values are reported in units of cm^{-1}.

Table 4.2: Biological activity of the compounds of zinc(II) complexes*

Complex/ ligand	*E.Coli*		*Staphylococus*		*Asp. Flavus*		*C. Albicans*	
	5μg	1μg	5μg	1μg	50μg	20μg	50μg	20μg
H_2L^1	17± 0.5	15± 0.5	19± 0.6	18± 0.4	9± 0.5		11± 0.5	10± 0.3
ZnL^1bip.(**17**)	15± 0.3	15± 0.6	15± 0.5	11± 0.5	11± 0.2		12± 0.45	11± 0.4
ZnL^1phen (**18**)	16± 0.4	15± 0.3	13± 0.4	11± 0.3	14± 0.3		18± 0.3	16± 0.2
H_2L^2	18± 0.3	17± 0.4	17± 0.3	16± 0.6	15± 0.4		11± 0.3	12± 0.5
ZnL^2bip (**19**)	15± 0.3	14± 0.3	19± 0.2	12± 0.4	14± 0.5		13± 0.3	12± 0. 6
CuL^2phen (**20**)	16± 0.4	15± 0.4	19± 0.4	11± 0.4	15± 0.3		15± 0.2	14± 0.3
H_2L^3	19± 0.5	16± 0.5	24± 0.5	22± 0.3	10.0		11.0	11.0
ZnL^3bip (**21**)	15± 0.4	16± 0.25	22± 0.6	20± 0.5	13± 0.2		17± 0.4	16± 0.3
ZnL^3phen (**22**)	17± 0.3	17± 0.3	24± 0.4	23± 0.3	14± 0.3		18± 0.3	17± 0.4
H_2L^4	14± 0.7	13± 0.5	17± 0.2	16± 0.4	09.0		10.0	10.0
ZnL^4bip (**23**)	15± 0.6	14± 0.2	18± 0.3	14± 0.3	12.0		13± 0.2	13.0
ZnL^4phen (**24**)	14± 0.5	13± 0.4	17± 0.4	13± 0.4	13.0		17± 0.3	16.0
Gentamycin/ Flucanazole#	26± 1.7	26± 2.0	30± 2.5	30± 2.5	20± 0.8		22± 0.4	22± 2.1

* All measurements are in mm diameter of inhibition zone (9.0 mm indicates no inhibition)

Commercially available anti-microbial agents.

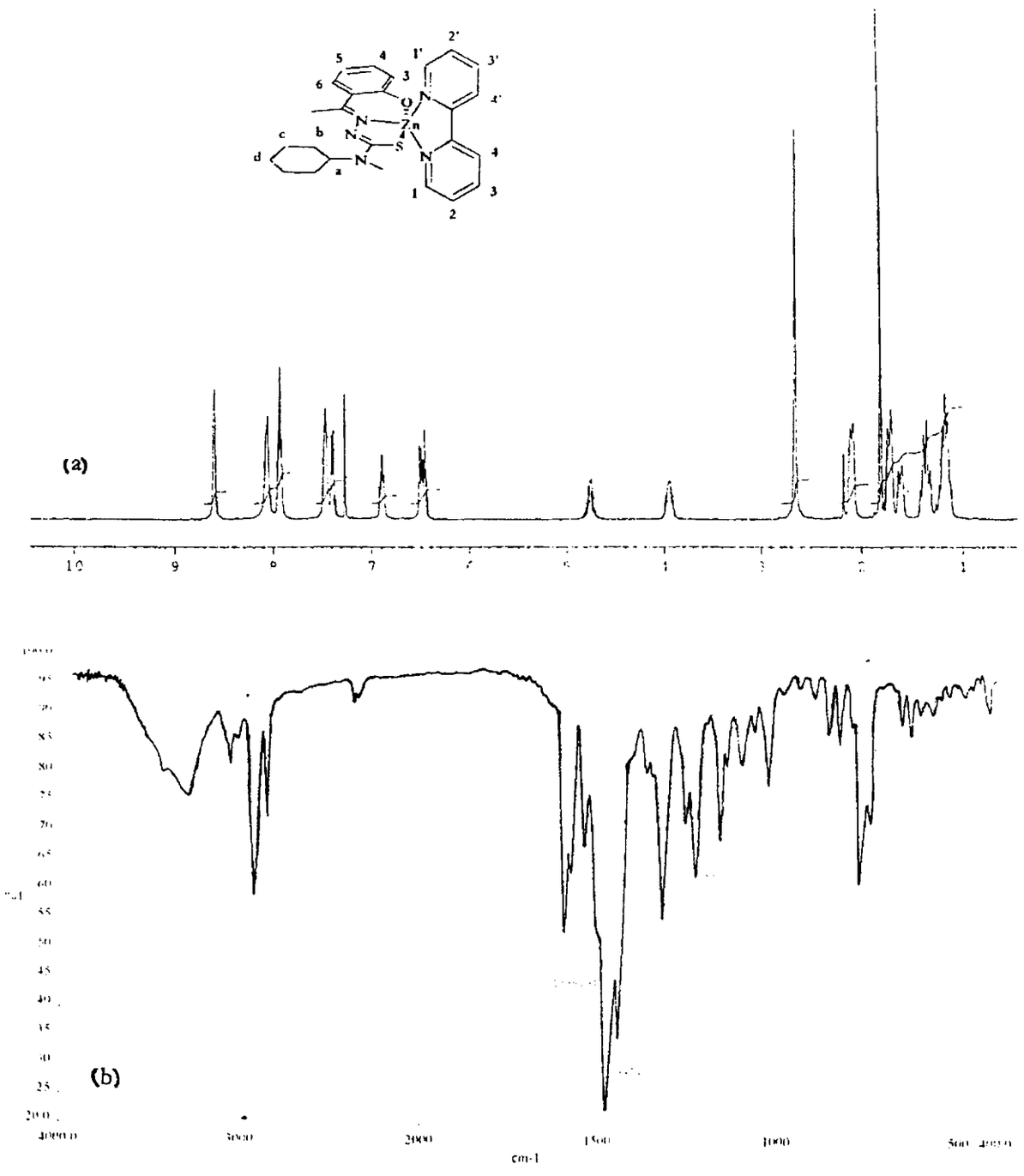

Figure 4.3:a) ^{1}H NMR spectrum of the compound **17**, b) IR spectrum of compound **17**

REFERENCES

1. R. P. J. Williams, *Endeavour, New. Ser.*, 1984, **8**, No. 2.
2. T. G. Spiro, *Zinc Enzymes*, Wiley, NY, 1983; I. Bertini, C. Luchinat, W. Maret and M. Zeppezauer, *Zinc Enzymes* , Birkhäuser, Boston, 1986.
3. H. Eklund, B. Nordstrom, E. Zeppezauer, G. Soderlund, I. Ohlsson, T. Bowie, B. O. Soderberg, O. Tapia, C. I. Branden, *J. Mol. Biol.*, 1976, **102**, 27.
4. M. H. Bracey, J. Christiansen, P. Towar, S. P. Cramer, S. G. Bartlet, *Biochemistry*, 1994, **33**, 13126.
5. A. J. Dent, D. Betersmann, C. Block, S. S. Hasnain, *Biochemistry*, 1990, **29**, 7822.
6. H. G. Petering, H. H. Buskirk and J. A. Crim, *Cancer Res.*, 1967, **27**, 1115; J. A. Crim and H. G. Petering, *Cancer Res.*, 1967, **27**, 1278.
7. G. J. Van Giessen, J. A. Crim, D. H. Petering and H. G. Petering, *J. Natl. Cancer Inst.*, 1973, **51**, 139.
8. M. B. Ferrari, G. G. Fava, C. Pelizzi, P. Tarasconi and G. Tosi, *J. Chem. Soc., Dalton Trans.*, 1987, 227; M. B. Ferrari, G. G. Fava, M. Lanfranchi, C. Pelizzi and P. Tarasconi, *Inorg. Chim. Acta.*, 1991, **181**, 253.
9. *D. X. West, G. A. Bain, R. J Butcher, J. P. Jasinski, R. Y. Pozdniakiv, Y. Lee, J. Valdez-Martinez, R. Toscano, S. Hernandez-Ortega, *Polyhedron*, 1996, **15**, 665; D. X. West, P. Ahrweiler, G. Ertem, J. P. Scovill, D. L. Klayman, J. L . Flippen-Anderson, R. Gilardi, C. George, L. K. Pannell, *Transition Met. Chem.*, 1985, **10**, 264.
10. G. C. Percy, D. A. Thornton, *J. Inorg. Nuclear. Chem.* 1972, **34**, 3351.
11. E. Bermejo, R. Carballo, A. Castineiras, R. Dominguez, A. E. Liberta, C. Maichle-Mossmer, D. X. West, *Z. Naturforsch.*, 1999.

CHAPTER 5

SYNTHESIS AND SPECTRAL STUDIES OF COBALT(III) COMPLEXES

5.1 INTRODUCTION

The enzyme nitrile hydratase (NHase) catalyzes conversion of nitriles to amides in several microorganisms and has found its use in the individual production of selected amides [1]. The active site of the hetero dimeric enzyme comprises either a low-spin non-heme Fe(III) or a noncorrin cobalt(III) center nested in a CXXCSC sequence of the α subunit. Recent crystallographic study on two *Rhodococcus* NHases have revealed that the single low-spin Fe(III) site in the $\alpha\beta$ heterodimer is coordinated to two deprotonated carboxamido nitrogens and the three Cys-S centers [2] with at least two of them modified to Cys-sulfenic and sulfinic groups [3]. The occurrence of the kinetically inert low-spin d^6 cobalt(III) center in NHase raises an interesting question regarding the role of the unusual donor set in the observed reactivity of the metal site. Though papers on Co(III) complexes of thiosemicarbazones are less in number compared to that of Cu(II) and Zn(II) complexes, recently there are some interesting reports on the Co(III) of mono and bis thiosemicarbazones [4]. Work on Co(III) complexes with carboxamido nitrogen(s) and thiolate sulfur(s) has been very scanty so far. Based on the above observations and the importance of thiosemicarbazones as good chelating agents [5], and potential growth inhibitors, we have attempted to prepare some novel Co(III) complexes of thiosemicarbazones of our interest and tried to establish the structural characteristics using various spectral techniques.

5.2. EXPERIMENTAL

5.2.1. Materials

The thiosemicarbazone ligands were prepared as described in chapter 2a. They were purified by recrystallization before complexation. The Sodium azide (Merck) and heterocyclic bases, viz., bipyridine and phenanthroline were of reagent grade (Merck), and were used as such. Co(II) acetatetetrahydrate (BDH) was purified by recrystallisation before complexation.

5.2.2 Preparation of complexes

The thiosemicarbazones (0.5 mmol) were dissolved in 20 mL of ethanol, to which was added 0.5 mmol of the heterocyclic base in the solid form. The mixture was slightly warmed to ensure complete dissolution of the ligands. To the above mixture was added about 10 mL of methanolic solution of cobalt(II) acetatetetrahydrate (0.5 mmol), with stirring. The stirring is continued for about 15 minutes. When a deep brown solution resulted, solid sodium azide (0.75 mmol) was added. Stirring was continued for about an hour. The solution was kept aside overnight for crystallization to occur. The compound was filtered washed with ethanol, water, and ether respectively. It was then dried over P_4O_{10} *in vacuo*.

Compound 25: $[C_{25}H_{28}CoN_8OS{\cdot}0.5H_2O]$ F.W. 555.84: Anal. Elemental Found C 53.77, H 4.93, N 19.93, Co 10.52; Calcd. C 53.09, H 5.09, N 20.20, Co 10.54; IR (KBr) 3338sh, 2029s, 1591m, 1566m, 1492s, 1435m, 1328m, 1231m, 1154s, 1030m, 864m, 762s, 730m, 626w, 413w, 482w cm^{-1}; ^{1}H-NMR δ 9.38(d, 1H, 1-bipy), 8.21(d, 1H, 1'-bipy), 8.11(d, 2H, 4&3-bipy), 8.04(d, 1H, 4'-bipy), 7.89(t, 1H, 3'-bipy), 7.67(t, 2-bipy), 7.59(d, 1H, H^6-Ph), 7.32(t, 1H, 2'-bipy), 6.95(t, 1H, H^4-Ph), 6.70(d, 1H, H^3-Ph), 6.55(t, 1H, H^5-Ph), 4.83(m, 1H, Ha-Cyclohexyl), 3.71(m, 1H, ^{4}NH), 3.14(s, 2H, methyl), 2.09(m, 4H, Cyclohexyl), 1.17-1.40(m, 6H, Cyclohexyl)

Compound 26: $[C_{27}H_{28}CoN_8OS.H_2O]$ F.W.589.58: Anal. Elemental Found C 54.86, H 5.03, N 19.20, Co 10.26; Calcd. C 55.00, H 5.13, N 19.01, Co10.00; IR (KBr) 3341w, 2022s, 1590m, 1562m, 1439s, 1466s, 1367m, 1335m, 1271m, 1198m, 1135m, 1086m, 1023m, 868m, 645w, 479w, 416w cm^{-1}; ^{1}H-NMR δ 9.37(d, 1H, 1-phen), 8.2(d, 1H, 1'-phen), 8.10(m, 2H, 4&2-phen), 8.05(s, 1H, 4'-phen), 7.88(t, 1H, 2'-phen), 7.62(m, 2H, 3-phen & H^6-Ph), 7.29(t, 1H, 3'-phen), 6.96(t, 1H, H^4-Ph), 6.71(d, 1H, H^3-Ph), 6.57(t, 1H, H^5-phen), 3.70(s, 2H, ^{4}NH & Ha-Cyclohexyl), 3.13(s, 3H, methyl), 1.75(m, 4H, Hb-Cyclohexyl), 1.61 & 1.48 (6H, Cyclohexyl).

Compound 27: $[C_{25}H_{28}CoN_8OS]$ F.W. 547.54 Anal. Elemental. Found C 54.62, H 4.89, N 20.42, Co 10.79; Calcd. C 54.94, H 4.98, N 20.50, Co 10.78; IR (KBr) 2018s(sh), 1588m, 1562m, 1437s, 1334s, 1272m, 1242m, 1204m, 1165m, 1135m, 1105m, 1060w, 1019w, 866m, 727w, 644w, 612w, 571w, 480w, 416w cm^{-1}; ^{1}H-NMR δ 9.30(d, 1H, 1-bipy), 8.12(d, 1H, 1'-bipy), 7.97-8.02(m, 2H, 3&4-bipy), 7.95(d, 1H, 4'-bipy), 7.79 (t, 1H, 3'-bipy), 7.56(t, 1H, 2-bipy), 7.52(d, 1H, H^6-Ph), 7.21(t, 1H, 2'-bipy), 6.87(t, H^4-Ph), 6.45(d, 1H, H^3-Ph), 6.47(t, 1H, H^5-Ph), 3.63(m, 4H, Ha), 3.06(s, 3H, methyl), 1.69(m, 4H, Hb), 1.42(m, 4H, Hc).

Compound 28: $[C_{27}H_{28}CoN_8OS.H_2O]$ F. W. 588.57 Found C 54.86, H 4.97, N 18.94, Co 10.03; Calcd. C 55.00, H 5.13, N 19.01, Co10.00; IR (KBr) 3448b, 2019s(sh), 1594m, 1564m, 1495s, 1438s, 1366m, 1339m, 1244m, 1194m, 1143w, 1020w, 846m, 752m, 721m, 521w, 413w, 442w cm^{-1}; ^{1}H-NMR 9.43(d, 1H, 1-phen), 88.46(d, 1H, 1'-phen), 8.35(d, 1H, 3-phen), 8.25(d, 1H, 3'-phen), 7.94(d, 1H, 4-phen), 7.86(d, 1H, 4'-phen), 7.87(dd, 1H, 2-phen), 7.55(d, 1H, H^6-Ph), 7.52(dd, 1H, 2'-phen), 6.86(t, 1H, H^4-Ph), 6.57(d,1H, H^3-Ph), 6.49(t,1H, H^5-Ph), 3.61(q, 4H, Ha), 3.12(s, 3H, methyl), 1.68(m, 4H, Hb), 1.42(m, 4H, Hc).

Compound 29: $[C_{23}H_{24}CoN_8O_2S]$ F.W. 535.49: Anal. Elemental. Found C 51.96, H 4.42, N 21.23, Co 11.07, Calcd C 51.59, H 4.52, N 20.93, Co 11.01; IR (KBr) 2022, 1594m, 1560m, 1497s, 1469s, 1387m, 1342m, 1269m, 1223m, 1155w, 1109m, 1026m, 887m, 727w, 646w, 504w, 421w, 402w cm^{-1}; ^{1}H-NMR δ 9.40(d, 1H, 1-bipy), 8.12(d, 3H, 1'-bipy, 4&3-bipy), 8.04(d, 1H, 4'-bipy), 7.89(t, 1H, 3'-bipy), 7.67(t, 1H, 2-bipy), 7.59(d, 1H, H^6-Ph), 7.31(t, 1H, 2'-bipy), 6.94(t, 1H, H^4-Ph), 6.69(d, 1H, H^3-Ph), 6.54(t, 1H, H^5-Ph), 3.72(s(br), 8H, Ha & Hb), 3.14(s, 3H, methyl).

Compound 30: $[C_{25}H_{24}CoN_8O_2S.3H_2O]$ F.W. 613.55 Anal. Elemental Found C 48.87, H 4.96, N 18.29, Co 9.56, Calcd C 48.94, H 4.93, N 18.26, Co 9.61; IR (KBr) 3428b, 2024S(sh), 1595m, 1563m, 1436m, 1342m, 1270m, 1227s, 1112m, 1030m, 845m, 721m, 652w, 556w, 443w, 410w cm^{-1}; ^{1}H-NMR δ 9.53(d, 1H, 1-phen), 8.57(d, 1H, 1'-phen), 8.35(d, 2H, 3&3'-phen), 8.03(t, 3H, 4, 4'& 2-phen) , 7.63(d,

2H, H^6-Ph & 2'-phen), 6.89(t, 1H, H^4-Ph), 6.61(d, 1H, H^3-Ph), 6.56(t, 1H, H^5-Ph), 3.70(s, 8H, Ha & Hb), 3.19(s, 3H, methyl). FAB (m/z) M^+ 613 (15), 558 (20), 516 (78).

Compound 31: $[C_{26}H_{24}CoN_8OS]$ F.W. 555.52: Anal. Elemental. Found C 55.99, H 4.14, N 19.97, Co 10.67, Calcd. C 56.21, H 4.35, N 20.17, Co 10.61; IR (KBr) 2025s(sh), 1596m, 1563m, 1437m, 1339m, 1287m, 1123m, 1010m, 866w, 733m, 702m, 572w, 551w, 441w, 411w; ^{1}H-NMR δ 9.31(d, 1H, 1-bipy), 8.16(d, 1H, 1'-bipy), 8.01(m, 3H, 4,3 & 4'-bipy), 7.58(t, 1H, 3'-bipy), 7.58(t, 2H, 2-bipy & H^6-Ph), 7.30(m, 5H, Ha, Hb & 2'-bipy), 7.16(d, 1H, Hc), 6.94(t, 1H, H^4-Ph), 6.70(d, 1H, H^3-Ph), 6.53(t, 1H, H^5-Ph), 3.58(s(b), 3H, N-CH_3), 3.16(s, 3H, methyl).

Compound 32: $[C_{28}H_{24}CoN_8OS]$ F.W. 579.54: Anal. Elemental Found C 58.10, 4.32, N 19.20, Co 10.07; Calcd. C 58.03, H 4.17, N 19.33, Co 10.17; IR (KBr) 2023s(sh), 1594m, 1562s, 1432m, 1344m, 1237m, 1125m, 1025w, 845m, 755m, 721m, 577w, 552w, 442w, 412w cm^{-1}; ^{1}H-NMR 9.70(d, 1H, 1-phen), 8.48(d, 1H, 1'-phen), 8.40(d, 1H, 3-phen), 8.32(d, 1H, 3'-phen), 7.90(m, 3H, 4, 4'& 2-phen), 7.64(m, 2H, 2'-phen & H^6-Ph), 7.29 (d, 2H, Ha-Ar), 7.24(t, 2H, Hb-Ar), 7.11(t, 1H, Hc-Ar), 6.91(t, 1H, H^4-Ph), 6.61(d, 1H, H^3-Ph), 6.56(t, 1H, H^5-Ph), 3.58(s, 3H, N-CH_3), 3.23(s, 3H, methyl).

5.2.3. Physical measurements

The details of various experimental techniques used for the characterization of the compounds are described in Chapter 2b.

5.3. RESULTS AND DISCUSSION

5.3.1 Preparation of complexes

It has been found that the Co(II) ion undergoes oxidation in the presence of methanol or chloroform [6] unlike in ethanol [7]. All the complexes are found to be brown in color but the crystalline nature may vary depending on their mode of formation. Complexes of H_2L^4 were found to give fine crystals on keeping while compounds of H_2L^1 and H_2L^2 were found to give the products more readily.

The elemental analysis data of compounds **25-32** suggests a formulation of $[MLBN_3]$. This indicates that the azide ion is coordinated to the metal as uninegative unidentate ligand. However, for the compound 25 the elemental data matches with a stochiometry containing 0.5 molecule of water of crystallization/lattice water. The compounds **26** and **28** contain one molecule of uncoordinated water and three molecules of water for the compound **30**. Compound **32** obtained in two different colors, viz., brown (**32a**) and green (**32b**). The elemental data indicate that **32a** is having one molecule of water, while the later **32b** is devoid of it. The elemental data of compound **32b** is reported here. Both give similar IR and UV spectra. The slight variations found in the elemental data for some of the compounds are due to the presence of non-stochiometric amount of water of crystallization present. All the complexes are found to

be diamagnetic confirming that the cobalt is in the +3 oxidation state and hence corresponds to d^6 ion in strong field. The molar conductance value indicates that the azide ion is within the coordination sphere. We were able to isolate X-ray quality single crystals of compound **31** by slow diffusion of ethanol into a solution of the compound in chloroform.

The thermal analysis of the compounds **25**, **26**, **28** and **30** showed that the non-stochiometric water of crystallization begins to lose in the 220-260°C range. The loss is gradual in **25**, **28** and in **29** but a sharp change at 250°C is found in the case of compound **26**. All the complexes started decomposing at 310°C and the changes are sharp at 330°C.

The FAB mass spectrum of the compound **30** gives a molecular ion(M^+) peak at m/z 613 (15) corresponding to trihydrated formulation. The next major peak at m/z 558 (20) corresponds to the non-hydrated formulation. The next lower but major fraction appears at m/z 516 (78) corresponding to a fraction stripped off its azido group.

5.3.2. Electronic and IR spectra

The electronic spectra (Figure 5.1) show broad bands in the visible region *ca.* 485-495 nm region and is characteristic of low-spin d^6 systems as cobalt(III) (Table 5.1) [8]. This is due to the $^1A_{1g} \rightarrow {}^1T_{1g}$ transition. However the tail of the charge transfer (CT) bands *ca.* 400 nm, mask the higher energy band due to $^1A_{1g} \rightarrow {}^1T_{2g}$ transition. The CT band is rather too broad and is explained as a combination of two bands resulting from the S→Co(III) and O→Co(III) charge transfer transitions. The broadband centered *ca.* 630 nm is due to the $^1A_{1g} \rightarrow {}^3T_{2g}$ transition [9]. Compound **32a** and **32b** dissolve to give a reddish brown solution in CH_2Cl_2 and give similar IR and UV spectra.

Compounds **25**, **28**, **29**, and **30** show broad bands *ca.* 3400 cm^{-1}, which is due to the O-H stretching modes of the uncoordinated water molecules. The infrared spectrum of the complexes show peaks *ca.* 1595 cm^{-1} due to the newly formed $^2N=^9C$ bond indicating that the coordination of the thiosemicarbazone takes place in the form of thiol rather than as thione. The lowering of the band *ca.* 1602 cm^{-1} ($^7C=^1N$) by 30 – 50 cm^{-1} (Table 5.2) is an explicit evidence for the coordination of the thiosemicarbazone through the azomethine nitrogen. The spectra of the complexes exhibit a systematic shift in the position of the bands 1600-1350 cm^{-1} region due to ν(C=C) and ν(C=N) vibrational modes, and their mixing patterns are different from those present in the ligand spectrum. Coordination of the bases is indicated by the presence of weak bands in the 410 – 485 cm^{-1} region due to Co-N stretching vibration. Weak bands in the range 510-565 cm^{-1} regions indicated the presence of Co-O bond resulting from coordination of phenolic oxygen. Besides the shifting of the bands due to $C\text{-}O_{(phenolic)}$ group to lower frequencies indicates the weakening of the C-O bond due to coordination. The presence of the azide group in the coordination sphere is evidenced from the very strong and sharp absorption peak *ca.* 2022 cm^{-1}. The azido group is bound to cobalt as terminal as it gives only one strong absorption at 2030 cm^{-1} characteristic of a terminal azido group [10]. The slight lowering in values is assumed to the result of its coordination to the metal [11]. The coordination via the thiolate sulfur is evidenced from the lowering of band due to the C-S stretching vibration *ca.* 1365 cm^{-1}, and C-S bending vibration *ca* 864cm^{-1}. The two very intense bands at 1495 and 1465 cm^{-1} show presence of different delocalised ligand molecules linked to the metal through the imine nitrogen.

5.3.3. ^{1}H-NMR spectra

The ^{1}H-NMR spectra of the complexes indicate signals corresponding to the heterocyclic bases and the thiosemicarbazone moiety. The resonance absorptions of some of the protons near to the coordinated nitrogens are shifted downfield, which is an evidence for the coordination of the ligand to the metal in higher oxidation state and subsequent decrease in the electron density in the ligand super structure. The non-homogeneity of the proton signals is due to an oriented geometry about the central metal. The approximate disposition of the ligands around the metal ion is shown in Figure 5.2, the atom labeling scheme and the ^{1}H NMR assignments of compound 28 is shown in Figure 5.2a, b respectively.

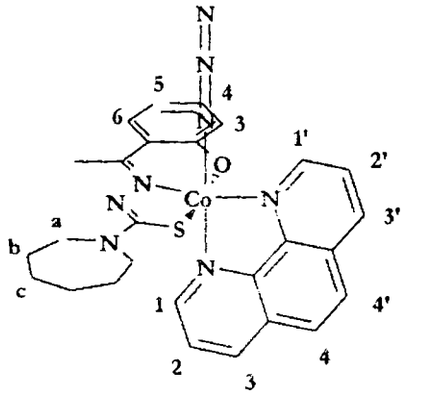

a

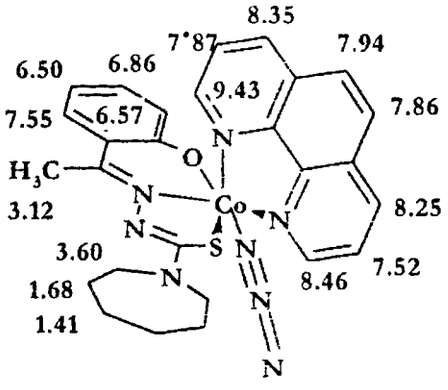

b

Figure 5.2.(a).: Atom labeling scheme for ^{1}H-NMR assignments for the compound 28.
(b) Approximate ^{1}H-NMR assignments for the compound 28

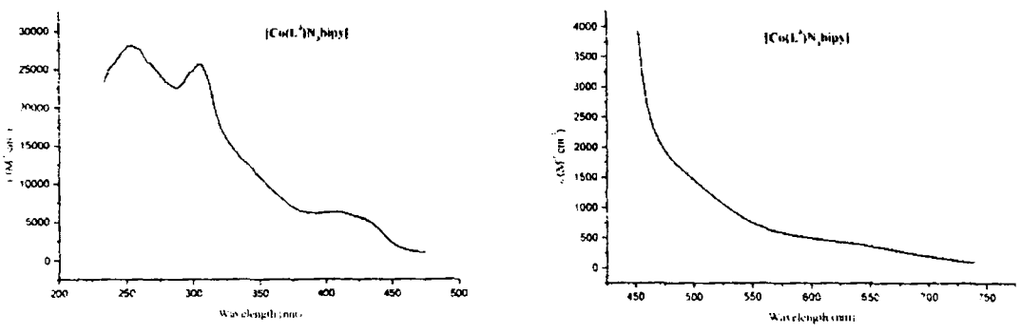

Figure 5.1a: Electronic spectrum of Compound **29** [$CoL^3(N_3)bipy$]

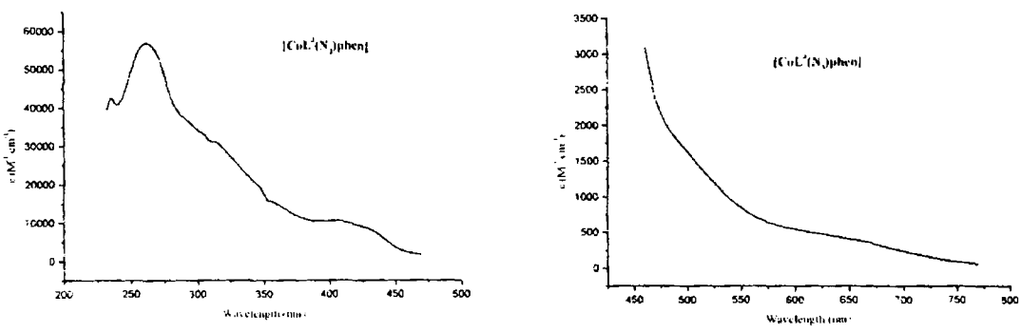

Figure 5.1b: Electronic spectrum of Compound **30** [$CoL^3(N_3)phen$]

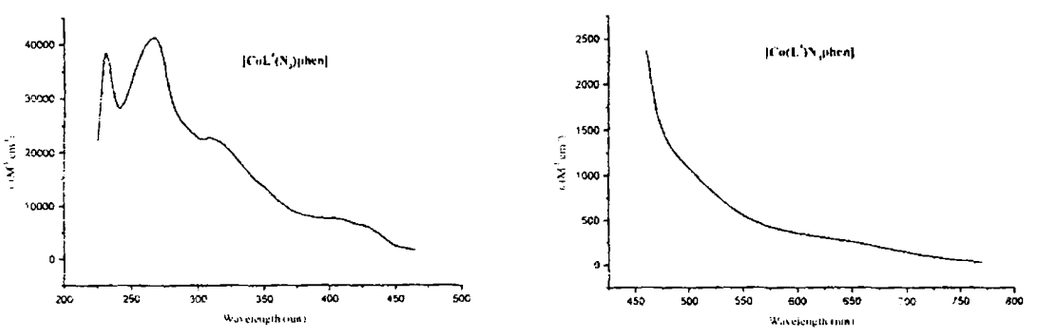

Figure 5.1c: Electronic spectrum of Compound **32** [$CoL^4(N_3)phen$]

Table 5.1.: Electronic spectral assignments, λ/cm $^{-1}$(logε^{a}) for compound **25-32**

Compound	d-d	LMCT	n→π*	π→π*
$CoL^{1}(N_3)$bipy (**25**)	17094(2.49), 20583(3.18)	24937 (3.82) 29154 sh (4.10)	33003 (4.43),	39525 (4.48), 37453 (4.47)
$CoL^{1}(N_3)$phen (**26**)	16528(2.42), 20202(2.80)	24691 sh (3.90)	32520 (4.52)	43478 (4.22), 39604 (4.54)
$CoL^{2}(N_3)$bipy (**27**)	16949(2.20), 20000(2.76)	24570 (4.01)	32573 (4.56), 33333 sh (4.45)	40241 (4.52), 36630 (4.62)
$CoL^{2}(N_3)$phen(**28**)	16530(2.47), 20408(3.22)	24937 (4.02)	32051 (4.50), 34722 sh (4.55)	37313 (4.75), 43197 (4.72)
$CoL^{3}(N_3)$bipy (**29**)	16758(2.70), 20636(3.23)	24498 (3.80)	29485 sh (4.12), 32786 (4.40)	39683 (4.44)
$CoL^{3}(N_3)$phen (**30**)	16474(2.71), 20080(2.82)	24938 (4.02)	32258 (4.49), 34222 sh (4.57)	38168 (4.75), 42735 (4.63)
$CoL^{4}(N_3)$bipy (**31**)	17035(2.74), 20202(3.25)	24570 (3.75)	29762 sh (4.10), 32679 (4.35)	40322 (4.34), 36630 (4.29)
$CoL^{4}(N_3)$phen (**32**)	16612(2.55), 20325(3.07)	24570 (4.00)	32363 (4.35), 34628 sh (4.47)	37453 (4.62), 43290 (4.58)

^{a} = ε is expressed in (l mol $^{-1}$cm $^{-1}$)

Table 5.2.: Infra Red spectral assignment for compounds 25-32

Compound	ν ($^{7}C=N^{1}$)	ν ($^{2}N=C^{9}$)	ν (N_3)	ν (Zn-N)	ν/ δ (C=S)	ν (C-O)	ν (Co-O)	Bands due to heterocyclic base
H_2L^1	1599s	-			1365s, 864m	1219 s	--	-
$CoL^1(N_3)$bip (**25**)[a]	1564m	1593s	2029s	482w, 413w	1329s, 762m	1154 s	525w	1492 m, 1435s, 730m
$CoL^1(N_3)$phen (**26**)	1562m	1590s	2022s	479w, 415w	1335s, 766m	1135 s	571w	1497s, 1439s, 1367m, 868w
H_2L^2	1603s	-			1383s, 839m	1252 s	--	-
$CoL^2(N_3)$bip (**27**)	1562m	1588	2018s	479w, 416 w	1334s, 765m	1203 m	541w	1498m, 1438m, 1367m, 866m
$CoL^2(N_3)$phen (**28**)	1564m	1594s	2018s	414w, 443w	1339s, 753m	1195 m	542w	1495m, 1438m, 1366 m, 845m
H_2L^3	1605s	-			1374s, 835m	1219 s	--	-
$CoL^3(N_3)$bip (**29**)	1560m	1594s	2022s	412m, 403w	1342m, 761	1156 m	545w	1497s, 1440s, 1387m, 727m
$CoL^3(N_3)$phen (**30**)	1563m	1595s	2024s	443w, 410w	1342m, 751m	1145 m	542w	1469s, 1436s, 1356m, 761m, 849w, 642m
H_2L^4	1601s	-			1375s, 791m	1222 s	--	-
$CoL^4(N_3)$bip (**31**)	1563m	1596s	2025s	411w, 441w	1340m, 771m	1123	567w	1463s, 1409s, 1351m, 856m, 705m
$CoL^4(N_3)$phen (**32**)	1562m	1594s	2022s	442m, 412w	1344s, 756m	1125 s	552w	1494m, 1432m, 846m, 727m, 700w

[a] peak 3338sh, due to 4NH vibration.

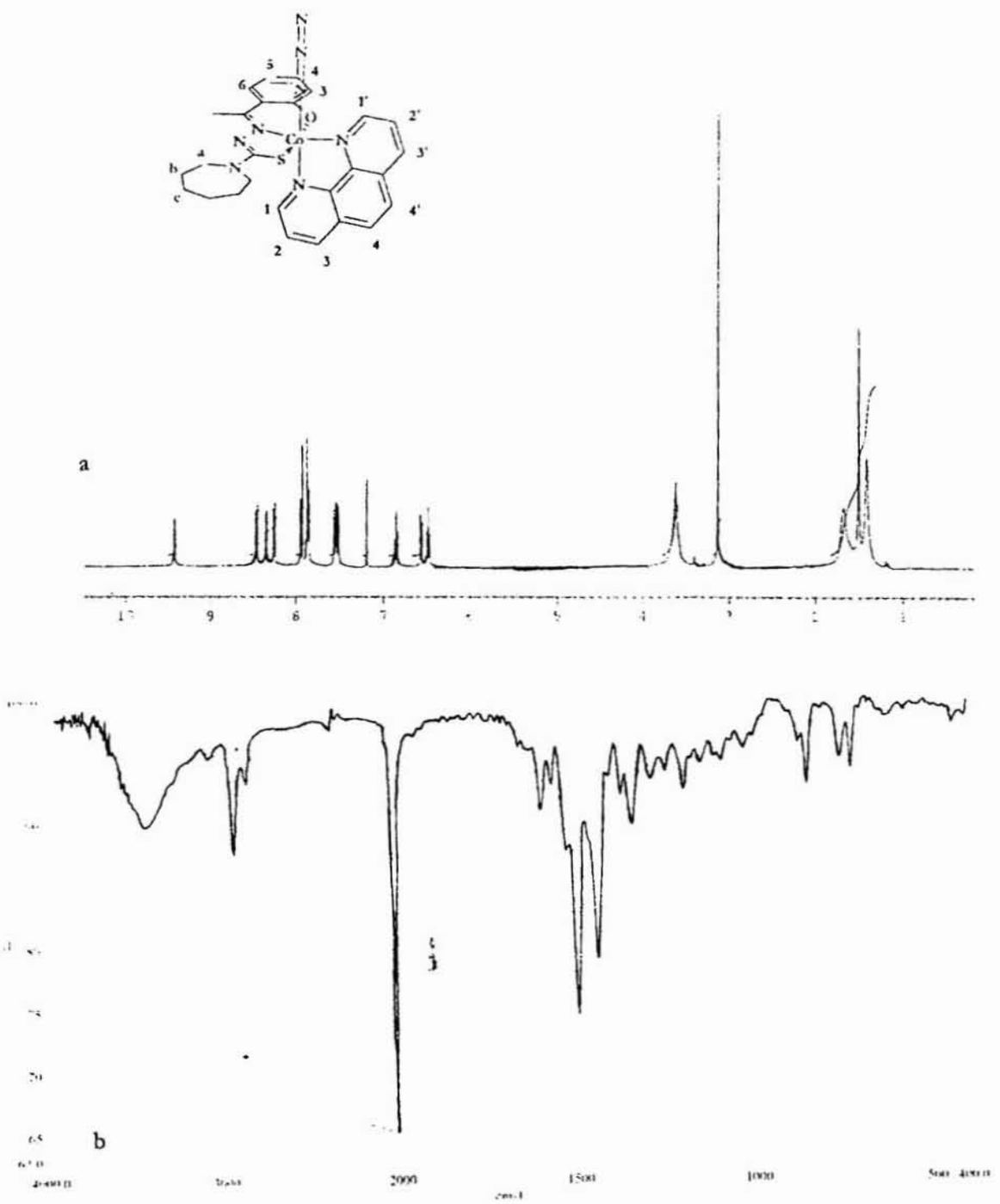

Figure 5. 3:a) ^{1}H NMR spectrum of the compound **28,** b) IR spectrum of compound **28**

REFERENCES

1. M. Kobayashi, S. Shimizu, *Eur. J. Biochem.*, 1999, **261**, 1; M. Kobayashi, S. Shimizu, *Nature Biotechnol.*, 1998, **16**, 733; T. Nagasawa, H. Yamada, *Trends Biotechnol.*, 1989, **7**. 153.
2. W. Huang, J. Jia, J. Cummings, M. Nelson, G. Shneider, Y. Lindqvist, *Structure*, 1997, 5, 691.
3. S. Nagashima, M. Nakasako, N. Dohmae, M. Tsujimura, K. Takio, M. Odaka, M. Yohda, N. Kamiya, I. Endo, *Nature Struct. Biol.* 1998, 5, 347.
4. M. B. Ferrari, G. G. Fava, C. Pelizzi, P. Tarasconi, *J. Chem. Soc. Dalton Trans.* 1992, 2153; M. B. Ferrari, G. G. Fava, C. Pelosi, M. C. Rodriguez-ArgÉelles, P. Tarasconi, *J. Chem. Soc. Dalton Trans.* 1995, 3035; M. B. Ferrari, G. G. Fava, C. Pelizzi, P. Tarasconi, *J. Chem. Soc. Dalton Trans.* 1991, 1951.
5. M. B. Ferrari, G. G. Fava, C. Pelosi, M. C. Rodriguez-ArgÉelles and P. Tarasconi, *Polyhedron*, 2000, 19, 1895.
6. M. B. Ferrari, G. G. Fava, M. Lanfranchi, C. Pelizzi and A. Tarasconi, *J. Chem. Soc. Dalton Trans.*, 1991, 1951.
7. M. B. Ferrari, G. G. Fava, E. Leporati, C. Pelizzi, A. Tarasconi and G. Tosi, *J. Chem. Soc. Dalton Trans.*, 1987, 227.
8. D. X. West, P. M. Ahrweiler, G. Ertem, J. P. Scovill, D. L. Klayman, J. S. Flippen –Anderson, R. Gilardi, C. George, L. K. Pannel, *Trans. Met. Chem.*, 1985, 10, 264.
9. D. X. West, J. K. Swearingen, J. Vades-Martinez, S. Hernandez-Ortega, A. K. El-Sawaf, F. van Meurs, A. Castineiras, I. Garcia and E. Bermejo, *Polyhedron*, 1999, 18, 2919.
10. A. L. Balch, L. A. Fosset, R. R. Guimerans, M. M. Olmstead, P. E. Reedy and F. E. Wood. *Inorg. Chem.* 1986, 25, 1248.
11. K. Nakamoto, *Infrared and Raman Spectra of Inorganic and Coordination Compounds*, 3rd edn, John Wiley and Sons, NY, 1978, p 124.

CHAPTER 6

SYNTHESIS AND SPECTRAL STUDIES OF SOME DIOXOURANIUM(VI) COMPLEXES.

6.1 INTRODUCTION

There has been considerable interest on theoretical and experimental chemistry of metal oxocations. Dioxouranium(VI) or UO_2^{2+} is one of the stable oxocations [1] and the complexes of UO_2^{2+} have been studied extensively [2,3], because of the theoretical interest in the linear O=U=O group, different structures, detection of uranium compounds in sea water and its importance in relation to energy problems. Though much work was reported on d-block element sulfur systems, little attention has been paid to that of *f*-block element sulfur systems [4]. In most cases the sulfur donor centers are in thioether environment in a potentially chelating molecule containing nitrogen and oxygen donor centers at the suitable positions [5]. Hydroxy containing molecules possessing N and O donor groups, where N is present as an imine are of interest in developing coordination chemistry in general and biomimetic chemistry in particular for a number of metal ions including that of vanadium [6]. In view of the emerging interest in extraction of uranium from different sources and importance of the coordination chemistry of UO_2^{2+}, we have tried to explore the structural aspect of the dioxouranium complexes of the thiosemicarbazones.

6.2 EXPERIMENTAL

6.2.1. Materials

The ligands used for the preparation of the complexes were synthesized as described in Chapter 2a. Uranyl acetate-dihydrate (Fluka), bipyridine and phenanthroline were used as received.

6.2.2. Preparation of the complexes

The complex **33** was prepared as follows: The thiosemicarbazone ligand 0.5 mmol was dissolved in 15 mL of ethanol. To this solution was added a 0.5 mmol of the uranyl acetatedihydrate in ethanol. The mixture was stirred for about 2 hours. An orange solid appeared in a few minutes. The solid formed was filtered, washed with ethanol, water and then with ether and dried *in vacuo* over P_4O_{10}.

Other complexes (**34-37**) were prepared as follows: To a hot ethanolic solution (10mL) of uranyl acetate (0.5 mmol), thiosemicarbazone ligand (0.5mmol) in 15 mL of ethanol along with a stochiometric ratio of the heterocyclic base was added. A deep colored solution resulted from which an amorphous solid precipitated. The compound is filtered washed with hot ethanol, water and ether. The compound was then dried over P_4O_{10}, *in vacuo*.

Compound 33: $[C_{30}H_{38}N_6O_6S_2U_2]$ F.W. 1118.55: Anal. Elemental Found C 32.32, H 3.50, N 7.81; Calcd. C 32.20, H 3.42, N 7.51; IR (KBr) 3294br, 1597s, 1564s, 1433m, 1358m, 1309m, 1272m, 1204m, 1159m, 1096m, 1023w, 900s, 864m, 786m, 770m, 695w, 640w, 592w, 476w cm^{-1}; 1H-NMR 7.54(s, 2H, H^6-Ph), 7.25(t, 2H, H^4-Ph), 6.93(d, 2H, H^3-Ph), 6.57(t, 2H, H^5-Ph), 3.89(s, 8H, Ha), 2.60(s, 3H, NCH_3), 2.50(s, 3H, methyl), 1.80(s, 8H), 1.49(s, 8H)

Compound 34: $[C_{27}H_{27}N_5O_3SU]$ F. W. 739.63: Anal. Elemental Found C 44.18, H 3.81, N 9.31; Calcd C 43.85, H 3.68, N 9.47; IR (KBr) 1592m, 1571m, 1485s, 1433s, 1369m, 1296m, 1143m, 905s, 845m, 791m, 755m, 725m, 640w, 594w, 419w cm^{-1}; ^{1}H-NMR δ 11.30(bs, 1H, 1-bipy), 10.94(bs, 1H, 1'-bipy), 8.70(bs, 2H, 2&2'-bipy), 8.32(bs, 1H, 3-phen), 8.20(bs, 1H, 3'-phen), 8.12(s, 2H, 4&4'-Phen), 7.74(d, 1H, H^6-Ph), 7.39(t, 1H, H^4-Ph), 7.25(d, 1H, H^3-Ph), 6.73(t, 1H, H^5-Ph), 4.09(bs, 4H, Ha), 2.86(s, 3H, methyl), 1.93(s, 4H, Hb), 1.57(s, 4H, Hc)

Compound 35: $[C_{23}H_{23}N_4O_4SU]$ F. W. 703.56: Anal Elemental Found C 39.04, H 3.26, N 9.88; Calcd C 39.27, H 3.29, N 9.95; IR (KBr) 1596m, 1566m, 1482s, 1436s, 1356m, 1316m, 1247m, 1220s, 1159m, 1153m, 1030m, 909s, 824w, 765m, 646w, 597w, 537w, cm^{-1}; ^{1}H-NMR δ 11.0 (bs, 1H, 1-bipy), 10.5(bs, 1H, 1'-bipy), 7.98(bs, 2H, 3&3'-bipy), 7.75(d, 1H, H^6-Ph), 7.41(t, 1H, H^4-Ph), 7.09(d, 1H, H^3-Ph), 6.77(t, 1H, H^5-Ph) 6.49(d, 2H, 4&4'-bipy), 6.27(t, 2H, 2&2'-bipy), 4.11(t, 4H, Ha), 3.81(t, 4H, Hb), 2.81(s, 3H, methyl)

Compound 36: $[C_{23}H_{24}N_5O_4SU]$ F. W. 727.57 Anal Elemental Found C 41.47, H 3.29, N 9.73; Calcd C 41.27, H 3.19, N 9.63; IR (KBr) 1593m, 1572m, 1483s, 1435s, 1358m, 1298m, 1211s, 1114m, 1029m, 907s, 847m, 757m, 725m, 640w, 597w, 538w, 449w; ; ^{1}H-NMR δ 11.28(bs, 1H, 1-phen), 10.87(bs, 1H, 1'-phen), 9.72(bs, 2H, 2&2'-phen), 8.31(bs, 1H, 3-phen), 8.19(bs, 1H, 3'-phen) , 8.10(s, 2H, 4&4'-phen), 7.79(d, 1H, H^6-Ph) , 7.46(t, 1H, H^4-Ph), 7.18(d, 1H, H^3-Ph), 6.76(t, 1H, H^5-Ph), 4.18(s, 4H, Ha) 3.87(s, 4H, Hb), 2.88(s, 3H, methyl),

Compound 37: $[C_{23}H_{23}N_4O_4SU]$ F. W. 747.61 Anal Elemental Found C 44.75, H 3.20, N 9.25; Calcd C 44.98, H 3.10, H 9.37; IR (KBr) 1591m, 1541m, 1485s, 1429m, 1345m, 1294m, 1249m, 1119m, 900s, 846m, 770m, 725m, 703m, 639m, 596w, 556w, 464w, 422w cm^{-1}; ^{1}H-NMR δ 11.27(bs, 1H, 1-phen), 10.67(bs, 1H, 1'-phen), 8.69(bs, 2H, 2&2'-phen), 8.32(bs, 1H, 3-bipy), 8.13(bs, 3H, 3'-phen, 4&4:-phen), 7.80(d, 1H, H^6-Ph), 7.55(d, 2H, Ha-Ar), 7.42(t, 3H, Hb-Ar & H^4-Ph), 7.29(m, 1H, Hc-Ar), 7.22(d, 1H, H^3-Ph), 6.75(t, 1H, H^5-Ph), 3.77(s, 3H, NCH_3), 2.86(s, 3H, methyl)

6.2.3. Physical measurements.

The various experimental techniques used for the characterization of the compounds are described in previous chapters.

6.3. RESULTS AND DISCUSSION

6.3.1 Preparation of the complexes

The elemental data of the complexes **34-37** (Table 6.1) indicate that they are having the stochiometry $[UO_2LB]$, where B is phenanthroline in compound **35**, **36** and **37**, bipyridine in compound **34**. The principal ligand in compound **33** and **35** is H_2L^2; **34** and **36** contain ligand H_2L^3; **37** contains H_2L^4. All the compounds were diamagnetic consistent with a $5f^0$ system. The compound **33** dissolves only in DMSO, upon dissolution the color gets faded. This is suggested to have a stoichiometry $[UO_2L]_2$, however further investigations were hampered by the lack of consistency in the synthesis of the complex and scanty amount of the samples prepared. Complexes **34-37** are soluble in DMF, DMSO, $CHCl_3$ and CH_2Cl_2. They are stable in CH_2Cl_2 but not in DMSO and DMF. Hence, CH_2Cl_2 was chosen as the solvent for electronic spectral measurement.

6.3.2. IR spectra

The details of the IR spectra are listed in Table 6.2. The IR spectra of all compounds show strong absorption peaks at 1595 and 1565 cm^{-1}, which is an evidence for the formation of thiol and coordination *via* the azomethine nitrogen. The lowering of the stretching frequency of the C=N bond by 30 to 40 cm^{-1} is an evidence for a strong coordination of the azomethine nitrogen to uranium. The presence of a band at 864 cm^{-1} is an evidence for the presence of tetrameric M$\overset{O}{\underset{O}{}}$M bridging [7]. The large numbers of peaks in the range 1500 to 750cm^{-1} are suggestive of the heterocyclic ring vibrations and are an evidence for the presence of the heterocyclic base in the compound. The coordination of the base and the azomethine nitrogen to the metal center is indicated by the presence of weak bands in the 400-470 cm^{-1} region. The bands appearing in the 520 to 570 cm^{-1} regions is an evidence for the formation of the U-$O_{(phenolic)}$ bond. The lowering in the C-S stretching/bending frequency of the compounds *ca.* 20 to 30 cm^{-1}, indicates the coordination of thiolate sulfur to uranium. The complexes exhibit a strong band in the 900 to 920 cm^{-1}region corresponding to ν_s(O=U=O) and ν_{as}(O=U=O) characteristic of uranyl complexes [8].

6.3.3 Electronic spectra

The two bands and the related shoulders in the range 230-260 nm and 330-350 nm in the electronic spectra (Table 6.3) may be due to intra –ligand charge transfer bands [9]. The complexes show transitions in the 360 –410 nm range, seen as a shoulder, may be due to apical oxygen to $\rightarrow f^{*}$ (U) ($^{1}Eg^{+} \rightarrow {}^{3}\pi_{\omega}$) transition typical of O=U=O moiety [10]. The uranyl ion possess two highest occupied orbitals π_v and σ_v and lowest unoccupied orbitals Φ_v andσ^{*}_v. A series of excited state configurations are generated from the ground state configurations [$(\pi_v)^4$, $(\sigma_v)^2$] [11]. The other shoulder in the visible region 480-530 nm can be due to the charge transfer from the reduced sulfur center to 5*f* and or 6*d* orbital of the uranium atom S$\pi \rightarrow$5*f* (6*d*) and S$\sigma \rightarrow$5*f*(6*d*) [5]. The electronic spectra of compounds **35** and **36** are shown in Figure 6.1.

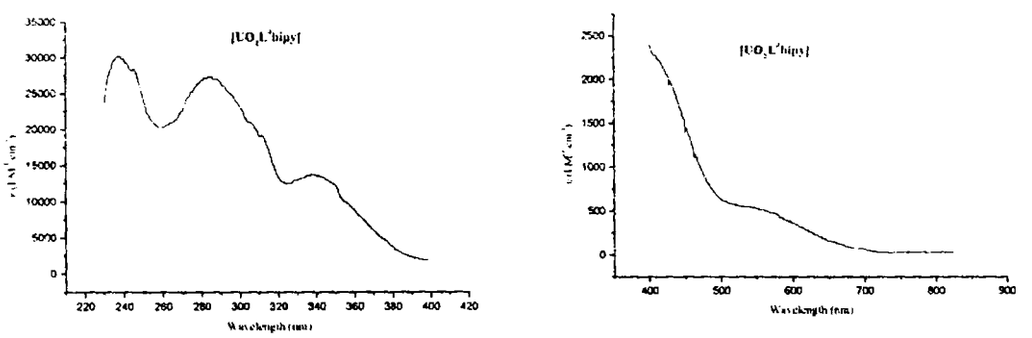

Figure 6.1a.: Electronic spectrum of Compound **35**

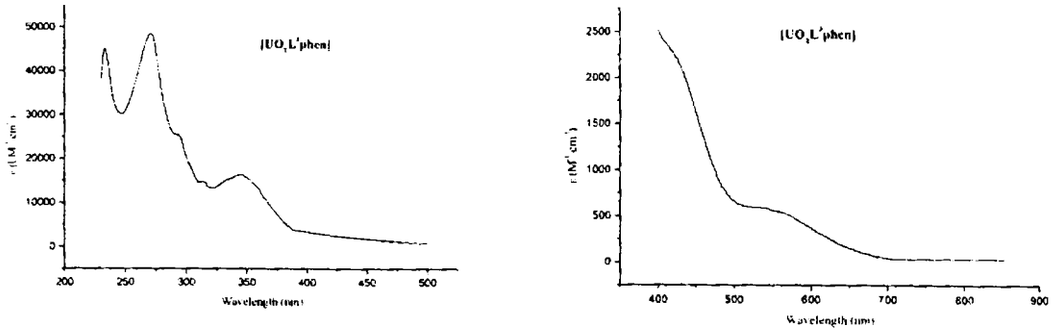

Figure 6.1b.: Electronic spectrum of compound **36**

6.3.4 ^{1}H-NMR spectra

The ^{1}H-NMR spectrum of the compound **33** confirms its dimeric structure. The equivalence of the proton signals of either thiosemicarbazone moiety indicates an approximate equatorial arrangement of the thiosemicarbazone. The two O=U=O bonds are perpendicular to the plane formed by the thiosemicarbazone ligands. However, the signals corresponding to the methyl group attached to the C=N bond are at different chemical shift positions indicating a distortion of the rings from planarity at some locations. Thus the compound can be assumed to have a dimeric structure in which the phenolic oxygen is acting as the bridging group (Figure 6.2).

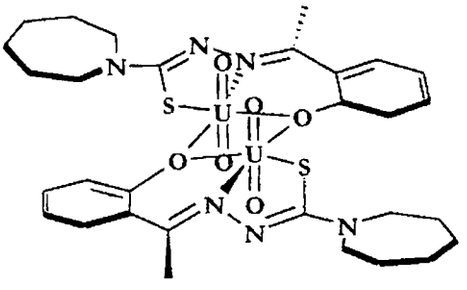

Figure 6.2.: The approximate structure of compound **33**

The ^{1}H-NMR of compounds **34–37** show some fluxional character. The room temperature ^{1}H-NMR spectrum of the compound **34** shows broad signals corresponding to the 1,1', 2,2' and 3, 3' phenanthroline protons. At –20°C the broadened signals assumes fine structure (Figure 6.3). Simultaneously, the signal corresponding to the "**a**" position of the azepine group, i.e., the proton adjacent to the nitrogen of the azepine splits into two, presumably because of the spatial distortion of the azepine moiety, pushing the two adjacent carbon atoms and the hydrogens attached to two different position in space. At lower temperature the averaging of the chemical shift positions is not attained.The approximate structure of compound **34** (proton labeled) is given in Figure 6.4. A similar observation is seen in the case of compound **36**, with respect to the fluxionality of the coordinated heterocyclic base. In this compound the signal corresponding to the hydrogen α to the nitrogen in the morpholine substituents labeled as "**a**", broadens at lower temperature, viz., -20°C. The broadening of the signals increases further at still lower temperature, i.e., -40°C (Figure 6.5).

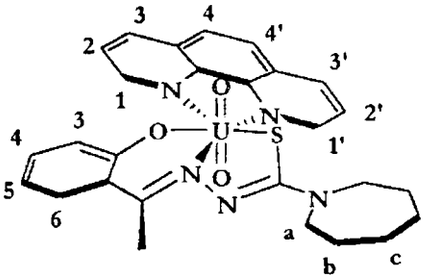

Figure 6.4.: Approximate structure of compound **34**

This can be explained due to effective quadruple interactions from adjacent nitrogen atoms at lower temperature resulting from reduced freedom of movement of the protons about the bonds. On exchanging with D_2O the signals corresponding to 1,1' and 3,3' of the heterocyclic base broadens further lowering the intensity. This can be attributed for a slow exchange of proton with deuterium (Figure 6.6). This phenomenon can be explained only if some acidic nature is assumed for the protons at the 1 and 3 positions of the heterocyclic base. The acidity can be regarded as a result of the coordination of the base to the highly positively charged UO_2^{2+} oxocation, the electron withdrawal from the ring is 'felt' more at 1 and 3 positions. The in homogeneity of the proton chemical shift positions can be explained by suggesting a distorted arrangement of the heterocyclic base with respect to the O=U=O bonds and the thiosemicarbazone skeletal frame work. The proposed structure is shown in Figure 6.7.

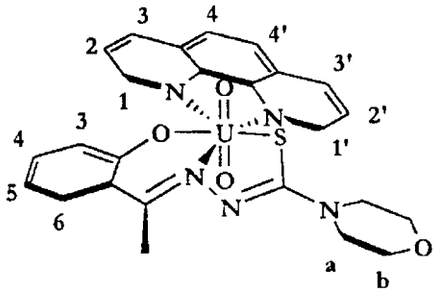

Figure 6.7.: Approximate structure of compound **36**

Table 6.1: Elemental analysis data of dioxouranium complexes

Compound	color	Found (Calcd)%		
		C	H	N
$[UO_2L^2]_2$	Orange	32.32 32.20	3.50 3.42	7.51 7.81
UO_2L^2phen	Olive green	44.18 43.85	3.81 3.68	9.31 9.47
UO_2L^3bipy	Olive green	39.04 39.27	3.26 3.29	9.88 9.95
UO_2L^3phen	Coffee brown	41.47 41.27	3.29 3.19	9.73 9.63
UO_2L^4phen	Coffee brown	44.75 44.98	3.20 3.10	9.25 9.37

Table 6.2: IR spectral assignments for dioxouranium(VI) complexes

Compound	ν (^{7}C=N^1)	ν (^{2}N=C^9)	ν (O=U=O)	ν (U-N)	ν/ δ (C=S)	ν (C-O)	ν (U-O)	Bands due to heterocyclic base
H_2L^2	1603s	-		-	1383s, 839m	1252 s	--	-
$[UO_2L]_2$ (**33**)	1565m	1597m	900s	439w, 404 w	1358m, 770m	1204 m	593m	
UO_2L^2phen (**34**)	1570m	1592 m	905s	419w	1368m, 755m	1194 m	580w	1433m, 1143,791w
H_2L^3	1605s			-	1374s, 835m	1219 s	--	-
UO_2L^3bipy (**35**)	1566m	1596m	910s	413w	1357m, 824m	1160m	537w	1436s, 1220s, 1030m, 646m
UO_2L^3phen (**36**)	1571m	1593m	907s	404w	1358m, 792m	1114	538w	1435s, 1211m, 640w
H_2L^4	1601s	-		-	1375s, 791m	1222 s	--	-
UO_2L^4phen (**37**)	1541m	1591m	900s	422w, 464w	1340m, 771m	1119s	556w	1429m, 1030,639w

Table 6. 3. UV-Visible spectral assignments for Dioxouranium complexes (**34-37**)

Compound	d-d	LMCT	n→π*	π→π*
UO_2L^2phen (**34**)	18903 (2.76)	24155 (3.37)	28985 (4.20), 34246 sh (4.39)	36764 (4.67), 42918 (4.66)
UO_2L^3bipy (**35**)	19305 (2.76)	24330 (3.36)	29586 (4.13),	42248 (4.47), 35335 (4.43)
UO_2L^3phen (**36**)	19300 (2.77)	24450 (3.38)	28985 (4.21), 34130 sh (4.40)	36900 (4.69), 43103 (4.65)
UO_2L^4phen (**37**)	18832 (2.76)	23923 (3.37)	29498 (4.20), 34246 sh (4.43)	37765 (4.66), 42500 (4.65)

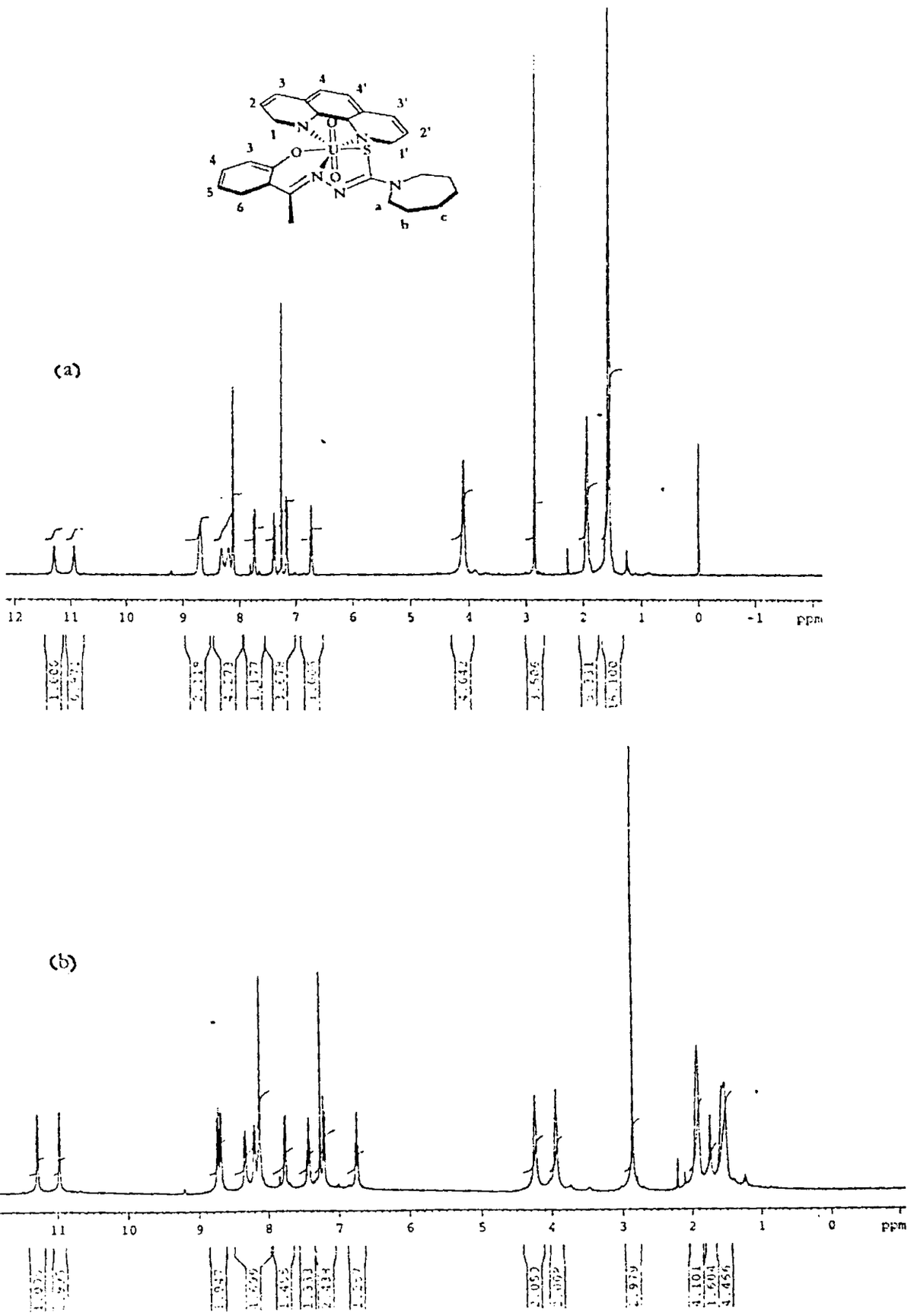

Figure 6.3: ^{1}H NMR spectra of the compound **34** at different temperatures; a) T = 298K, b) T = 253K

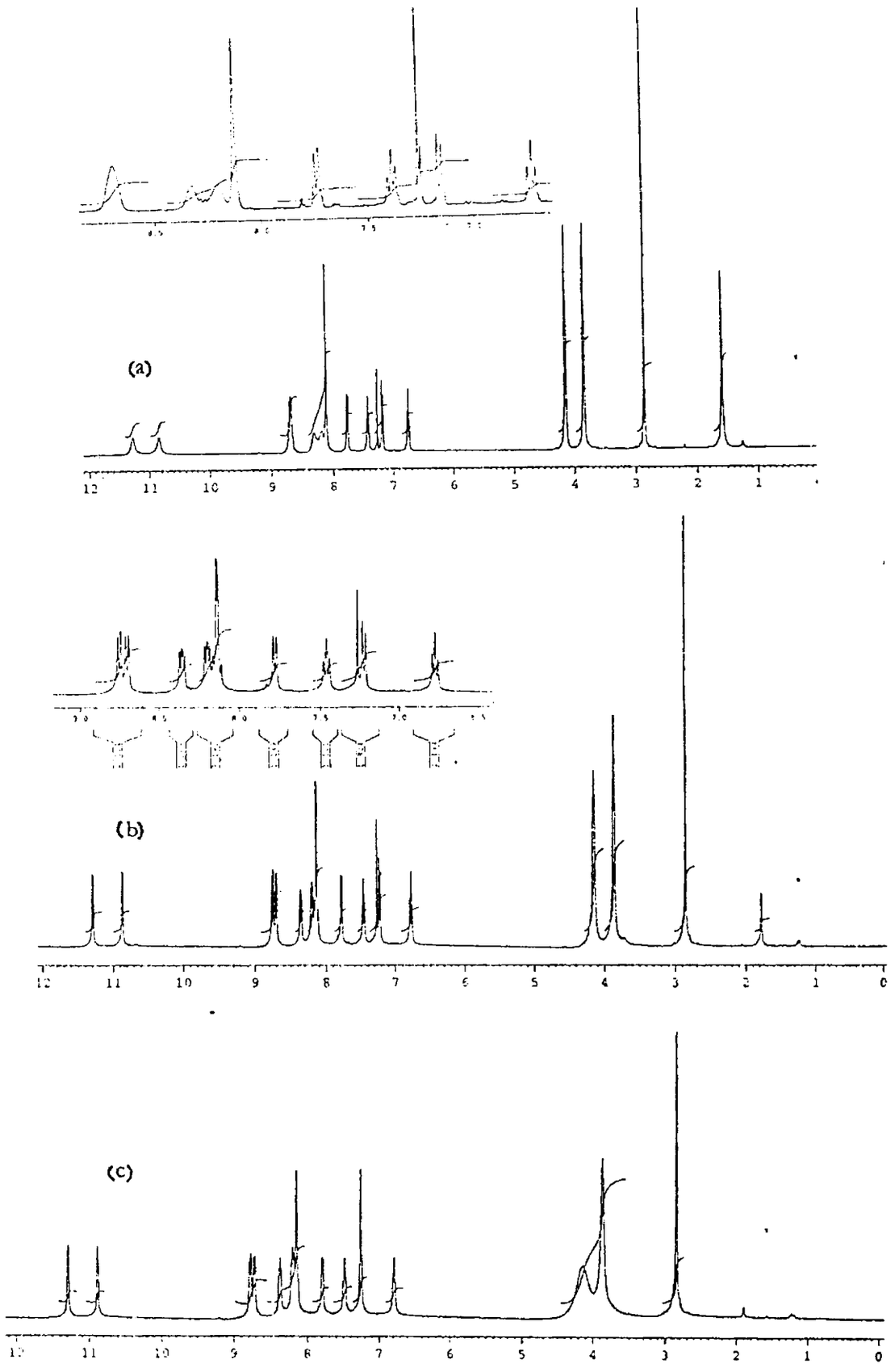

Figure 6.5: ^{1}H NMR spectra of the compound **36** at different temperatures; a) T = 298 K, b) T = 253 K, c) T = 233 K

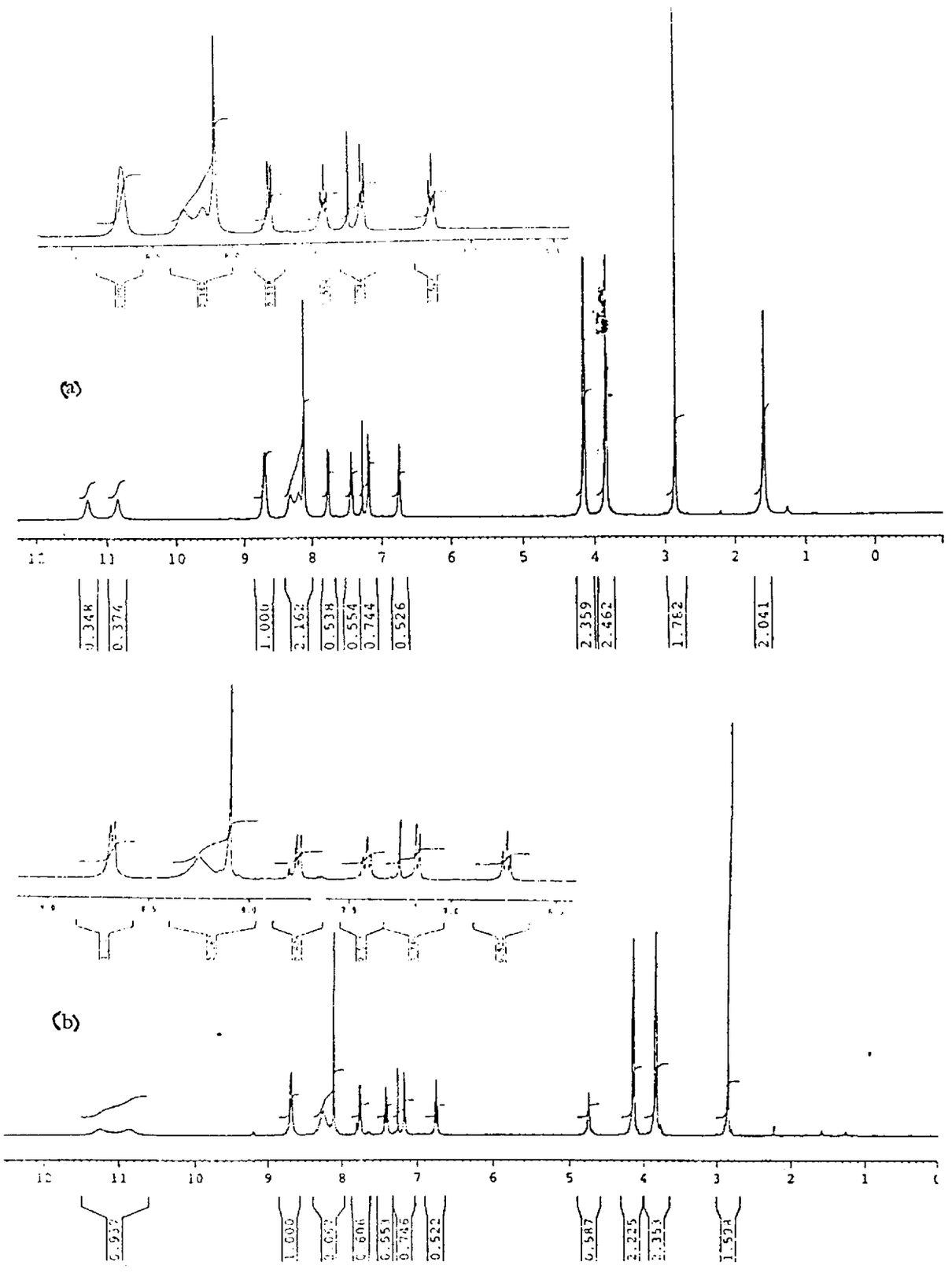

Figure 6.6: ^{1}HNMR spectra of the compound **36** a) with D_2O exchange; b) without D_2O exchange

REFERENCES

1. N. N. Greenwood, A. Ernshaw, *Chemistry of elements*, (Pergamon Press, Oxford), 1986, p 1467.
2. I. Tabushi, Y. Kobuke, K. Ando, M. Kishimoto and E. Oharo, *J. Am. Chem. Soc.*, 1980(102), 5947.
3. S. Shikai, H. Koreshi, K. Ueda and O. Manabe, *J. Chem. Soc., Chem. Commun*, 1986, 233; S. Shikai, T. Subak, T. Sone and O. Manabe, *Tetrahedron Lett.*, 1985, **26**, 3343.
4. U. Casellato, D. Fergona, S. Sitran, S. Tamburini, P. A. Vigato and D. E. Fenton, *Inorg. Chim. Acta*, 1985, **110**, 181.
5. P. Chattopadhyay and C. Sinha, *Ind. J. Chem.* 1995, **34A**, 76;
6. C. R. Cornman, G. J. Colpas, J. D. Hoeschele, J. Kampf and V. L. Pecoraro, J. Am. Chem. Soc., 1992, **114**, 9925; C. J. Carrano, C. M. Nunn, R. Quan, J. A. Bondais and V. L. Pecoraro, *Inorg. Chem.*, 1990, **29**, 944.
7. A. Pasini, M. Gullotti and E, Cesarotti, *J. Inorg. Nucl. Chem.*, 1972, **34**, 3821; A.E. Commyns, B. M. Gatehouse and E. Wait, J. Chem. Soc., 1958, 4655; S. P. McGlynn, J. K. Smith and W. C. Neely, *J. Chem. Phys.*, 1955, **23**, 2105.
8. R. M. Silverstein, G. C. Bassler and T. C. Morril, Spectrometric identification of organic compounds, (John Wiley, NY) 1981.
9. S.P. McGlynn, J. K. Smith, *J. Molec. Spectrosc.*, 1961, **6**, 164.
10. J. Vicente, M. T. Chicote, P. G. Herrero and P. G. Jones, *J. Chem Soc., Dalton Trans.*, 1994, 3183.
11. Denning, R. G, Snellgrove, T. R and Woodwork D. R, *Mol. Phys*, 1979, **30**, 1109; Groller-walrand C and Colen W, *Inorg. Chim. Acta*, 1984, **84**, 183.

CHAPTER 7

SPECTRAL, MAGNETIC AND CYCLIC VOLTAMMETRIC STUDIES OF MANGANESE(IV) COMPLEXES

7.1 INTRODUCTION

The relevance of manganese lies in its role in biological systems as an essential element. Manganese(II) in biological systems act as an effective enzyme activator and are important active sites in metalloproteins. In these metalloproteins manganese can exist in any of the five oxidation states or in mixed valence states. The significance of manganese in biological systems is also evident from their role as good water oxidation catalysts in photosynthesis. The oxygen-evolving complex (OEC) of photosystem-II is a tetrameric manganese cluster with di(μ-oxo)dimanganese as its key structural feature [1]. This mixture of tetrameric manganese(IV) complexes has led to a spurt in research in this field, and as a consequence different OEC model complexes were synthesized and their properties investigated [2]. In the course of such investigations, complexes of manganese in different oxidation states and also of mixed valence complexes were obtained [3]. Their spectral and magnetic properties had been of interest for inorganic chemists. The chapter deals with synthesis, spectral characterization and cyclic voltammetric studies of manganese(IV) complexes of three ligands H_2L^2, H_2L^3 and H_2L^4.

7.2 EXPERIMENTAL

7.2.1. Materials and Methods

The thiosemicarbazones H_2L^2, H_2L^3 and H_2L^4 were prepared as described in chapter 2a. Manganese(II) acetate tetrahydrate (Reagent grade, E. Merck) was purified by standard methods. The solvents were purified by standard procedures before use.

7.2.2. Physical Measurements

The details of elemental, IR, and UV-Visible spectral techniques are described in Chapter 2b. The content of manganese was estimated by Atomic Absorption Spectroscopy in a Perkin-Elmer Analyst 700 spectrometer, after decomposing the compounds by standard methods. The details of magnetic measurements, EPR spectra, cyclic voltammetry and conductance measurements are also described in Chapter 2b.

7.2.3. Preparation of the complexes

The general method of synthesis of the manganese complexes (**38-40**) is as described below:

To a hot ethanolic solution (25 mL) of the thiosemicarbazone (1.0 mmol) was added 10 mL of ethanolic solution of manganese(II) acetate tetrahydrate (0.5 mmol) with stirring. The solution after refluxing for about 2 hrs, was allowed to cool, when microcrystals of the manganese(IV) complex crystallized out. The complex was filtered off, washed with hot ethanol, water and ether respectively and dried *in vacuo*. The details of elemental analysis, physical characteristics and the magnetic properties are listed in Table 7.1.

Compound **38:** $[C_{30}H_{38}MnN_6O_2S_2]$ F.W. 633.73: Analytical data; elemental. Found: C 57.26, H 6.09, N 13.42, Mn 8.82; Calcd C 56.77, H 6.19, N 13.24, Mn 8.66; IR (cm^{-1}) 1591, 1558, 1522, 1489, 1367, 1292, 1263, 1192,1132, 1086, 864, 808, 758, 617, 441; Electronic (nm) (CH_2Cl_2) 236.5, 298.3, 362.5, 450sh, 509sh, 622sh, 752sh; EPR g_{iso} (solid) 2.69.

Compound **39:** $[C_{26}H_{30}MnN_6O_4S_2.H_2O]$ F.W. 627.63: Analytical data; FAB M^+(m/z) 610 [627.63 -18.01]; elemental. Found: C 50.05, H 5.22, N 12.94, Mn 8.83; Calcd C 49.76, H 5.14, N 13.39, Mn 8.75; IR (cm^{-1}) 1591, 1566, 1526, 1487, 1356, 1300, 1267, 1228, 1113, 1086, 1030, 887, 754, 613, 545, 457, 439; Electronic (nm) (in CH_2Cl_2) 240, 305, 318, 364, 443sh, 510sh, 613sh, 780sh; EPR g_{iso} (solid) 2.66, g_{iso} (in DMF at 77 K) 1.998, A_{iso} 68 G (63.44 x 10^{-4} cm^{-1}).

Compound **40:** $[C_{32}H_{30}MnN_6O_2S_2]$ F.W. 649.69: analytical data. Elemental; Found: C 59.32, H 4.74, N 13.05, Mn 8.47; Calcd C 59.16, H 4.65, N 12.94, Mn 8.46; IR (cm^{-1}) 1591, 1558, 1522, 1479, 1361, 1307, 1273, 1240, 1124, 1024, 862, 756, 694, 565, 547, 456, 443; Electronic (nm) (in CH_2Cl_2) 237, 305, 364, 440sh, 513sh, 605sh, 760sh; EPR g_{iso} (solid) 2.698, g_{iso} (in DMF at 77 K) 2.0021, A_{iso} 94.8 G (88.6 x 10^{-4} cm^{-1}).

7.3. RESULTS AND DISCUSSION

7.3.1. Preparation of the compounds

The mixing of the ligand and the metal salt results in an immediate deepening of the color of the solution into dark brown or even black. The complexes could also be precipitated on stirring the two solutions for about an hour. When stirring was adopted the precipitation started immediately. Though we have attempted the preparation of the manganese(II) complex of all the four ligands we have observed the serendipitous formation of manganese(IV) complex in all the cases except for H_2L^1, in which case the decomposition of the ligand occurred upon refluxing for about an hour. The physical characteristics and elemental analysis details are reported in Table 7.1. The elemental analysis and the FAB mass spectra of all the prepared complexes are in agreement with the stochiometry $M^{IV}L_2$. However, for the compound **39** the elemental data are in conformity with a molecule of water of crystallization. The magnetic susceptibility values are in agreement with the spin only value for d^3 electronic configuration for manganese viz, 3.9-4.2 BM. The molar conductance values are similar to that of non-electrolytes. Our attempts to isolate compound from DMF was not successful since compound was not stable in DMF solution. However slow diffusion technique using chloroform and ethanol were found to give results.

7.3.2. Electronic spectra

The details of the electronic spectra recorded in dichloromethane are given in Table 7.2. The compound is stable in dichloromethane and chloroform. The unusually intense peaks in the visible region (logε ≈3) (Figure 7.3) is attributed to the "intensity stealing" influence of the sulfur containing ligands, where by the ligands steal the intensity of the CT bands into transitions in the visible region. The high intensity peak at *ca.* 28000 cm^{-1} is due to the LWM charge transfer bands. The shoulders of unexpected intensity in the 22000, 19000, 16000 cm^{-1} are attributed to the phenolate → Mn(IV) charge-transfer band (LMCT) and a thiolate→ Mn(IV) charge transfer[4a,b]. The

shoulders seen *ca.* 22000, 19000, 16000 and 13000 cm^{-1} are respectively due to the $^4B_{1g}W^4A_{2g}(F)$, $^4B_{1g}W^4E_g(F)$, $^4B_{1g}W^4B_{2g}$ and $^4B_{1g}W^4E_g$ transitions characteristic of a tetragonally distorted octahedral d^3 ion. The peaks due to the $^4B_{1g}W^4A_{2g}(P)$ and $^4B_{1g}W^4E_g(P)$ are involved in the tail of the charge transfer band *ca.* 28000 cm^{-1}. The solution in DMF also gives a similar spectrum. However, the bands in the visible region are found to shift to lower frequencies and lowers in intensity when a solution in DMF is allowed to stand for a day. This is assumed to be due to the coordination of DMF with manganese metal center.

7.3.3. IR spectra

The infrared spectral details are given in Table 7.3. The stretching vibration in the region 1591 cm^{-1} in all complexes indicates the formation of a new $^2N=^9C$ bond due to the enolisation of the ligand before complexation. The absence of bands in the higher frequency region is another evidence to the formation of thiol during complexation. The enol formation is further supported by the increase in the $\nu_{(N\text{-}N)}$ stretching frequency by *ca.* 20cm^{-1}. The shifting of the band at 1605 cm^{-1} region in the ligand to 1558 cm^{-1} is due to the weakening of the $^8C=^1N$ bond resulting from coordination of the azomethine nitrogen with the metal ion. The lowering in the phenolic C-O absorption by *ca.* 100 cm^{-1} is due to the binding of the phenolic oxygen to the metal. The six coordinate, octahedral, complex is assumed to have a distorted structure with the azomethine nitrogens occupying the apical positions and the phenolic oxygen and thiolate sulfur atoms occupying four corners of the distorted square. The coordination of the C-S bond is indicated by the lowering in the $\nu_{(C=S)}$ stretching frequency, found in the ligand *ca.* 1380 cm^{-1} to *ca.* 1300 cm^{-1}. This is also indicated by the lowering in the $\delta_{(C=S)}$ by *ca.* 30 cm^{-1}. The structure of the complex can be shown tentatively as in Figure 7.4.a and b. and as in Figure 7.5.

7.3.4. EPR spectra

The EPR spectra for manganese(IV) may be described by the spin Hamiltonian (1) [5]

$$? = g\beta H \cdot q + D[q_z^2 - 5/4] + E(q_x^2 - q_y^2) + q \cdot A \cdot I \qquad (1)$$

If the zero-field splitting constants, D and E are very small compared to $g\beta Hq$, three EPR transitions are to be obtained (corresponding to d^3 system) with g value just below 2.0. However if D is very large, then only the transition between +1/2 Y -1/2 will be observed.

The room temperature spectra (Figure 7.1) in the polycrystalline state are very broad due to dipolar interactions and enhanced spin lattice relaxation [6]. But the g_{av} values are higher than the expected values. The higher g values can be attributed to the promotion of the electrons in the inner filled ligand levels to the half-filled levels containing the unpaired electrons [7]. In other words, there is a mixing in of excited states due to spin-orbit coupling that produces a positive contribution to g.

However, none of the manganese complexes in DMF solution at room temperature produce any spectra. This is not an abnormal observation as only a few do give the solution spectra at room temperature. This is attributed to the zero-field effect

and is controlled by the zero-field splitting parameters D and E [8]. In distorted manganese(IV) complexes, i.e., the one lacking cubic symmetry, the zero-field splitting may be quite significant. Its magnitude depends on the relative orientation of the molecular axis and the magnetic field direction, molecular tumbling will modulate this interaction and the line broadening will be so large as to cause the EPR signal often go undetected [9].

The frozen DMF solution spectrum (77 K) of the compound **38** was found to be EPR silent, which can be due to the broadening resulting from large spin-orbit coupling [10]. The DMF solution of the compound **39** (Figure 7.2) at 77 K gives six line EPR signal of 340 G wide with a hyperfine coupling constant of A_0 = 68 G. The g value of 1.998 is consistent with the typical manganese ion in the higher oxidation states reported [11]. This hyperfine splitting is due to electron spin-nuclear spin interaction (^{55}Mn, I = 5/2). The six lines corresponds to M_I = +5/2, +3/2, +1/2, ..,-5/2 ΔM_I=0 for all transitions. However, for compound **40** the frozen solution gives a typical EPR spectrum of an Mn(II) system. The hyperfine coupling constant is about 95 G and the g_0 value is close to the spin only value of 2.002. The A_0 values are consistent with the octahedral coordination [12]. In addition to this a pair of low intensity forbidden lines lying between each of the main hyperfine lines is observed. This corresponds to $\Delta M_I = \pm 1$, due to the mixing of nuclear hyperfine levels by the zero-field splitting factor of the Hamiltonian [13]. The A_0 values are somewhat lower than that of pure ionic compounds, and reflect the covalent nature of the metal ligand bonds.

7.3.5. Cyclic Voltammetry

Cyclic voltammograms recorded in DMF (10^{-3} M) are not very informative (Figure 7.6). However, a scan at 20 mV/s scan rate for the compound **39** gives an irreversible reduction peak corresponding to $Mn^{IV/III}$ couple at about –0.15 V. The couple due to $Mn^{III/II}$ reduction *ca.* –0.95 V is rather obscured by the ligand reduction couple. The irreversible peak is more pronounced at higher scan rates (200 mV/s). The oxidation peaks are obscurely seen at ca. +0.39 V and at higher potentials, viz., +0.49 V, +0.65 V, +0.95 V.

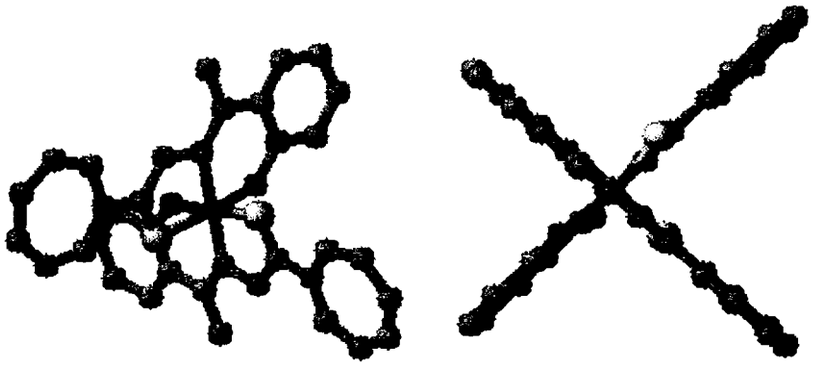

Perspective 1 Perspective 2

Figure.7.4.: Approximate structure of compound **38**
[Atoms: Black –carbon, Blue- oxygen, Yellow-sulfur, Red- manganese and Green-nitrogen]

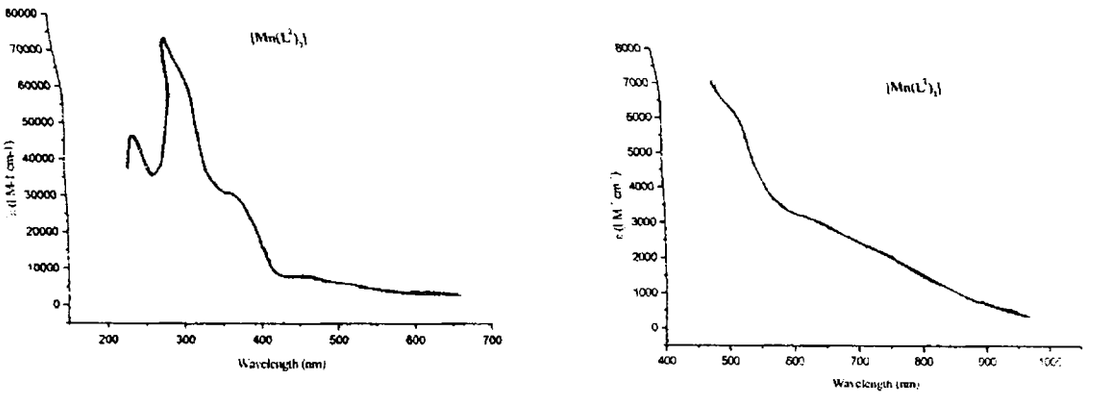

Compound **38**

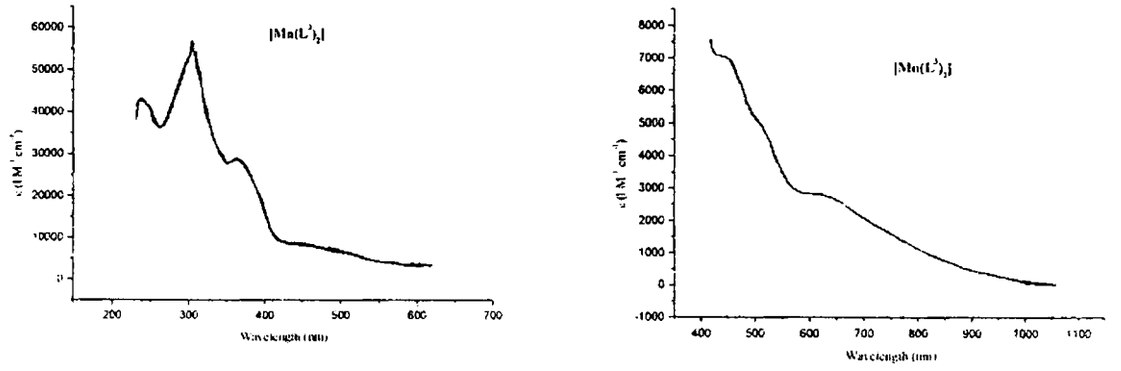

Compound **39**

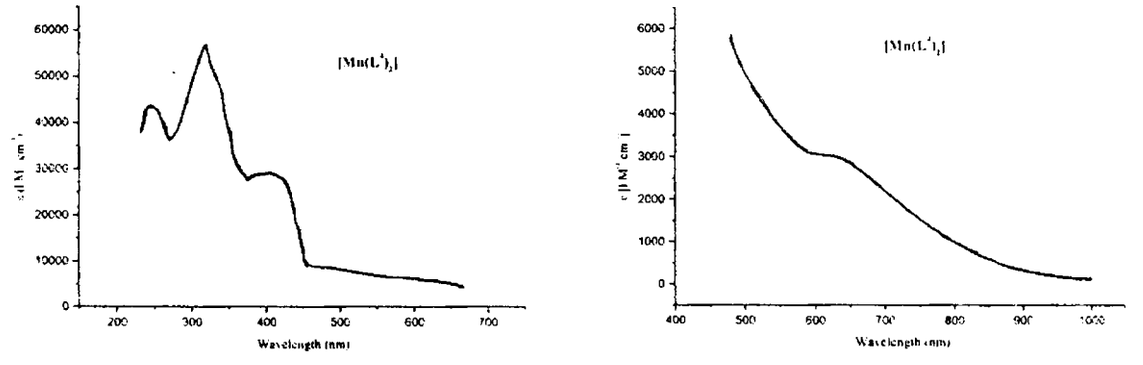

Compound **40**

Figure 7.3.: UV(left) and Visible (right) spectra of the compounds **38**, **39** and **40** inCH_2Cl_2.

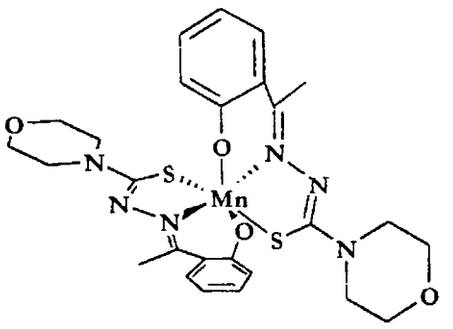

Figure 7.5.: The suggested distorted octahedral structure of compound **39**

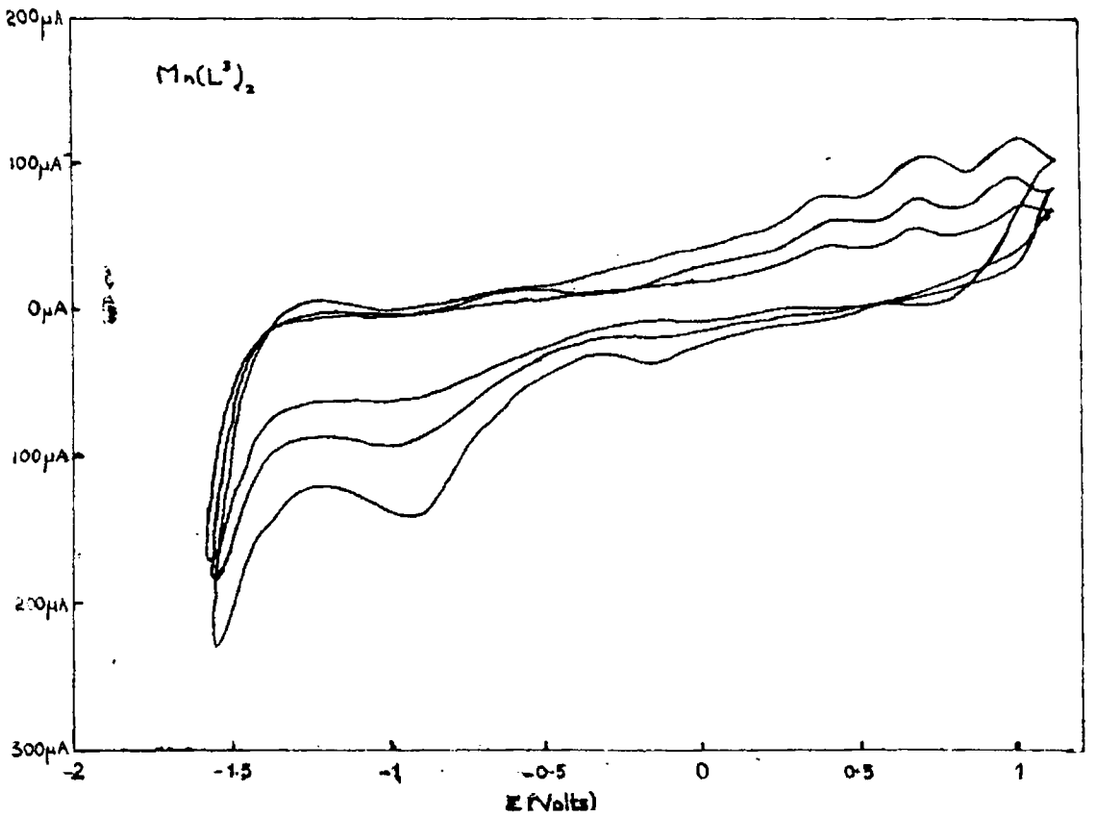

Figure 7.6. : Cyclic voltammograms recorded in DMF (10^{-3} M) of $Mn(L^3)_2$

Table 7.1: Elemental analysis and EPR data for manganese complexes

Compound	Color	Found (Calcd.) (%)				Magnetic moment BM	g_0 solid	g_0 in DMF 77 K	A_{II} (DMF) 77 K (G)
		C	H	N	Mn				
$Mn(L^2)_2$ (**38**)	Brownish black	57.26 (56.86)	6.09 (6.04)	13.42 (13.26)	8.82 (8.66)	4.04	2.69	---	---
$Mn(L^3)_2.H_2O$ (**39**)	Black	50.05 (49.76)	5.22 (5.14)	12.94 (13.39)	8.83 (8.75)	4.07	2.66	1.998	68
$Mn(L^4)_2$ (**40**)	Black	59.32 (59.12)	4.74 (4.65)	13.05 (12.94)	8.47 (8.46)	3.94	2.70	2.002	94.8

Table 7.2.: Electronic spectral data, $\lambda/cm^{-1}(log\varepsilon)$, and cyclic voltammetric data for the ligands and their manganese(IV) complexes.

Compound	d-d	L→M	n→π*	π→π*	Oxidation $E_{1/2}$/V	Reduction $E_{1/2}$/V
H_2L^2	---	---	30581 (4.19) 32372sh (4.23)	35587 (4.48)		
$Mn(L^2)_2$ (**38**)	22222 (4.01), 19646 (3.80), 16077 (3.50), 13298 (3.29)	27586 (4.58)	33523 (4.95)	42283 (4.75)	0.12, 0.65, 0.75	0.45, 0.85[a], 1.2[a]
H_2L^3	---	---	30030 (4.43) 32895sh (4.41)	42370 (4.25)		
$Mn(L^3)_2.H_2O$ (**39**)	22573 (3.95), 19607 (3.73), 16312 (3.48), 12820 (3.15)	27472 (4.47)	32787 (4.70), 31446sh (4.64)	41656 (4.64)	0.39, 0.49, 0.65, 0.95	0.15, 0.95
H_2L^4	---	---	30211 (4.19) 35524sh (4.40)	42370 (4.32)		
$Mn(L^4)_2$ (**40**)	22727 (3.83), 19493 (3.65), 16529 (3.49), 13158 (3.15)	27473 (4.36)	32787 (4.65)	42194 (4.52)	0.40, 0.65	0.85

a = quasireversible i.e., $i_{pa}>i_{pc}$

Table 7.3: IR spectral bands /cm^{-1} for the manganese complexes

Compound	ν (^{7}C=^{1}N)	ν (^{2}N=^{9}C)	ν (^{1}N-^{2}N)	ν (Mn-N)	ν (C=S)	δ (C=S)	ν (C-O)
H_2L^2	1603s	-	997m	-	1383s	839m	1252s
$Mn(L^2)_2$ **(38)**	1559m	1591	1017m	442w	1367s	810m	1132s
H_2L^3	1605s	-	1017m	-	1374s	835m	1219s
$Mn(L^3)_2.H_2O$ **(39)**	1566m	1591s	1030m	439w	1300s	808m	1113s
H_2L^4	1601s	-	995m	-	1375s	791m	1222s
$Mn(L^4)_2$ **(40)**	1558m	1592s	1024m	444w	1307s	764 m	1124s

s = strong, m = medium, w = weak, sh = sharp

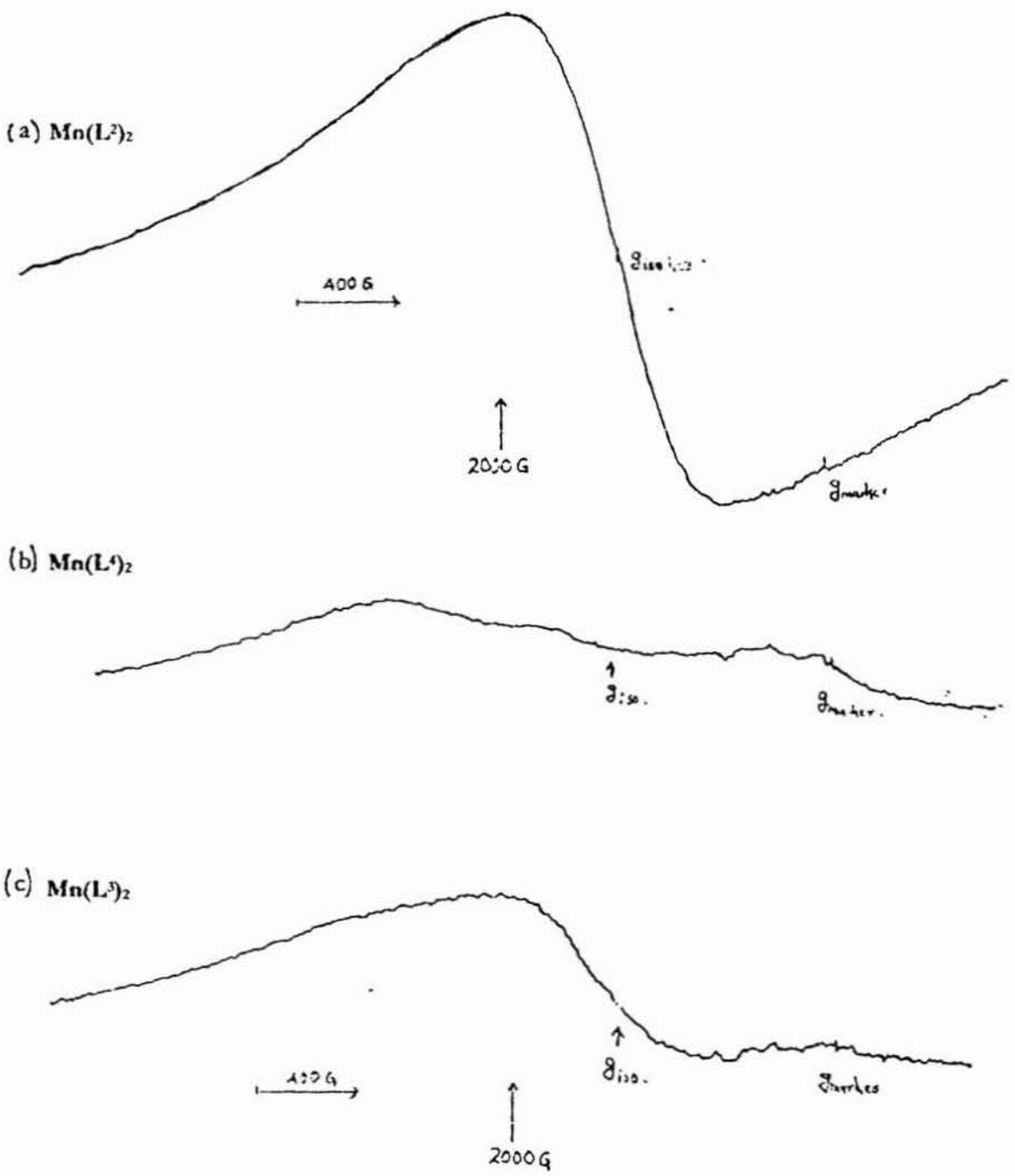

Figure 7.1: EPR spectra of manganese complexes in polycrystalline state at 298 K. a) compound **39**, b) compound **38**, c) compound **40**.

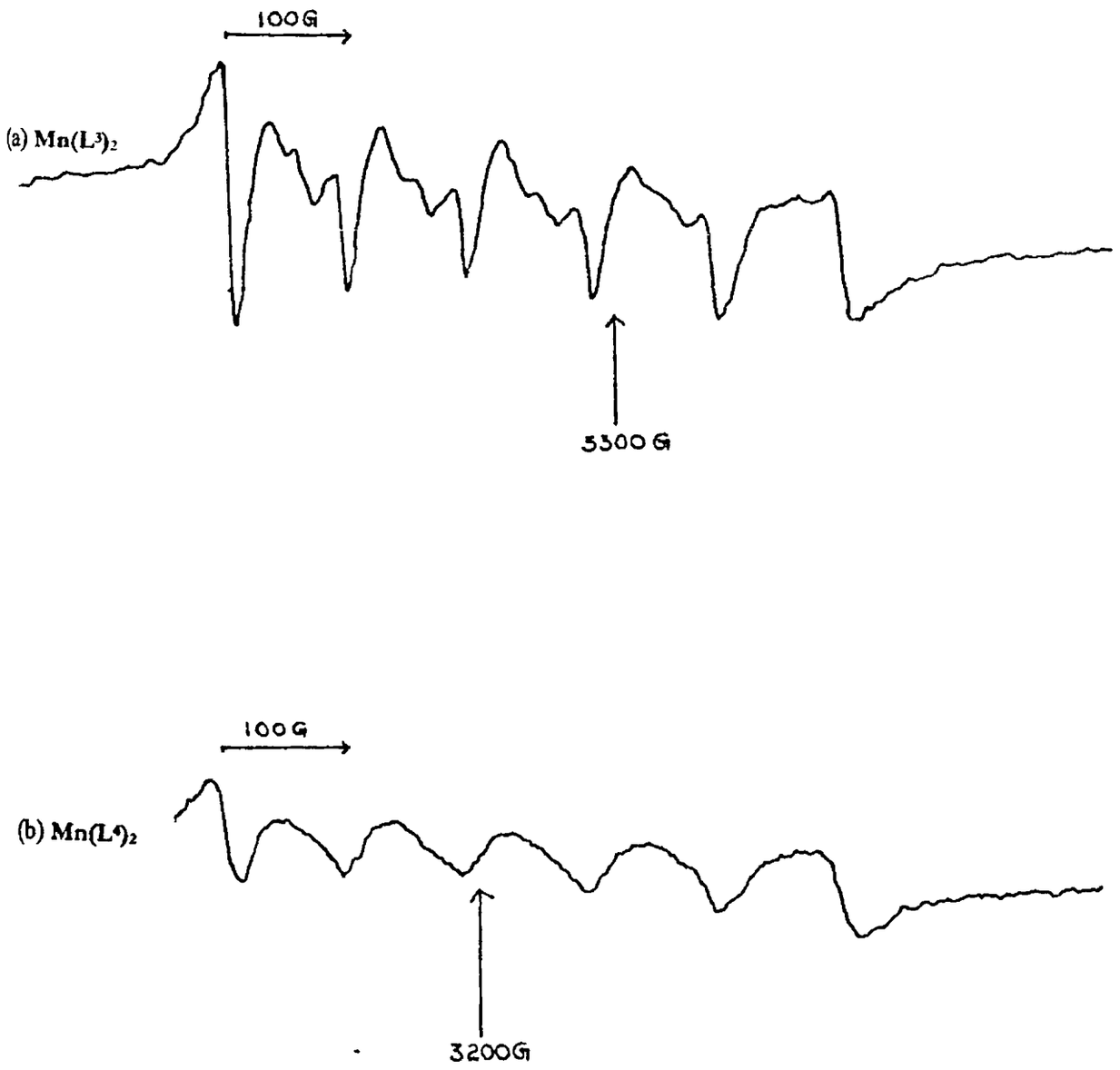

Figure 7.2: EPR spectra of manganese complexes in DMF at 77K. a) compound **39**, b) compound **40**

REFERENCES:

7.1 V. K. Yachandra, K. Sauer and M. P. Klein, *Chem. Rev.*, 1996, **96**, 2927.

7.2 K. Wieghardt, *Angew. Chem., Int. Ed. Engl.*, 1994, **33**, 725; R. Manchandra, G. W. Bradvig and R. A. Crabtree, *Coord. Chem. Rev.*, 1995, **144**, 1.

7.3 G. Blandin, R. Davydov, C. Philonze, M. F. Charlot, S. Styring, B. Akermark, J. J. Girerd and A. Boussac, *J. Chem. Soc. Dalton Trans.*, 1997, 4069.

7.4 a) U. Auerbach, T. WeyhermCller, K. Wieghardt, B. Nuber, E. Bill, C. Butzlaff, A.X. Trautwein, *Inorg. Chem.*, 1993, 32, 508; b) M. J. Baldwin, T. L. Stemmler, P. J. Riggs-Gelasco, M. L. Kirk, J. E. Penner-Hahn, V. L. Pecararo, J. Am. Chem. Soc., 1994, 116, 11349.

7.5 D. J. E. Ingram, *Spectroscopy at radio and microwave frequencies*, Butterworth, London, 2nd Edn. 1967.

7.6 A. Carrington, and A. D. Mchachlan, *Introduction to Magnetic Resonance*, Harper and Row, NY, 1969, p. 173.

7.7 I. Fidone, and K.W. H. Stevens, *Proc. Phys. Soc. (London)* 1958, **73**, 116.

7.8 B. R. McGarvey, *J. Phy. Chem.*, 1957, **61**, 1232; N. Blombergen and L. O. Morgan, *J. Chem. Phys.*, 1961, **34**, 842; H. Levanon and Z. Luz, *J. Chem. Phys.*, 1968, **49**, 2031.

7.9 S. I. Chan, B. M. Fung, and H. Lutje, *J. Chem. Phys.*, 1967, **47**, 2121.

7.10 J. E. Wertz and J. R. Bolton, *Electron Spin Resonance Elemental Theory and Practical Applications*, p 335.

7.11 W. E. Buschmann, C. Vazquez, M. D. Ward, N. C. Jones and J. S. Miller, *Chem. Comm.*, 1997, 409.

7.12 B. A. Goodman, and J. B. Raynor, *Adv. Inorg. Chem. Radiochem.*, 1970, **13**, 135.

7.13 J. E. Drumheller and R. S. Rubins, *Phys. Rev.*, 1964, **133**, 1099.

SUMMARY AND CONCLUSION

The thesis deals with synthesis, structural characterization, electrochemical and biological studies of metal complexes of four, ^{4}N substituted thiosemicarbazones of 2-hydroxyacetophenone. The entire thesis is divided into eight chapters.

Chapter 1 embodies a brief introduction into the field of thiosemicarbazones, its significance and an extensive literature survey. It also contains a brief outline of various instrumental techniques adopted in the characterization process in the field of inorganic chemistry. It defines the objectives, and provides an outline of the scope of the present work.

Chapter 2 is divided into two portions *viz*., chapter 2a and chapter 2b. Chapter 2a deals with synthesis and spectral characterization of four thiosemicarbazone ligands used for complexation, using IR, UV-Visible, ^{1}H and ^{13}C-NMR spectroscopy.

Chapter 2b deals with the synthesis of eight heterocyclic base adducts of copper(II) complexes of the four thiosemicarbazone ligands, structural characterization using, elemental, IR, UV-Visible, EPR spectroscopy and X-ray diffraction techniques. The bases used were bipyridine and phenanthroline. The EPR spectra at room temperature in the polycrystalline state, at room temperature in solution, and at 77K in solution were recorded. The information obtained was used for calculating the bonding parameters of the compounds. EPR simulations were carried out to obtain accurate magnetic parameters. The compounds are found to possess axial symmetry in the solid state and retain the symmetry in the solution state. Single crystal X-ray diffraction studies were carried out to establish the exact structure of the compounds as a distorted square pyramid. Cyclic voltammetric measurements were done to study the redox behavior of the complexes in solution. The copper$^{II/I}$ reductions and copper$^{II/III}$ oxidations were found to be masked by the redox properties of the ligands. The biological activity of the complexes were tested against commonly found fungal and bacterial strains viz, *E. Coli, Staphylococcus Aureus, Asp. Flavus and Candida Albicans.* All complexes showed increased activity against bacterial cultures and moderate activity against the tested fungal cultures. The complexes of ligands H_2L^1 and H_2L^2 are more active. The phenanthroline base adducts of the copper(II) complexes are found to be more active than their bipyridyl counter parts.

Chapter 3 deals with the synthesis of eight ternary complexes of oxovanadium(IV). In addition to the four thiosemicarbazone ligands heterocyclic bases such as bipyridine and phenanthroline were used as auxiliary ligands for complexation. The prepared complexes were analyzed by UV-Visible, IR, and EPR spectroscopic techniques. The electronic and EPR spectroscopy were used to obtain magnetic and spectral parameters of the complexes. EPR simulations were used to get the best-fit data from the EPR spectral measurements. The data obtained were used to calculate various bonding parameters. The structural alternations and formation of new species in solution were monitored using electronic and EPR spectroscopy. The geometry of the compound was arrived at with the help of the above techniques, as a distorted octahedral.

Chapter 4 contains details regarding synthesis of eight novel base adducts of zinc(II) and thiosemicarbazone ligands. It describes the ^{1}H NMR spectroscopy used for establishing the structure of the complexes. The zinc complexes were suggested to have trigonal bipyramidal geometry. Biological activity studies of the complexes were also discussed in this chapter.

Chapter 5 discusses the synthesis of eight quaternary complexes of cobalt(III) and their spectral characterizations. The thiosemicarbazones, heterocyclic bases *viz.*, phenanthroline/bipyridine and azide ion acts as ligands. The magnetic data are in conformity with cobalt in the +3 oxidation state. The compounds are diamagnetic. The IR, electronic and ^{1}H-NMR spectra suggests a distorted octahedral geometry for the cobalt(III) complexes.

Chapter 6 deals with the five dioxouranium(VI) complexes. The elemental, IR, electronic and ^{1}H-NMR spectra of the compounds suggests an oxo-bridged dimer for the complex $[UO_2L^2]_2$ formed by H_2L^2. The electronic spectra are characteristic of the dioxouranium(VI) species. The NMR spectra of the other dioxouranium(VI) compounds indicate fluxional behaviour for the coordinated heterocyclic moiety. The geometry of the compounds was suggested to be a five-coordinated uranium atom with the dioxo group lying along axis. The ligands are suggested to be misaligned from the equatorial plane.

Chapter 7 discuses the synthesis and spectral characterizations of three manganese(IV) complexes. Magnetic, electronic, IR and EPR measurements suggest the metal in the +4 oxidation state. The compound is suggested to have a distorted octahedral geometry.